
**Novel interaction partners of the chromatin
remodeler CHD7, a protein mutated in CHARGE
syndrome**



Dissertation

zur Erlangung des Doktorgrades
der Mathematisch-Naturwissenschaftlichen Fakultäten
der Georg-August-Universität zu Göttingen

vorgelegt von

Tserendulam Batsukh
aus Ulaanbaatar, Mongolei

Göttingen, 2012

D7

Referent: Prof. Dr. Dr. Wolfgang Engel

Korreferent: Prof. Dr. Sigrid Hoyer-Fender

Tag der mündlichen Prüfung:

*Dedicated to my family,
whose love and supports were always present and encouraged me in my path.*

Table of contents

Table of Contents	i
List of Tables and Figures	ii
1. Zusammenfassung	1
1. Summary.....	3
2. Introduction	5
2.1 Chromodomain helicase DNA-binding family of chromatin remodelers.....	5
2.2 Function of CHD7.....	7
2.3 Role of CHDs in human diseases.....	9
2.4 CHD7 and CHARGE syndrome.....	10
3. Results	14
3.1 CHD8 interacts with CHD7, a protein which is mutated in CHARGE Syndrome.....	15
3.2 Identification and characterization of FAM124B as a novel component of a CHD7 and CHD8 containing complex.....	26
4. Discussion	51
4.1 Known CHD7 complexes and function.....	51
4.2 Known CHD8 complexes and function.....	53
4.3 CHD8 builds together with CHD7 a complex.....	55
4.4 Evaluating the effect of 4 CHD7 missense mutations on the interaction between CHD8 and CHD7.....	57
4.5 FAM124B is associated with CHD7 and CHD8.....	58
4.6 Subcellular localization and expression profile of Fam124B in comparison of Chd7 and Chd8.....	59
4.7 Structure and Function of FAM124B.....	63
4.8 Future endeavors and perspectives.....	64
5. References	67
6. Abbreviations	80
7. Acknowledgments	83
8. Curriculum Vitae	84
9. List of Publications	85

List of Tables and Figures

Figure 2.1. Mechanism for ATP-dependent chromatin remodeling.....	5
Figure 2.2. Structural domains of human CHD family of proteins	6
Table 2.1. Overview of the functions of the CHD family of proteins	8
Table 2.2. Human diseases associated with CHD proteins.....	10
Figure 2.3. Distribution of pathogenic mutation types in the <i>CHD7</i> gene.....	12
Figure 4.1. Models for CHD7 complexes.....	53
Figure 4.2. Models for CHD8 complexes.....	55
Figure 4.3. CHD7 and CHD8 endogenous interaction in HeLa cells shown by the Duolink PLA method.....	56
Figure 4.4. Hypothetical Enhancer and Promoter interaction via CHD7 and CHD8 containing protein/transcription factors (TF) complex mediated DNA-loop model.....	58
Figure 4.5. Immunostaining Fam124B of adult brain shown in comparison with Chd7 and Chd8.....	60
Figure 4.6. Chd7, Chd8 and Fam124B immunostainings on sagittal section of an E12.5 wildtype embryo	61
Figure 4.7. Chd7, Chd8 and Fam124B immunostaining on coronal section of the E12.5 mouse embryo.....	62
Figure 4.8. A homologous part of FAM124B protein alignment from Human to Zebrafish by Constraint-based Multiple alignment tool.....	64
Figure 4.9. Effect of CHD7 knockdown on expression of transcription factor Twist involved in neural crest formation.....	65

1. Zusammenfassung

CHARGE Syndrom, ein autosomal dominant vererbtes Malformationssyndrom wird durch Mutationen im Chromodomänen Helikase DNA bindenden protein 7 (CHD7) Gen hervorgerufen. In 10% der „typischen“ und 40-50% der „atypischen“ CHARGE Patienten findet sich keine Mutation im *CHD7* Gen und somit bleibt die Ursache der Symptomatik in diesen Fällen unklar. CHD7 ist ein nukleär lokalisierter chromatin *remodeler*, der in großen Multiproteinkomplexen detektiert werden konnte und die Expression verschiedener Gene reguliert. Die Charakterisierung von CHD7 Interaktionspartnern ist möglicherweise hilfreich um die Pathogenese des CHARGE Syndroms zu verstehen. Für einige andere genetisch bedingte Erkrankungen konnte gezeigt werden, dass Mutationen in Interaktionspartnern zu demselben oder einem ähnlichen Krankheitsbild führen. Daher vermuten wir, dass CHD7 Interaktionspartner gute Kandidaten sind, die möglicherweise im mutierten Zustand ebenfalls zum CHARGE Syndrom führen.

Im ersten Teil dieser Arbeit wurde CHD8 als ein Interaktionspartner von CHD7 identifiziert. Die Interaktion des CHD7 Teilstückes (Aminosäuren: 1593-2178) mit einem CHD8 Teilstück (Aminosäuren: 1789-2302) wurde mittels verschiedener molekularer Techniken validiert. Zusätzlich konnten wir zeigen, dass die Interaktion im Nucleoplasma stattfindet. Darüber hinaus wurde der Einfluss von 3 in der Literatur beschriebenen Mutationen (p.His2096Arg, p.Val2102Ile und p.Gly2108Arg) und einer neu identifizierten (p.Trp2091Arg) CHD7 missense Mutation auf die CHD7-CHD8 Interaktion mittels Yeast two hybrid (Y2H) und Co-Immunopräzipitation (Co-IP) untersucht. Während wir mittels Y2H zeigen konnten, dass die CHD7-CHD8 Interaktion durch die CHD7 missense Mutationen p.Trp2091Arg, p.His2096Arg und p.Gly2108Arg aufgehoben wird, konnte dieser Effekt mittels Co-IP nicht nachgewiesen werden. Daher vermuten wir, dass CHD7 und CHD8 einerseits direkt miteinander interagieren (gezeigt durch die direkten Y2H Experimente) und zusätzlich indirekt über sog. Linker Proteine, die zusammen mit CHD7 und CHD8 einen großen Proteinkomplex formen (Erklärung für die Co-IP Ergebnisse). Zusätzlich haben wir CHD7 negative CHARGE Patienten auf Mutationen im *CHD8* Gen untersucht.

Im zweiten Teil der Doktorarbeit zeigen wir die Ergebnisse der SILAC und Massenspektrometrie Analyse, bei der wir das bisher uncharakterisierte Protein FAM124B als eine Komponente eines CHD7-CHD8 enthaltenden Komplexes identifizierten. Die Interaktion mit dem CHD8 Teilstück (Aminosäuren 1789-2302) wurde mittels direktem Y2H und Co-IPs

validiert, während eine Interaktion mit dem CHD7 Teilstück (Aminosäuren 1593-2178) nur mittels Co-IP bestätigt werden konnte, wodurch gezeigt wurde, dass FAM124B nicht direkt mit der o.g. CHD7 Region interagiert. Zusätzlich erfolgte eine Charakterisierung von FAM124B. Wir konnten zeigen, dass FAM124B, wie CHD7 und CHD8 im Zellkern lokalisiert ist. Fam124B wird bei der Maus in den Organen, die beim CHARGE Syndrom betroffen sind expremiert. Eine starke Expression konnte in dem sich entwickelnden Gehirn, Herzen, Lunge und im Rückenmark von E12.5 Mausembryonen nachgewiesen werden. Kürzlich konnte gezeigt werden, dass Mutationen in CHD8 Autismus (ASD) und Entwicklungsstörungen des Nervensystems (NDD) bewirken können. Zusammenfassend, weisen unsere Daten darauf hin, dass das bisher uncharakterisierte Protein FAM124B eine sehr wichtige Funktion in der Embryonalentwicklung hat und möglicherweise an der Pathogenese des CHARGE Syndroms und ASD/NDD beteiligt ist.

Um eine mögliche Rolle von FAM124B an der Pathogenese des CHARGE Syndroms und Neurocristopathien zu analysieren, planen wir die Herunterregulierung von Fam124B in *Xenopus laevis* um anschließend den Einfluss von Fam124B auf Gene, die an der Neuralleistenzellformation beteiligt sind zu testen. Die Generierung eines Fam124B knockout Mausmodels und die weitere Charakterisierung von CHD7 Interaktionspartnern werden zur Erlangung tiefgreifender Kenntnisse des molekularen Mechanismus des CHARGE Syndroms und Autismus Erkrankungen hilfreich sein.

1. Summary

CHARGE syndrome, an autosomal dominant inherited multiple malformation syndrome is caused by mutations in the chromodomain helicase DNA binding protein 7 gene (*CHD7*). In 10% of 'typical' CHARGE patients and 40-50% of 'atypical' CHARGE patients no mutation in the *CHD7* gene is detectable and therefore the molecular cause is still unknown. *CHD7* is a nuclear chromatin remodeling protein found in big protein complexes and regulating gene expression of various genes. We suggested that the characterization of *CHD7* interacting partners can be useful for understanding the pathogenesis of CHARGE syndrome. Furthermore, for other genetic diseases it was shown that mutations in interacting partners lead to the same or a similar phenotype. Therefore, we hypothesized that *CHD7* interacting partners are good candidates, leading to CHARGE syndrome when they are mutated.

In the first part of the thesis, *CHD8* was identified as an interacting partner of *CHD7*. The interaction of the *CHD7* part (1593 – 2178aa) with the *CHD8* part (1789 – 2302aa) was validated by different molecular techniques. Additionally, we could show that the interaction takes place in the nucleoplasm. Furthermore, the influence of 3 known (p.His2096Arg, p.Val2102Ile and p.Gly2108Arg) and one (p.Trp2091Arg) newly identified *CHD7* missense mutation on the *CHD7-CHD8* interaction was elucidated by direct Yeast two hybrid (Y2H) and co-immunoprecipitation (Co-IP) methods. By Y2H we could demonstrate that the missense mutations p.Trp2091Arg, p.His2096Arg and p.Gly2108Arg disrupt the *CHD7-CHD8* interaction, while no influence on the interaction could be seen in Co-IP assays. Therefore, we suggest that *CHD7* and *CHD8* interact directly (shown by Y2H) and indirectly via additional linker proteins which build together with *CHD7* and *CHD8* a large protein complex (explaining the Co-IP result). In addition, we reported about the sequence analysis of the *CHD8* gene in *CHD7* mutation negative patients with CHARGE syndrome.

In the second part of the thesis, we showed the results of a SILAC and mass-spectrometry approach that identified the hitherto unknown protein FAM124B as a member of *CHD7-CHD8* containing complex. The interaction with the *CHD8* part (1789 – 2302aa) was validated by direct Y2H and Co-IP methods whereas the interaction with the *CHD7* part (1593 – 2178aa) could be only confirmed with the Co-IP assay, demonstrating that FAM124B interacts not directly with the analyzed *CHD7* region. Furthermore, we characterized FAM124B. We could show that FAM124B is localized in the nucleoplasm like *CHD7* and *CHD8*. Murine Fam124B is expressed in the organs affected in CHARGE syndrome. High expression could be observed in the developing brain, heart, lung and spinal cord of E12.5 mouse embryos. Recently, *CHD8*

mutations are shown to be a cause of autism spectrum disorders (ASD) as well as neurodevelopmental disorders (NDD). In conclusion, our results indicate that the hitherto uncharacterized protein FAM124B might be very important for embryonic development and could be involved in the pathogenesis of CHARGE syndrome and ASD/NDDs.

Moreover, to analyse the possible role of FAM124B in the pathogenesis of CHARGE and neurocristopathies, we plan to perform a knockdown of FAM124B in *Xenopus laevis* and test its influence on genes related to neural crest formation. Generation of a knockout mouse model for Fam124B and further characterization of the CHD7 interacting complex members will help to learn more about the molecular mechanism behind CHARGE syndrome and ASD/NDDs.

2. Introduction

2.1 Chromodomain helicase DNA-binding family of chromatin remodelers

Chromatin is a DNA-protein complex offering the possibility to package large amounts of DNA into the small area of the nucleus by wrapping the DNA. The basic unit of the chromatin assembly is called nucleosome that consists of eight histone proteins (Ho & Crabtree 2010). Depending on the chromatin condensation grade (loosely or tightly packed DNA), the transcription of a certain gene is possible or not, because transcription factors and RNA-polymerases need free access to their binding sites. Therefore, the condensation of DNA provides an important mechanism to regulate gene expression in living cells (Wolffe 1992, Hall & Georgel 2007). Chromatin remodelers can alter the structure of chromatin by different mechanisms: nucleosome sliding, histone exchange, nucleosome eviction and alteration of the nucleosome structure (Wolffe 1992, Allis et al. Epigenetics 2007, Hall & Georgel 2007) (Fig. 2.1).

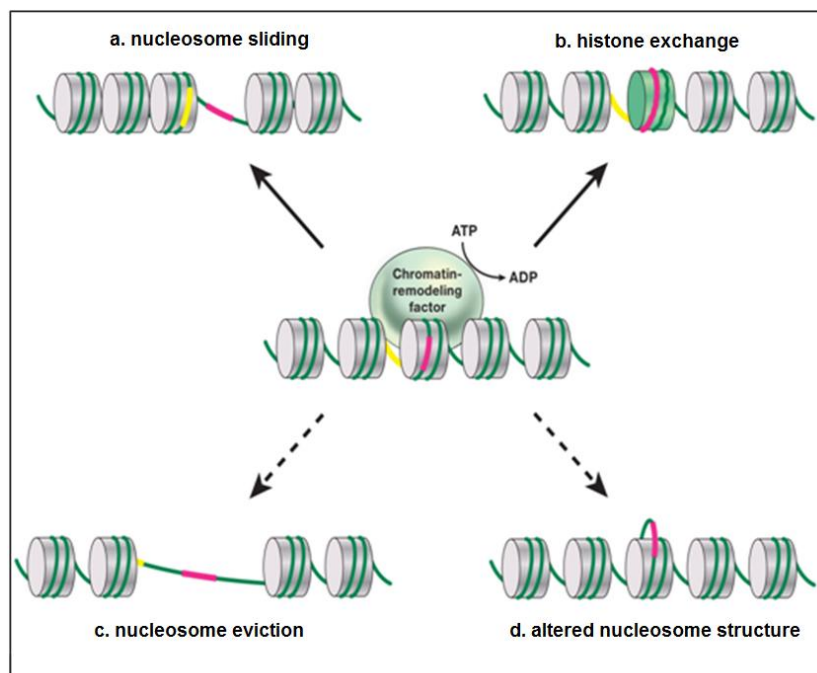


Figure 2.1. Mechanism for ATP-dependent chromatin remodeling. Different chromatin remodeling models are described by showing the change in position or composition of nucleosomes relative to the DNA wrapped around it. The central panel indicates a starting chromatin region where linker DNA is indicated in yellow and nucleosomal DNA in red. **a:** nucleosome sliding movement along the DNA, **b:** exchange of a variant histone for a standard histone to create a variant nucleosome, **c:** eviction of nucleosomes to open a large region of DNA. This mechanism might depend on other proteins, such as histone chaperones or DNA-binding factors, in addition of remodeling proteins, **d:** creating a loop on the surface of the nucleosome (Adapted and modified from Allis et al. Epigenetics 2007).

Several chromatin remodeling complexes are known. The Chromodomain Helicase DNA binding (CHD) gene family belongs to the group of ATP-dependent chromatin remodelers (Ho & Crabtree 2010). In human, the CHD family consists of 9 members. All of them share the unique combination of two chromodomains (chromatin organization modifier) (Messmer et al. 1992), a sucrose non-fermenting (SNF2)-like helicase/ATPase domain and DNA-binding domains (Hall & Georgel 2007; Marfella & Imbalzano 2007) (Fig. 2.2).

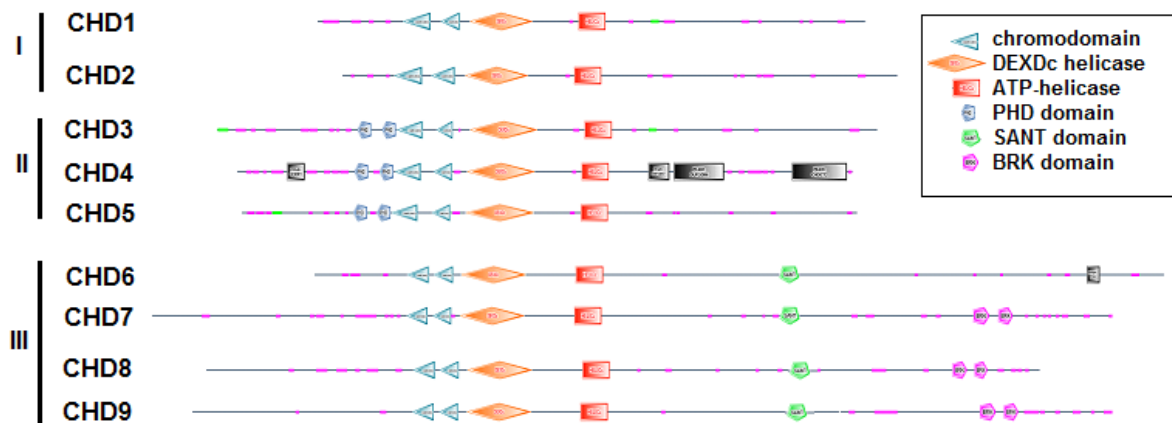


Figure 2.2. Structural domains of human CHD family of proteins. Full length protein sequences were analyzed by SMART program and modified. (<http://smart.embl-heidelberg.de/>). CHD1-2 (Subgroup I) have the simplest protein structure which is N-terminal 2 chromodomains, in the middle part a DEXDc helicase (DEAD like helicase), ATP-helicase (ATPase) domain and C-terminal a DNA-binding domain. CHD3-5 (Subgroup II) have in addition N-terminal double PHD (Plant homeo domain) domains followed by the chromodomains. CHD6-9 (Subgroup III) proteins have in addition a C-terminal SANT domain followed by two BRK domains.

The SNF2-like ATPase domain was found in many proteins which are involved in chromatin assembly, transcription regulation, DNA repair, DNA replication, development and differentiation (Tsukiyama 2002, Smith & Peterson 2005, de la Serna et al. 2006).

Mutational analysis of helicase and chromodomains revealed their crucial role for proper binding with chromatin (Kelley et al. 1999). Detailed functional analysis of chromodomains led to the suggestion that they mediate chromatin interactions through the direct binding of DNA, RNA, and methylated histone H3 (Akhtar et al. 2000, Bouazoune et al. 2002, Fischle et al. 2003, Min et al. 2003, Brehm et al. 2004, Flanagan et al. 2005, Pray-Grant et al. 2005, Sims et al. 2005, Kim et al. 2006).

Because of additional domains, the CHD family of protein members is further divided into 3 subgroups (Hall & Georgel 2007, Marfella & Imbalzano 2007) (Fig. 2.2). *CHD1* and *CHD2* belong to the first subgroup. They have the simplest protein structure among the other family members consisting of 2 chromodomains, a SNF2-like helicase/ATPase domain and DNA-

binding domains. Although the subgroup I members are highly homologous to one another, they are significantly divergent in the 3' region.

The second subgroup contains *CHD3*, *CHD4* and *CHD5*. They share in addition two N-terminal PHD (plant homeo domain) zinc finger domains (Sims & Wade 2011) which are known to be involved in special chromatin remodeling mechanisms (Eberharter et al. 2004, Ragvin et al. 2004) as well as in epigenetic processes by binding to methylated histone peptides (Pena et al. 2006, Shi et al. 2006).

CHD6-9 belong to subgroup III. All subgroup III members have two BRK domains (*Brahma* and *Kismet* domain) at C-terminus with unknown function, three conserved regions (CR1-3) with unknown function and a SANT domain (*Switching-defective protein 3*, *Adaptor 2*, *Nuclear receptor corepressor*, *Transcription factor IIIB*) (Janssen et al. 2012). The SANT domain is suggested to act as a histone tail binding module (Boyer et al. 2004, Hall & Georgel 2007) (Fig. 2.2).

2.2 Function of CHD7

Table 2.1 gives an overview of all human *CHD* family members and their possible or known functions in humans or other species as well as their existing mutant models. A more detailed description is given for the *CHD7* gene. *CHD7* is involved in transcriptional regulation (Schnetz et al. 2009) and mutations in this gene lead to CHARGE syndrome (see 2.4) (Vissers et al. 2004).

The *CHD7* gene is located on chromosome 8q12.1 and consists of 38 exons with the ATG in exon 2 and the stop codon in exon 38. The genomic size is 188kb and the gene encodes a protein with a predicted size of 336kDa (<http://www.sciencegateway.org/tools/proteinmw.htm>). *CHD7* is evolutionary highly conserved among species (orthologs were described in *Xenopus*, mouse, chicken, zebrafish, *C.elegans* and *Drosophila melanogaster* (Bosman et al. 2005, Aramaki et al. 2007, Shrinivasan et al. 2008, Bajpai et al. 2010)). *CHD7* expression is tissue and embryonic stage dependent and its expression pattern in human, mouse, chicken, zebrafish and in other species match with the developmental defects in CHARGE syndrome (Bosman et al. 2005, Lalani et al. 2006, Sanlaville et al. 2006, Aramaki et al. 2007). Since the discovery that *CHD7* mutations lead to CHARGE syndrome in human, the *CHD7* gene has been studied more functionally. Several animal models for CHARGE syndrome were created (Table 2.1) (Siebert et al. 1985, Bergman et al. 2005, Hurd et al. 2007, Bajpai et al. 2010, Schnetz et al. 2010, Zentner et al. 2010, Patten et al. 2012).

Genes	Molecular functions	Mutants phenotype and in vivo function
<i>CHD1</i>	Transcriptional repressor. Interacts with SSRP1. Transcription elongation, Transcription activator (Gaspar-Maia A. et al. 2009)	Maintenance of mouse embryonic stem cell. (Gaspar-Maia A. et al. 2009)
<i>CHD2</i>	Unknown	Chd2 null mice embryos have growth retardation and die before birth, Decreased neonatal viability, non-neoblastic lesions (Marfella et al., 2006)
<i>CHD3</i>	Component of Nurd complex (Tong et al. 1998, Xue et al. 1998, Zong et al. 1998) <i>Drosophila</i> : Nucleosome-stimulated ATPase activity and mobilizes nucleosomes (Brehm et al. 2004) Transcriptional repression (Sims et al. 2003)	Several deficient model system of CHD3 suggest that it has a role in transcription repression (Kehle et al. 1998, Wade et al. 1998, Solari & Ahringer et al. 2000)
<i>CHD4</i>	Component of Nurd complex (Tong et al. 1998, Xue et al. 1998, Zong et al. 1998) Transcriptional repression (Sims et al. 2003)	T-cell development, Lymphocyte differentiation (Williams et al. 2004)
<i>CHD5</i>	Unknown	Potential tumor suppressor in breast, colon, and neuroectodermal cancers (Sims and Wade 2011)
<i>CHD6</i>	Localizes to sites of transcription and is induced by DNA damage (Jennifer et al. 2011)	One patient with translocation t(18;20)(q21.1;q11.2) has mild to moderate mental retardation and minor facial anomalies, including a broad, square face, hypertelorism, flat nasal bridge, prominent ears, and a short neck. (Karlscheuer et al. 2008) CHD6 mutation in some transitional cell carcinoma (Gui et al. 2011)
<i>CHD7</i>	CHD7 binds in a cell type and developmental stage specific manner to methylated histone H3K4 in enhancer region (Bergman et al. 2005) Transcriptional regulation of nuclear genes (Schnetz el al. 2010) Transcriptional regulation of ribosomal RNA biogenesis in nucleolus. Interacts through rDNA with treacle, the protein involved in Treacher Collins syndrome (Zentner et al. 2010) Fine tuning effect on ES specific genes in mutant null mouse ESCs. Chd7 colocalizes with ES cell master regulators Oct4, Sox2 and Nanog. (Schnetz el al. 2010)	Whirligig Chd7 null mouse embryo dies at E10.5. Heterozygous mice shows head bobbing and circling behavior due to inner ear defect, heart malformations, cleft palate, choanal atresia, genital anomalies etc. (Bergman et al. 2005, Bosman et al. 2010) Homozygous Chd7 gene trap mutant mice die pränatally. Heterozygous associated with defects in multiple developing tissues (Hurd et al. 2007) Xenopus and human neural crest cell study showed it is essential role for formation of multipotent migratory neural stem cells. Chd7 is required for the organization of the neural retina in zebrafish. Knockdown of Chd7 display an abnormal organization of motor neurons and severe loss of the facial nerves (Siebert et al. 1985, Bajpai et al. 2010, Patten et al. 2012)
<i>CHD8</i>	CTCF-CHD8 has a role in insulation and epigenetic regulation at active insulator sites. (Ishihara et al. 2006) CHD8 regulates HOXA2 gene expression negatively (Yates et al. 2010) Coregulator of androgen-responsive transcription (Menon et al. 2010) <i>Xenopus</i> : Duplin regulates Wnt signalling negatively by binding beta-catenin (Sacamoto et al. 2010) CHD8 regulates beta-catenin targeted genes negatively. CHD8 interacts with the WAR complex members (Thompson et al. 2008)	Duplin knockout mice show early embryonic lethality and growth retardation (Nishiyama et al. 2004)
<i>CHD9</i>	It might be involved in differentiation of osteogenic cells (Shur and Benayahu. 2005, Shur et al. 2006)	

Table 2.1. Overview of the functions of the CHD family of proteins.

Most of the malformations present in CHARGE patients have been observed in animal models of mouse, xenopus and zebrafish, e.g craniofacial malformations and heart defects etc

(Bosman et al. 2005, Adams et al. 2007, Hurd et al. 2007, Cleary et al. 2009, Layman et al. 2009, Randall et al. 2009, Bajpai et al. 2010, Bergman et al. 2010, Jacobs-McDaniels & Albertson 2011, Layman et al. 2011, Patten et al. 2012). Recent functional studies could show that CHD7 binding sites have features of enhancer elements (Heintzman et al. 2009). Indeed, a comparative gene expression study in embryonic stem cells (ESCs) derived from wild type, heterozygous and homozygous *CHD7* mutant mice demonstrated that CHD7 binds predominantly to methylated histone H3K4 in enhancer elements and regulates genes in a cell type and stage specific manner (Schnetz et al. 2009, 2010).

Kismet is the ortholog of CHD subgroup III (CHD6-9) members in *Drosophila*. Srinivasan et al. (2008) studied *Kismet* and could demonstrate that it regulates gene transcription by recruiting the ASH1 (Absent, Small or Homeotic 1) and TRX (Trithorax) histone methyltransferases to chromatin.

In addition, a *Chd7* knockdown in *Xenopus* multipotent migratory neural crest cells revealed that crucial transcription factors like *Sox2*, *Slug*, and *Twist* are diminished. Therefore, the authors suggest an important role for CHD7 in gene expression programs for neural crest cell migration and specification (Bajpai et al. 2010). However, a recent study of Randall et al. (2009) demonstrated that a *Chd7* rescue in only neural crest cells cannot correct the phenotype of pharyngeal arch defects, while a *Chd7* rescue in both neural crest cells and in ectoderm could do it. These findings demonstrate the necessity of CHD7 expression in ectoderm.

2.3. Role of CHDs in human diseases

To date, *CHD3*, *CHD4*, *CHD5*, *CHD7* and *CHD8* are known to be involved in human diseases (Table 2.2). In dermatomyositis, which is a connective tissue disease, *CHD3* and *CHD4* have been characterized as autoantigens in inflammation of both muscle and skin (Airio et al. 1995, Ge et al. 1995, Seelig et al. 1995, 1996). *CHD3* is also suggested to play a role in the pathogenesis of Hodgkin's lymphoma by interacting with Ki-1/57 (Lemos et al. 2003), an intracellular phosphoprotein which is a marker for malignant cells in Hodgkin's lymphoma (Schwab et al. 1982, Rhode et al. 1992).

CHD5 is found to be deleted in neuroblastoma and glioma cell lines (Thompson et al. 2003, Law et al. 2005, White et al. 2005). Neuroblastoma is an embryonal malignancy of the sympathetic nervous system arising from neuroblasts. It frequently affects infants, usually under two years old (www.nhs.uk/conditions/Neuroblastoma/Pages/Introduction.aspx). *CHD5* is located on chromosome 1p36.31. Deletions of 1p36 are common in human neuronal,

epithelial and hematopoietic cancers. Bagchi et al. (2007) demonstrated that CHD5 acts as a tumor suppressor that controls proliferation, apoptosis, and senescence.

Recent bioinformatic studies of Neale et al. (2011), O’Roak et al. (2012) and Talkowski et al. (2012) revealed chromosomal rearrangements, nonsense and missense mutations disrupting the *CHD8* in patients with Autism Spectrum Disorders (ASD) and neurodevelopmental disorders (NDD), suggesting a role of *CHD8* in the pathogenesis of these diseases (Neale et al. 2011, O’Roak et al. 2012, Talkowski et al. 2012).

CHD Protein	Disease	Reference
CHD3	Dermatomyositis	Nilasena et al. 1995, Seelig et al. 1995, Seelig et al. 1996
	Hodgkin's lymphoma	Schwab U et al. 1982
CHD4	Dermatomyositis	Nilasena et al. 1995, Seelig et al. 1995, Seelig et al. 1996
CHD5	Neuroblastoma	Thompson et al. 2003, Law et al. 2005, White et al. 2005 Bagchi et al 2007
CHD8	Autism spectrum disorders and NDD	Neale et al. 2011, Talkowski et al. 2012, O’Roak et al. 2012
CHD7	CHARGE Syndrome	Visser et al. 2004, Williams et al.2005
	Kallman syndrome, normosmic IHH	Kim et al. 2008, Jongmans et al. 2009, Bergman et al. 2011a

Table 2.2. Human diseases associated with CHD proteins (Adapted and modified from Marfella & Imbalzano 2007). NDD = neurodevelopmental disorders, IHH = idiopathic hypogonadotropic hypogonadism.

2.4 CHD7 and CHARGE syndrome

CHARGE syndrome is an autosomal dominant inherited disease caused by heterozygous *CHD7* mutations (Vissers et al. 2004). The name “CHARGE” is an acronym describing commonly occurring clinical symptoms like Coloboma, Hear malformation, Atresia of the choanae, Retardation of Growth and development and Genital anomalies (Pagon et al. 1981, Blake et al. 1998, Jongmans et al. 2006, Lalani et al. 2006, Bergman et al. 2011b). Additional symptoms like cleft lip/palate and tracheoesophageal fistula can occur, leading to a high variability in the clinical presentation of CHARGE syndrome patients. Therefore, diagnostic criteria were set up to help clinicians finding the right diagnosis. The currently used criteria for CHARGE syndrome were defined by Blake et al. (1998) and updated by Verloes in 2005.

According to Blake et al. (1998), major criteria are: anomalies of ear (90-100% of patients with *CHD7* mutation), ocular coloboma and/or microphthalmia (80-90%), cranial nerve dysfunction, swallowing and breathing difficulties (70-90%). Minor criteria according to Blake are: genital anomalies, developmental and growth retardation, congenital heart defects, cleft lip/palate, tracheoesophageal fistulas and facial dysmorphism (Horsch & Scheele 2011). If four

main or three main and three minor criteria are present, patients will be clinically diagnosed with CHARGE syndrome. In Verloes's criteria (2005) eight key features are proposed, three major (coloboma, choanal atresia, semicircular canals anomalies) and five minors (rhombencephalic anomalies, hypothalamic-hypophyseal dysfunction, external/middle ear malformations, malformation of mediastinal viscera, and mental retardation). If 2/3 major elements and at least 3/5 minor traits are present, CHARGE can be diagnosed. Verloes also classified CHARGE "borderline phenotypes" in two groups: partial (or incomplete) CHARGE and atypical CHARGE. The diagnosis "partial CHARGE" get those patients who present 2 major and only 1 minor sign, whereas the diagnosis "atypical CHARGE" is given to those patients who have 2 major and no minor, or 1 major and at least 3 minor signs (Verloes 2005).

CHD7 mutations have been found also in patients with Kallman Syndrome (KS) (Table 2.2) (Kim et al. 2008, Jongmans et al. 2009, Bergman et al. 2011a). Kallman syndrome is a clinically and genetically heterogenous disease which combines the absence of puberty (Hypogonadotropic Hypogonadism) with defective sense of smell (hyposmia or anosmia) (Dodé & Hardelin 2009). It is suggested that Kallmann syndrome is a mild variant of the phenotypic spectrum of CHARGE syndrome.

Mutations in the *CHD7* gene are distributed along the coding region, no mutation hotspots could be observed. Most frequent are nonsense and frameshift mutations (approximately 75% of all mutations) followed by missense and splice site mutations (20 % of all mutations). Complete and partial deletions/duplications and chromosomal rearrangements are rarely found in CHARGE syndrome patients (Fig. 2.3) (Janssen et al. 2012).

But not in all clinically diagnosed patients with CHARGE syndrome mutations in the *CHD7* gene were found (Jongmans et al. 2006, Lalani et al. 2006, Bergman et al. 2011a). Depending on different studies and which diagnostic criteria are used, the *CHD7* mutation detection rate is in range of 33-100% for patients suspected of CHARGE syndrome and in average calculated as 58% (Vissers et al. 2004, Aramaki et al. 2006, Felix et al. 2006, Jongmans et al. 2006, Lalani et al. 2006, Sanlaville et al. 2006, Vuorela et al. 2007, Asakura et al. 2008, Wincent et al. 2008, Lee et al. 2009, Wessels et al. 2010). The average detection rate is much higher in patients diagnosed as "typical CHARGE syndrome patients". For instance, Jongmans et al. (2006) found *CHD7* mutations in more than 90% of patients who fulfilled the diagnostic criteria of Blake et al. (1998) and/or Verloes (2005). Therefore, in 10% of typical

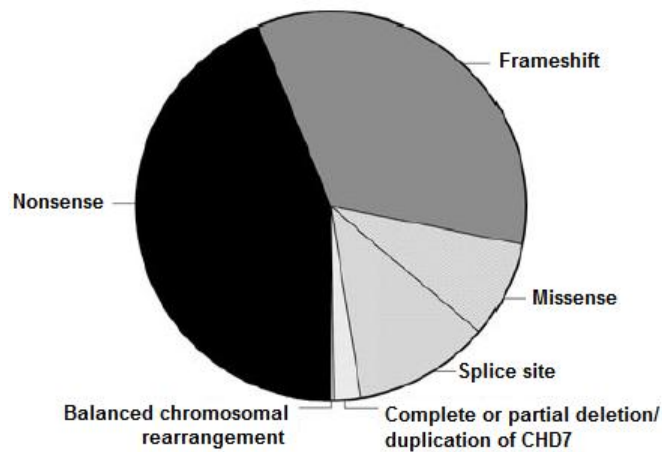


Figure 2.3. Distribution of pathogenic mutation types in the *CHD7* gene. Nonsense and frameshift mutations are in over 75% of the patients with CHARGE syndrome. Missense and splice site mutations occur in 20%. Complete and partial deletions/duplications and chromosomal rearrangements happen rarely (Adapted from Janssen et al. 2012).

CHARGE syndrome patients the molecular cause of the disease is unknown. Similar as in many other autosomal dominant diseases, also in CHARGE syndrome, genetic heterogeneity of more than one gene resulting in the disease is realized. For example, Noonan syndrome is caused by mutations in Ras/MAP kinase pathway genes such as *PTPN11*, *SOS1*, *KRAS*, *RAF1*, *NRAS*, *BRAF* or *MAP2K1* (Tartaglia et al. 2001, Carta et al. 2006, Schubbert et al. 2006, Nava et al. 2007, Razzaque et al. 2007, Roberts et al. 2007, Zenker et al. 2007, Sarkozy et al. 2009, Cirstea et al. 2010), while Cornelia de Lange syndrome is caused by mutations in *NIPBL*, *SMC1A* and *SMC3* (interaction partner of *SMC1A*) (Krantz et al. 2004, Tonkin et al. 2004, Musio et al. 2006, Deardorff et al. 2007).

Therefore, we suggest genetic heterogeneity in CHARGE syndrome. Possibly, mutations in *CHD7* interaction partners lead also to a CHARGE syndrome phenotype. Thus, aim of the study was:

- ❖ to identify and characterize *CHD7* interaction partners in order to understand the genetic basis behind CHARGE syndrome
 - Identification, validation and characterization of exact interacting area of *CHD7* and *CHD8*
 - What is the influence of some missense mutations of *CHD7* to its' interacting capacity to *CHD8*

- Identification of a novel interacting member of the CHD7-CHD8 complex by SILAC (Stable isotope labeling by amino acids in cell culture) and mass-spectrometry approach
- Characterization of FAM124B protein, a novel hitherto unknown interacting member of CHD7 and CHD8 containing complex.

3. Results

3.1 CHD8 interacts with CHD7, a protein which is mutated in CHARGE syndrome

3.2 Identification and characterization of FAM124B as a novel component of a CHD7 and CHD8 containing complex

Each chapter within the results starts with a brief description of the aims of the particular manuscript in context of the complete thesis, the status of the manuscript, and the author's contribution to the work.

3.1 CHD8 interacts with CHD7, a protein which is mutated in CHARGE syndrome

In this part of my thesis, we identified CHD8, another member of the CHD family of proteins, as an interaction partner of CHD7. *CHD7* mutations are found in two-third of patients with CHARGE syndrome. Because of the information that some hereditary diseases are caused by alterations in several genes (genetic heterogeneity) of whom some of the gene products interact with each other, we studied interaction partners of CHD7. We used a part of CHD7 (amino acid 1593-2183) for a yeast two hybrid library screen and found CHD8 (amino acid 1789-2091) as a potential interaction partner. The exact interacting area of both CHD proteins was identified by direct yeast two hybrid. The interaction of CHD7 and CHD8 was confirmed by direct yeast two-hybrid, co-immunoprecipitation and bimolecular fluorescence complementation assays. Furthermore, we studied the influence of 3 known (p.His2096Arg, p.Val2102Ile and p.Gly2108Arg) and one newly identified missense mutation (p.Trp2091Arg) of the *CHD7* gene on the CHD7 and CHD8 interaction. Therefore, we performed direct Y2H and CoIP experiments. Interestingly, the CHD7–CHD8 interaction was disrupted by the missense mutations p.Trp2091Arg, p.His2096Arg and p.Gly2108Arg in the direct Y2H experiment, while no influence on the CHD7-CHD8 binding capacity could be observed in Co-IP studies. We explained the different findings of direct Yeast two hybrid and Co-IP results in that way that with Yeast two hybrid experiments a direct interaction between two proteins could be tested while Co-IPs cleaned up a whole complex and possible linker proteins can bridge the mutated area. In addition, twenty five CHD7 negative CHARGE patients were screened for CHD8 mutations. But no mutation could be detected in the candidate gene CHD8 in our patients. As a result we hypothesized that CHD7 and CHD8 interact directly and indirectly via linker proteins. Further characterization of the complexes might help to better understand the pathogenesis of CHARGE syndrome.

Tserendulam Batsukh, Lasse Pieper, Anna M. Koszucka, Nina von Velsen, Sigrid Hoyer-Fender, Miriam Elbracht, Jorieke E.H. Bergman, Lies H. Hoefsloot, Silke Pauli

Status: Published in *Human Molecular Genetics* (Impact Factor 8.058). Volume 19, No. 14, 2010, pp.2858–2866, (doi:10.1093/hmg/ddq189)

Author contributions to the work:

1. **Tserendulam Batsukh:** Performed direct yeast two hybrid and Co-Immunoprecipitation experiments; made the constructs of 4 missense mutations in

pGBKT7-CHD7 and Co-IP constructs pCMV-Ha-CHD7 (wild type and mutated) and pCMV-Myc-CHD8; involved in manuscript preparation.

2. Lasse Pieper: performed BiFC-assay and made the constructs of pGBKT7-CHD7 wildtype and pGBKT7-CHD8 wildtype; performed direct Y2H experiments.
3. Anna M.Koszucka: performed the yeast two hybrid library screening.
4. Nina von Velsen: performed the *CHD8* mutational analysis in *CHD7* mutation negative CHARGE patients.
5. Sigrid Hoyer-Fender: generated the BiFC assay vectors FPCA-V1 and FPCA-V2 from pEGFP-N1 vector (BD-Bioscience).
6. Miriam Elbracht: patient care; providing patient data and DNA samples
7. Jorieke E.H. Bergman: patient care; providing patient data and DNA samples
8. Lies H. Hoefsloot: patient care; providing patient data and DNA samples
9. Silke Pauli: Concept and research design; interpretation of the results and preparation of the manuscript.

CHD8 interacts with CHD7, a protein which is mutated in CHARGE syndrome

Tserendulam Batsukh¹, Lasse Pieper¹, Anna M. Koszucka^{1,3}, Nina von Velsen¹, Sigr d Hoyer-Fender², Miriam Elbracht⁴, Jorieke E.H. Bergman⁵, Lies H. Hoefsloot⁶ and Silke Pauli^{1,*}

¹Institute of Human Genetics, University of G ttingen, 37073 G ttingen, Germany, ²Johann-Friedrich-Blumenbach Institute of Zoology and Anthropology-Developmental Biology, University of G ttingen, 37077 G ttingen, Germany, ³Department of Biochemistry, University of Erlangen-N rnberg, 91058 Erlangen, Germany, ⁴Institute of Human Genetics, RWTH Aachen University, 52074 Aachen, Germany, ⁵Department of Genetics, University Medical Centre Groningen, University of Groningen, 9700 RB Groningen, The Netherlands and ⁶Department of Human Genetics, Institute of Genetic and Metabolic Disease, Radboud University Nijmegen Medical Center, 6500 HB Nijmegen, The Netherlands

Received February 25, 2010; Revised April 5, 2010; Accepted May 5, 2010

CHARGE syndrome is an autosomal dominant disorder caused in about two-third of cases by mutations in the *CHD7* gene. For other genetic diseases e.g. hereditary spastic paraplegia, it was shown that interacting partners are involved in the underlying cause of the disease. These data encouraged us to search for CHD7 binding partners by a yeast two-hybrid library screen and CHD8 was identified as an interacting partner. The result was confirmed by a direct yeast two-hybrid analysis, co-immunoprecipitation studies and by a bimolecular fluorescence complementation assay. To investigate the function of *CHD7* missense mutations in the CHD7–CHD8 interacting area on the binding capacity of both proteins, we included three known missense mutations (p.His2096Arg, p.Val2102Ile and p.Gly2108Arg) and one newly identified missense mutation (p.Trp2091Arg) in the *CHD7* gene and performed both direct yeast two-hybrid and co-immunoprecipitation studies. In the direct yeast two-hybrid system, the CHD7–CHD8 interaction was disrupted by the missense mutations p.Trp2091Arg, p.His2096Arg and p.Gly2108Arg, whereas in the co-immunoprecipitation studies disruption of the CHD7–CHD8 interaction by the mutations could not be observed. The results lead to the hypothesis that CHD7 and CHD8 proteins are interacting directly and indirectly via additional linker proteins. Disruption of the direct CHD7–CHD8 interaction might change the conformation of a putative large CHD7–CHD8 complex and could be a disease mechanism in CHARGE syndrome.

INTRODUCTION

CHARGE syndrome (OMIM 214800) is an autosomal dominant malformation syndrome. The disorder is characterized by variable combinations of coloboma, heart defects, atresia of the choanae, retarded growth and development, genital hypoplasia, ear anomalies and deafness (1–3). Additional features such as cranial nerve palsy, semicircular canal agenesis, cleft lip/palate, tracheo-oesophageal fistula and renal anomalies are described (4–6).

Mutations in the *CHD7* gene are the major cause of CHARGE syndrome (4,5,7–10). A large cohort of patients, who had received the clinical diagnosis CHARGE syndrome, was tested for *CHD7* mutations and the clinical spectrum was studied. Prominent differences in the phenotype could not be observed between the mutation-positive and the mutation-negative groups (4).

CHD7 belongs to the CHD (chromodomain helicase DNA binding) family of proteins, which share the combination of two N-terminal chromodomains, followed by a

*To whom correspondence should be addressed at: Institute of Human Genetics, Heinrich-D lker-Weg 12, D-37073 G ttingen, Germany. Tel: +49 551399016; Fax: +49 551397567; Email: spauli@gwdg.de

SWI2/SNF2-like ATPase/helicase domain (11–13). The CHD group can be further divided into three subgroups according to sequence similarities and additional functional domains. CHD7 belongs together with CHD6, CHD8 and CHD9 to subgroup III. Distinctive features of this subgroup are the presence of three conserved regions (CR1–CR3), a SANT domain and two BRK domains (14,15). To date, the molecular functions of subgroup III members are poorly understood.

CHD family members are involved in chromatin remodelling as it was shown for CHD1 (14,16). Alterations in chromatin structure are important for the regulation of gene transcription, DNA repair, replication and recombination. Chromatin remodelling enzymes can be divided into two categories, those that alter chromatin structure by histone modification (17) and those that alter the histone-DNA contacts within the nucleosome by using energy of ATP hydrolysis (18). Members of the CHD group belong to the SNF2 superfamily of ATP-dependent chromatin remodelers (12,15). For most SNF2-like ATPases, it was shown that they are components of large multi-subunit complexes. For some CHD family members, several protein–protein interactions have been described. Chd1 of *S. cerevisiae* is a component of the two highly homologous acetyltransferase complexes SAGA and SLIK (19), CHD3 acts together with CHD4 as components of the nucleosome-remodelling and histone deacetylase (NuRD) complex (14). CHD8 interacts directly with WDR5 (20), a component of the histone H3 Lys-4 methyltransferase MLL complex (21).

CHD7 interacts *in vitro* with its chromodomains with methylated forms of H3K4 (22). It was shown that during mouse ES cell differentiation, the CHD7 sites change with the H3K4 pattern and the CHD7 sites are predominantly located distal to transcription start sites (22). Because of these observations, it was suggested that CHD7 plays a role in enhancer mediated transcription of key target genes (22).

On the basis of sequence similarities between CHD7 and other CHD members, it can be suggested that CHD7 acts in a large multisubunit complex. Therefore, binding partners of CHD7 could be candidate genes for CHARGE syndrome.

For other diseases, e.g. hereditary spastic paraplegia (HSP), it was shown that interacting partners are involved in the underlying cause of the disease. Mutations in spastin (SPG4) and in its binding partner ZFYVE27 (SPG33) lead to HSP (23). In Cornelia de Lange syndrome, mutations in the cohesion regulators NIPBL and ESCO2 and in different components of the cohesion complex (SMC1A and SMC3) were reported (24). These data from the literature encouraged us to search for CHD7 binding partners by a yeast two-hybrid library screen using a part of CHD7 as bait. In our yeast two-hybrid library screen, we identified CHD8, another CHD subgroup III member, as a specific interaction partner of CHD7. We confirmed this result by direct yeast two-hybrid studies, co-immunoprecipitation experiments and by a bimolecular fluorescence complementation assay (BiFC-Assay). Furthermore, we characterized the interacting part of CHD7 and CHD8, introduced four missense mutations in the CHD7 interacting part and performed direct yeast two-hybrid experiments and co-immunoprecipitation studies. In the yeast two-hybrid system, the CHD7–CHD8 interaction was disrupted by three missense mutations (p.Trp2091Arg, p.His2096Arg and p.Gly2108Arg), whereas in the co-immunoprecipitation

studies no disruption of the CHD7–CHD8 interaction by the mutations could be observed. These findings indicate that CHD7 and CHD8 are interacting directly and indirectly via additional linker proteins. Loss of the direct CHD7–CHD8 interaction might change the conformation of a possible CHD7–CHD8 containing complex, which might be a disease mechanism in CHARGE syndrome.

RESULTS

Identification of CHD8 as a potential binding partner of CHD7 by Y2H library screening

To identify CHD7 interacting proteins, we screened a human foetal brain cDNA library (BD Clontech). The plasmid CHD7-CR1-3-pGBKT7 (amino acids 1591–2181) containing the three conserved regions CR1–CR3 and the SANT domain of the CHD7 protein was used as bait. We screened 3.34×10^7 clones and identified 21 clones, which were able to grow in selective media. Eighteen clones were also positive for α -galactosidase expression. From these clones, plasmids were isolated and sequenced. Eleven clones contained parts of the coding region of CHD8. One clone showed a correct reading frame, whereas in 10 clones the reading frame of the CHD8 region to the GAL4 activation domain was incorrect. The correct clone encodes the protein region from amino acids 1789–2091 (NP_065971.2) of the CHD8 protein and this clone was used in further experiments.

Confirmation of the CHD7–CHD8 interaction by direct Y2H experiments

To specify the CHD7–CHD8 interacting area, we performed direct Y2H experiments using the plasmids CHD7-CR1-pGBKT7 (amino acids 1593–1768), CHD7-CR2-pGBKT7 (amino acids 1701–1948) and CHD7-CR3-pGBKT7 (amino acids 1950–2172) as bait, respectively. These plasmids contain either the conserved region 1, or 2 or 3 (Figs 1 and 2A). CHD7–CHD8 interaction could only be observed in the part-spanning amino acids 1950–2172, containing the conserved region 3 (CR3) of the CHD7 protein (Fig. 2A). The three known missense mutations p.His2096Arg, p.Val2102Ile and p.Gly2108Arg (4,25,26) identified in CHARGE patients are located within this CHD7–CHD8 interacting area. Furthermore, we identified in a patient with atypical CHARGE syndrome another new missense mutation (p.Trp2091Arg) which resides also in this region. We created four new bait constructs for the interacting region (amino acids 1950–2172), each containing one of these missense mutations (CHD7-His2096Arg-pGBKT7, CHD7-Val2102Ile-pGBKT7, CHD7-Gly2108Arg-pGBKT7 and CHD7-Trp2091Arg-pGBKT7, Fig. 1) and performed direct yeast two-hybrid experiments with the CHD8-pGADT7-Rec plasmid as prey. The CHD7–CHD8 interaction was disrupted by the missense mutations p.Trp2091Arg, p.His2096Arg and p.Gly2108Arg, but not by the missense mutation p.Val2102Ile.

To narrow down the interacting area of CHD8, we created two new prey constructs, CHD8-pGADT7-1 (amino acids 1789–1983) and CHD8-pGADT7-2 (amino acids 1985–2091). The CHD8-pGADT7-2 includes the first BRK domain, while

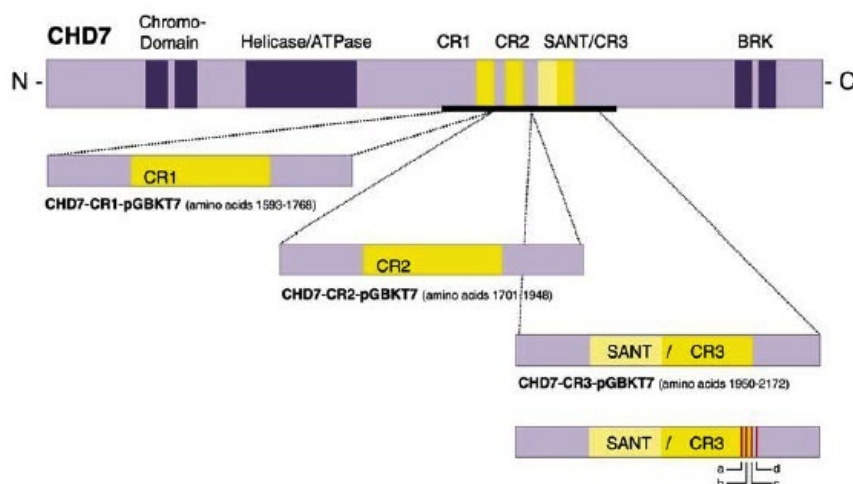


Figure 1. Schematic overview of the CHD7 protein and the constructs used as baits in the yeast two-hybrid assay. CHD7 consists of two N-terminal chromo-domains, followed by a SWI2/SNF2-like ATPase/helicase domain, three conserved regions (CR1–CR3), a SANT domain and two BRK domains. The plasmids CHD7-CR1-pGBKT7, CHD7-CR2-pGBKT7 and CHD7-CR3-pGBKT7 divide the CHD7-CR1-3-pGBKT7 bait plasmids (black lane spanning amino acids 1591–2181) in three different parts. The bait plasmids (a) CHD7-Trp2091Arg-pGBKT7, (b) CHD7-His2096Arg-pGBKT7, (c) CHD7-Val2102Ile-pGBKT7 and (d) CHD7-Gly2108Arg-pGBKT7 were generated by introducing one of the missense mutations (Trp2091Arg, His2096Arg and Val2102Ile/Gly2108Arg) into the CHD7-CR3-pGBKT7 part spanning the amino acids 1950–2172 of the CHD7 protein.

CHD8-pGADT7-1 does not code for a known protein domain. We performed again a direct yeast two hybrid with all four CHD7 plasmids containing missense mutations and with the plasmid CHD7-CR3-pGBKT7 as positive control and the plasmid CHD7-CR1-pGBKT7 as negative control. We identified the CHD7–CHD8 interaction within the CHD8 part spanning the amino acids 1789–1983. This result supports our observation that the missense mutations p.Trp2091Arg, p.His2096Arg and p.Gly2108Arg disrupt the interaction (Fig. 2B).

CHD7–CHD8 interaction analysed by bimolecular fluorescence complementation assay (BiFC-Assay)

To confirm the CHD7–CHD8 interaction, we performed a BiFC-Assay. The principle of this technique is based on the observation that splitted N- and C-terminal EGFP fragments do not emit a bright fluorescence. If the two splitted non-functional EGFP halves are fused to proteins that interact, they can functionally complement and emit a bright fluorescence (27). HeLa cells were either transiently co-transfected with the plasmids CHD7-FPCA-V1 and CHD8-FPCA-V2 or transfected with a single plasmid as negative control. After 24 h, the cells were analysed for the presence of fluorescence complementation. As shown in Figure 3, we observed in co-transfected cells a bright green fluorescence in the nucleus. Single-transfected cells did not show any fluorescence signal. Because fluorescence complementation was only observed in CHD7–CHD8 co-transfected cells, these results confirm the CHD7–CHD8 interaction shown in the yeast two-hybrid system.

CHD8 co-immunoprecipitates with CHD7

To further verify the CHD7–CHD8 interaction, we performed co-immunoprecipitation studies in HeLa cells. After transfection

and cell culture for 24 h, the cells were lysed and protein extracts were prepared. A part of the CHD7 protein (amino acids 1593–2178) was fused to an HA-tag, while a part of the CHD8 protein (amino acids 1789–2302) was fused to a c-Myc tag. The CHD7 part fused to the HA-tag was estimated to produce a ~70 kDa protein fragment, while the CHD8 part labelled with a c-Myc tag was calculated to have a size of approximately 61 kDa. Using a c-Myc antibody for precipitation, we detected with an HA antibody a ~70 kDa band corresponding to the estimated size of the CHD7 part (Fig. 4A). The reciprocal experiment, precipitation with an HA antibody and detection with the c-Myc antibody lead to a specific band of about 68 kDa in size (Fig. 4B). To further confirm the specificity of the observed bands, we precipitated with c-Myc and detected with the c-Myc antibody again the specific 68 kDa band, strongly supporting that this band corresponds to the CHD8-c-Myc fusion protein. The reciprocal experiment was also performed (Fig. 4C and D).

To investigate the influence of the missense mutations in the CHD7 gene in the CHD7–CHD8 interacting area in an *in vivo* system, we performed co-immunoprecipitation studies with the CHD7-His2096Arg-pCMV-HA, CHD7-Val2102Ile-pCMV-HA, CHD7-Gly2108Arg-pCMV-HA and CHD7-Trp2091Arg-pCMV-HA plasmids, respectively. Interestingly, in all four cases, the mutated CHD7 part was co-immunoprecipitated with the CHD8 part (Fig. 4E and F).

DISCUSSION

Mutations in the CHD7 gene lead to CHARGE syndrome, which is a well-known congenital malformation syndrome. The CHD7 protein belongs to the CHD (chromodomain helicase DNA-binding domain) family of ATP-dependent chromatin remodelling enzymes. The human CHD family consists of

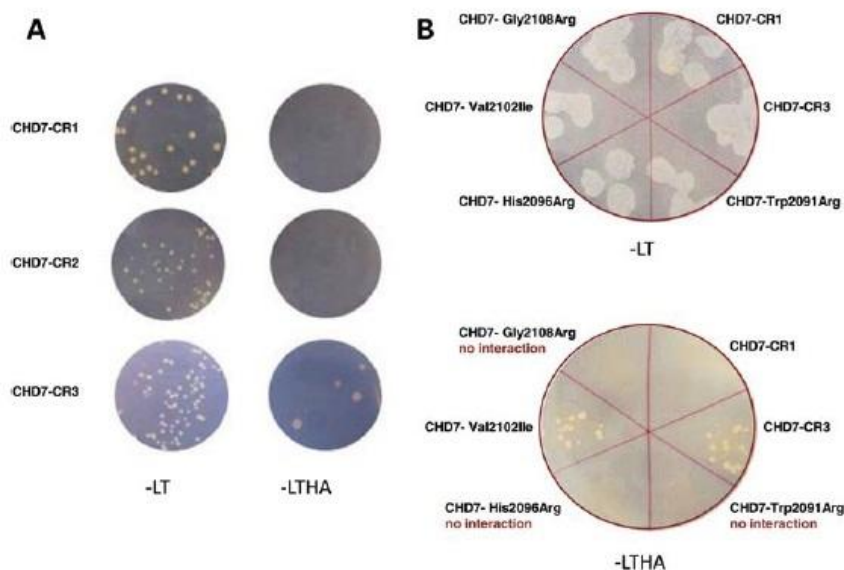


Figure 2. Yeast two-hybrid assay. (A) Direct yeast two-hybrid experiment with the constructs CHD7-CR1-pGBKT7, CHD7-CR2-pGBKT7 and CHD7-CR3-pGBKT7 as baits, which divide the CHD7-CR1-3-pGBKT7 bait plasmids (amino acids 1591–2181) in three different parts. CHD7–CHD8 interaction takes place in the part spanning amino acids 1950–2172, containing the conserved region 3 (CR3) of the CHD7 protein. (B) Direct yeast two-hybrid experiment with all four CHD7 plasmids containing a missense mutation and the plasmid CHD7-CR3-pGBKT7 as positive control and the plasmid CHD7-CR1-pGBKT7 as negative control. The CHD8 plasmid CHD8-pGADT7-1 (amino acids 1789–1983) was used as prey. The CHD7–CHD8 interaction was disrupted by the missense mutations p.Trp2091Arg, p.His2096Arg and p.Gly2108Arg.

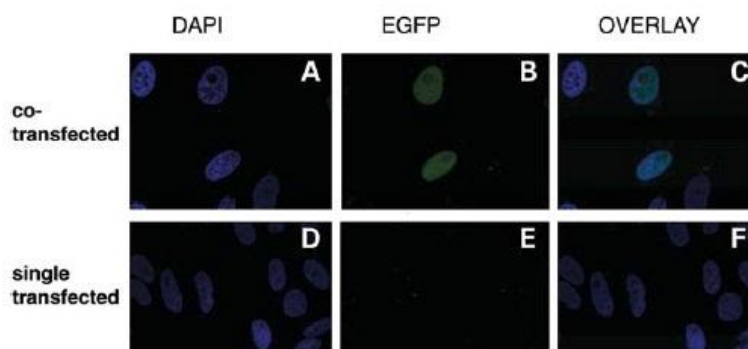


Figure 3. BiFC-Assay. HeLa cells were transiently co-transfected with the plasmids CHD7-FPCA-V1 (spanning CHD7 amino acids 1596–2178) and CHD8-FPCA-V2 (spanning CHD8 amino acids 1791–2302). (A) Cell nuclei were stained with DAPI (blue), (B) co-transfected cells showed a bright green fluorescent signal demonstrating CHD7–CHD8 interaction by fluorescence complementation and with localization in the nucleus, (C) overlay of (A) and (B). As negative control HeLa cells were transfected with a single construct (D–F).

nine members, which can be grouped in three subgroups based on homologies in the sequence and domain architecture (12). Chromatin remodelling is an important mechanism for the regulation of gene expression and it is known that chromatin remodelling is carried out by multi-protein complexes (28). It can be hypothesized that CHD7 is also a component of a multisubunit complex. Identification and characterization of CHD7 binding proteins might provide insights into the molecular mechanism in which CHD7 is involved.

In this study, we identified CHD8, another subgroup III member of the CHD family of proteins, as an interacting

partner of CHD7 by a yeast two-hybrid library screen. The specificity of the interaction was confirmed by direct yeast two-hybrid studies, co-immunoprecipitation experiments and by a BiFC-Assay. CHD8 consists, such as CHD7, of two N-terminal chromodomains, followed by a SWI2/SNF2-like ATPase/helicase domain and specific for subgroup III members of three conserved regions (CR1–CR3), a SANT domain and two BRK domains (12). It has been shown that CHD8 interacts with human Staf (ZNF143), a zinc finger transcription factor, which controls the expression of the U6 gene (29). Furthermore, CHD8 was co-purified with components of

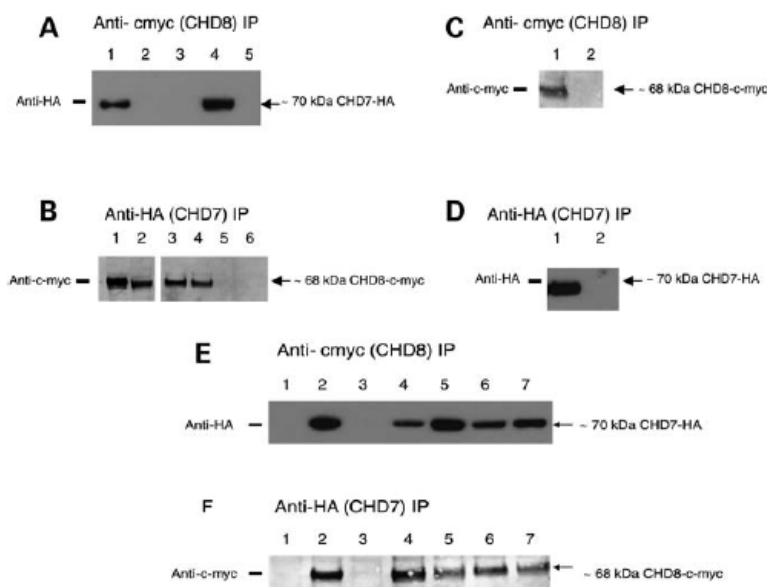


Figure 4. Co-immunoprecipitation of CHD7 and CHD8. A part of the CHD7 protein (amino acids 1593–2178) was fused to an HA-tag, while a part of the CHD8 protein (amino acids 1789–2302) was fused to a c-Myc tag. (A) Using a c-Myc antibody for precipitation, we detected a ~70 kDa band with an HA antibody corresponding to the estimated size of the CHD7 part (lane 1). Lane 1: co-transfected Co-IP, lane 2: CHD7 single-transfected HeLa cells and CHD7 co-IP as negative control, lane 3: untransfected HeLa cells as negative control, lane 4: co-transfected input, lane 5: untransfected input. (B) The reciprocal experiment, precipitation with an HA antibody and detection with the c-Myc antibody leads to a specific band of approximately 68 kDa. Lane 1: CHD8 input, lane 2: co-transfected input, lanes 3 and 4: co-transfected Co-IP, lane 5: CHD8 single-transfected HeLa cells and CHD8 Co-IP as negative control, lane 6: untransfected HeLa cells as negative control. (C) Precipitation with c-Myc and detection with the c-Myc antibody. Lane 1: co-transfected Co-IP, lane 2: untransfected Co-IP as negative control. A specific 68 kDa band was detected, strongly supporting that this band corresponds to the CHD8-c-Myc fusion protein. (D) The reciprocal experiment. Precipitation with HA and detection with the HA antibody. Lane 1: co-transfected Co-IP, lane 2: untransfected Co-IP as negative control. A specific ~70 kDa band, corresponding to the CHD7-HA fusion protein could be detected. (E and F) Investigation of the influence of four missense mutations in the CHD7 gene on the CHD7-CHD8 interaction by co-immunoprecipitation studies. Lane 1: untransfected Co-IP as negative control, lane 2: wild-type co-transfected Co-IP as positive control, lane 3: CHD7 single-transfected HeLa cells and CHD7 co-IP as negative control, lane 4: co-transfected Co-IP with the mutated CHD7-Trp2091Arg-pCMV-HA plasmid, lane 5: co-transfected Co-IP with the mutated CHD7-His2096Arg-pCMV-HA plasmid, lane 6: co-transfected Co-IP with the mutated CHD7-Val2102Ile-pCMV-HA plasmid, lane 7: co-transfected Co-IP with the mutated CHD7-Gly2108Arg-pCMV-HA plasmid. (E) Precipitation with c-Myc and detection with the HA antibody. (F) Precipitation with HA and detection with the c-Myc antibody.

the MLL1–WDR5 complex (20,30) and was found to interact directly with beta-catenin and playing a role in the regulation of beta-catenin target genes (20). Mouse Chd8 was shown to bind via its BRK domains Ctf, an insulator binding protein involved in insulation and epigenetic regulation (31). With its tandem chromodomains, CHD8 binds *in vitro* specifically to histone H3 di-methylated at lysine 4 (32). CHD8 was also found to be associated with the elongating form of RNA polymerase II and to control the expression of cyclin E2 and thymidylate synthetase (32).

In *Drosophila melanogaster*, *kismet* is the only gene related to the subgroup III members of the CHD gene family. *Kismet* encodes for two isoforms, a large protein with a molecular weight of 574 kDa (KIS-L) and a small isoform of 225 kDa (KIS-S) (33,34). Kis-L is highly related to the human CHD7 or other CHD subgroup III members. Kis-L belongs to the trithorax group and was shown to play an important role in body segmentation and segment identity of *Drosophila* larvae (33). Furthermore, it was suggested that kis-L is involved in an early step of transcriptional elongation by RNA Polymerase II (Pol II), because it is co-localized with most RNA-Polymerase II sites (32,35,36). In *kismet* mutant larvae, a reduction in the levels of elongating Pol II and the

elongation factors SPT6 and CHD1 was observed (35). In contrast to *Drosophila*, CHD8 depletion in mammals does not reduce in general the levels of Ser2-phosphorylated RNA Polymerase II (32). It was suggested that in mammals, the function of *kismet* is overtaken by several subgroup III members (CHD6–CHD9) and that depletion of one subgroup III member leads to a gene-specific and not a general effect (32). In the present study, we could show that two subgroup III members, namely CHD7 and CHD8, interact. We hypothesize that CHD7 and CHD8 together build a core component of a complex with similar functions such as *kismet*. Interestingly, the situation that two members of the same subgroup interact was found for the subgroup II members CHD3 and CHD4. In *Drosophila*, there is only a single gene related to subgroup II, named Mi-2. This *Drosophila* gene encodes also for two transcripts (15,37). In mammals, CHD3 and CHD4 were found to build together a core component of the NuRD complex (14,38).

Mutations in CHD7 interacting genes, which are involved in the same molecular mechanism, may also cause CHARGE syndrome. In three children with developmental delay, cognitive impairment and similar dysmorphic features a submicroscopic deletion on chromosome 14q11.2 was detected (39).

The minimal overlapping region of approximately 35 kb includes only the *SUPT16H* and the *CHD8* gene, leading to the suggestion that haploinsufficiency of *CHD8* plays a role in the patient's phenotype (39). Because the patient's phenotype is different from the phenotype seen in CHARGE syndrome patients, we suggested that the heterozygous deletion of *CHD8* is not a possible disease mechanism in CHARGE syndrome. However, nucleotide alterations (e.g. missense mutations) in a gene can lead to a more severe or different phenotype than gross deletions, because an aberrant protein can disturb the function of its interacting partner. Therefore, we performed *CHD8* sequence analysis in 25 patients suspected of CHARGE syndrome, where the sequence and MLPA analysis of the *CHD7* gene revealed no mutations or deletions/duplications. No pathogenic mutations in *CHD8* were identified (data not shown). However, small exon deletions or duplications in the *CHD8* gene were not excluded by the sequence analysis. Our results could neither indicate that *CHD8* mutations are causative for CHARGE syndrome, nor could *CHD8* be excluded as a candidate gene in the pathogenesis of this disease. Further investigations of the *CHD8* gene in a larger cohort of *CHD7* negative CHARGE patients are needed to clarify this aspect. To investigate the effect of *CHD7* missense mutations in the *CHD7*-*CHD8* interacting sequence on the binding capacity of both proteins, three known *CHD7* missense mutations were included (p.His2096Arg, p.Val2102Ile and p.Gly2108Arg) (4,25,26) as well as a new identified missense mutation (p.Trp2091Arg) in the *CHD7* gene recently found by our group in a CHARGE patient. We performed direct yeast two-hybrid analyses and co-immunoprecipitation studies. In the direct yeast two-hybrid system, the *CHD7*-*CHD8* interaction was disrupted by the missense mutations, p.Trp2091Arg, p.His2096Arg and p.Gly2108Arg. The missense mutation p.Gly2108Arg was described in two different families with five affected members (26). From the five affected members, only one fulfilled the diagnostic criteria for CHARGE syndrome while the others showed a very mild phenotype. Our patient with the missense mutation p.Trp2091Arg is also affected with atypical CHARGE syndrome. She has bilateral coloboma and microphthalmia of the left eye, microcephaly, mental retardation and unilateral deafness.

In contrast to the results obtained in the direct yeast two-hybrid experiments, co-immunoprecipitation studies did not reveal a disruption of the *CHD7*-*CHD8* interaction by the mutations described above. This discrepancy strongly indicates that *CHD7* and *CHD8* might be components of a larger complex. Direct yeast two-hybrid studies analyse the direct interaction of two proteins. A complex of proteins with different influences on binding partners, e.g. bridging proteins, cannot be studied by this method. However, co-immunoprecipitation studies can detect linker proteins between *CHD7* and *CHD8* which stabilizes a possible protein complex. For example, it was shown that mouse *Chd8* binds *Ctcf* via its BRK domains (31). For human *CHD7*, there was also an interaction with *CTCF* via its BRK domains observed (40). We suggest that *CHD7* and *CHD8* are interacting directly (as we showed by our yeast two-hybrid results) and indirectly via additional linker proteins such as *CTCF*. Further studies are needed to discover such linker pro-

teins, which could influence the severity of *CHD7* mutations or which could be another underlying cause of CHARGE syndrome, if present in a mutated condition.

MATERIALS AND METHODS

Yeast two-hybrid analysis

Yeast two-hybrid screen. For the identification of putative *CHD7* interacting partners, we used the MATCHMAKER™ human foetal brain cDNA library (BD, Clontech), which was pre-transformed into the yeast strain Y187. The bait plasmid *CHD7*-CR1-3-pGBKT7 was constructed by subcloning a fragment of *CHD7* (amino acids 1591–2181, containing the area of conserved regions 1–3) into the pGBKT7 vector (Clontech) in frame to the GAL4 DNA-binding domain. The correct reading frame and the correct sequence were confirmed by sequencing the plasmid.

The bait plasmid *CHD7*-CR1-3-pGBKT7 was transformed into AH109 yeast strain cells and was tested for toxicity and autoactivation of the bait reporter genes. No toxicity for the yeast cells and no self-activation of the bait reporter genes could be observed. The AH109 yeast strain cells containing the bait plasmid were mated with the MATCHMAKER library Y187 cells. After mating, diploids were plated on leucine-tryptophan-histidine-adenine lacking SD medium (-LTHA-SD medium) plates. Colonies growing on the -LTHA-SD medium plates were picked and spread on -LTHA-SD medium plates containing X- α -Gal. Blue colonies were cultured for plasmid isolation, which was carried out using the YEASTMAKER™ Yeast Plasmid Isolation Kit (BD, Clontech) according to the manufacturer's instructions. Isolated plasmids were subcloned into competent *E. coli* cells. Transformants were spread out on Ampicillin containing plates for the selection of clones bearing the pGADT7-Rec library vector. Inserts of the pGADT7-Rec vector were characterized by sequence analysis.

To avoid false positive results, the candidate plasmid *CHD8*-pGADT7-Rec (amino acids 1789–2091) was retransformed into AH109 yeast cells together with the empty bait vector pGBKT7 and selected on -LTHA-SD plates. No colonies were able to survive, indicating lack of self-activation of the system by the *CHD8*-pGADT7-Rec plasmid.

Direct yeast two hybrid. Direct yeast two-hybrid analysis was performed for confirmation of the *CHD7*-*CHD8* interaction. For this purpose, the identified *CHD8*-pGADT7-Rec prey plasmid and the *CHD7*-CR1-3-pGBKT7 bait plasmid were co-transformed into AH109 yeast strain cells. The co-transformants were grown on -LTHA-SD medium plates for transformation control and the interaction was verified on selective -LTHA-SD medium plates.

To specify the *CHD7*-*CHD8* interacting area, we generated three constructs *CHD7*-CR1-pGBKT7, *CHD7*-CR2-pGBKT7 and *CHD7*-CR3-pGBKT7 which divide the *CHD7*-CR1-3-pGBKT7 bait plasmids (amino acids 1591–2181) in three different parts (Figs 1 and 2A). The first fragment consists of the CR1 region and corresponds to amino acids 1593–1768. The second fragment spans the CR2 part (amino acids 1701–1948), while the third fragment consists

of the SANT domain and the CR3 region, corresponding to amino acids 1950–2172. These CHD7 fragments were subcloned into the pGBKT7 vector (Clontech) and the three constructs CHD7-CR1-pGBKT7, CHD7-CR2-pGBKT7 and CHD7-CR3-pGBKT7 were used as baits for direct yeast two-hybrid analysis.

To study the effect of known CHD7 missense mutations on the CHD7–CHD8 interaction, the bait plasmids CHD7-His2096Arg-pGBKT7, CHD7-Val2102Ile-pGBKT7, CHD7-Gly2108Arg-pGBKT7 and CHD7-Trp2091Arg-pGBKT7 were generated by introducing one of the missense mutations (His2096Arg, Val2102Ile, Gly2108Arg and Trp2091Arg) into the CHD7 region spanning amino acids 1950–2172. An overview of the used plasmids is given in Figure 1.

To narrow down the interacting area of CHD8, we created two prey constructs, CHD8-pGADT7-1 (amino acids 1789–1983) and CHD8-pGADT7-2 (amino acids 1985–2091) dividing the CHD8 interacting area found in the initial library screen. All plasmids were checked for the correct sequence and reading frame by sequence analysis.

Cell culture

HeLa cells were cultured in Dulbecco's modified Eagle's media (DMEM) (PAN BIOTECH), supplemented with 10% foetal calf serum (PAN BIOTECH) and 1% penicillin/streptomycin (PAN BIOTECH). For transfection, cells were plated into two chamber culture slides (BD Falcon) and 50 ml flasks (Sarstedt). After 24 h when the cells' confluence reached about 70–80%, they were transfected with the plasmid DNA using OptiMEM serum-free medium (Gibco) and Lipofectamine 2000 transfection reagent (Invitrogen) according to the manufacturer's instruction. After transfection, cells were grown for additional 24 h in DMEM.

Co-immunoprecipitation

For co-immunoprecipitation studies, we generated the plasmid CHD7-CR1-3-pCMV-HA by cloning a part of the *CHD7* gene (amino acids 1593–2178, NP_060250.2) in frame to the hemagglutinin (HA) epitope tag into the pCMV-HA vector (Clontech). A part of the *CHD8* gene (amino acids 1789–2302, NP_065971.2) was cloned in frame to the N-terminal c-Myc epitope tag into the pCMV-Myc vector (Clontech) for the construction of the CHD8-pCMV-c-Myc plasmid. The CHD7 missense mutations (His2096Arg, Val2102Ile, Gly2108Arg and Trp2091Arg) were introduced into the CHD7-CR1-3-pCMV-HA plasmid, leading to the four new plasmids CHD7-His2096Arg-pCMV-HA, CHD7-Val2102Ile-pCMV-HA, CHD7-Gly2108Arg-pCMV-HA and CHD7-Trp2091Arg-pCMV-HA. The correct reading frame and sequence was confirmed by sequence analysis.

HeLa cells cultured in 50 ml flasks (Sarstedt) were transiently co-transfected with one of the CHD7 constructs (wild-type plasmid CHD7-CR1-3-pCMV-HA or mutant constructs) and CHD8-pCMV-c-Myc. After incubation for 24 h at 37°C, transfected cells were washed twice with ice-cold DPBS. After washing, the cells were treated for 30 min on ice with 400 µl lysis buffer (Immunoprecipitation lysis buffer, Roche). Centrifugation at 14 000g for 20 min was carried out to remove

cell debris. Forty microlitre of total protein extract was used for western blot analysis. When both transfected proteins were detected by western blot analysis, the remaining protein extract which was stored at 4°C was incubated with either 1 µg of monoclonal anti-HA (Roche) or 1:100 diluted anti-c-Myc (Millipore) antibody at 4°C overnight. Eighty microlitre of protein G (Immunoprecipitation lysis buffer, Roche) was added to the immunocomplex and incubated for 2 h at 4°C. Centrifugation at 350 rpm for 3 min was carried out to collect the agarose beads. The beads were washed two times in 500 µl lysis buffer to remove unbound proteins. A resuspension of the beads in NuPAGE LDS Sample buffer (Invitrogen) with 0.1 M DTT followed. After denaturation for 10 min at 75°C, the denaturated beads were loaded onto a 4–12% NuPAGE Bis-Tris gel (Invitrogen). Proteins were immunoblotted with the anti-c-Myc antibody (Millipore) at a dilution of 1:500 or the anti-HA antibody (Roche) at a dilution of 1:1000. The following secondary antibodies were used: alkaline phosphatase labelled anti-mouse antibody produced in goat (SIGMA) was used for anti-c-Myc and horseradish peroxidase labelled anti-rat antibody produced in goat (Thermo Scientific) was used for anti-HA detection.

Bimolecular fluorescence complementation assay (BiFC-Assay)

For the BiFC-Assay, we cloned a part of the *CHD7* gene (amino acids 1596–2178, NP_060250.2) in the FPCA-V1 vector and a part of the *CHD8* gene (amino acids 1791–2302, NP_065971.2) in the FPCA-V2 vector. The FPCA-V1 vector was generated from the pEGFP-N1 vector (BD Bioscience). The FPCA-V1 vector contains a CMV promoter followed by a multiple cloning site in which we introduced the *CHD7* part, a spacer region and the C-terminal end of EGFP (amino acids 158–239). The FPCA-V2 vector, generated from the pQM-Ntag/B plasmid (Abcam, UK), contains a CMV promoter, followed by an E2 tag, the N-terminal part of EGFP (amino acids 1–157), a spacer and the multiple cloning site in which we introduced the *CHD8* part. HeLa cells were co-transfected with 0.5 µg of each construct. After incubation for 24 h at 37°C, the cells were washed with DPBS, fixed with 4% paraformaldehyde and again washed with DPBS. After the washing step, cover slips were attached onto slides using Vectashield mounting solution containing DAPI (4,6-diamidino-2-phenylindole). Fluorescence imaging was performed using the Olympus BX60 microscope (Olympus, Hamburg, Germany).

Mutational analysis

CHD8 analysis was performed in 25 patients suspected of CHARGE syndrome, where the sequence and deletion analysis (MLPA, MRC Holland) of the *CHD7* gene revealed no mutation. The coding sequence of all 37 coding exons and flanking intronic sequences of the *CHD8* gene were analysed by PCR and sequenced in both directions in CHD7 negative CHARGE patients. Primer sequences and PCR conditions are available on request.

The ethical approval was obtained from the Ethics Committee of the Georg-August University Göttingen.

ACKNOWLEDGEMENTS

We thank W. Engel for his support and helpful discussions. We also thank P. Burfeind for careful reading of the manuscript, S. Kaulfuss for her help in microscopy and imaging and M. Steckel for excellent technical assistance.

Conflict of Interest statement. None declared.

FUNDING

This work was supported by the Forschungsförderungsprogramm of the Medical School of the University of Göttingen (to S.P.).

REFERENCES

- Hall, B.D. (1979) Choanal atresia and associated multiple anomalies. *J. Pediatr.*, **95**, 395–398.
- Hittner, H.M., Hirsch, N.J., Kreh, G.M. and Rudolph, A.J. (1979) Colobomatous microphthalmia, heart disease, hearing loss, and mental retardation—a syndrome. *J. Pediatr. Ophthalmol. Strabismus*, **16**, 122–128.
- Pagon, R.A., Graham, J.M. Jr, Zonana, J. and Yong, S.L. (1981) Coloboma, congenital heart disease, and choanal atresia with multiple anomalies: CHARGE association. *J. Pediatr.*, **99**, 223–227.
- Lalani, S.R., Safullah, A.M., Fernbach, S.D., Harutyunyan, K.G., Thaller, C., Peterson, L.E., McPherson, J.D., Gibbs, R.A., White, L.D., Heiner, M. et al. (2006) Spectrum of CHD7 mutations in 110 individuals with CHARGE syndrome and genotype-phenotype correlation. *Am. J. Hum. Genet.*, **78**, 303–314.
- Jongmans, M.C., Admiraal, R.J., van der Donk, K.P., Vissers, L.E., Baas, A.F., Kapusta, L., van Hagen, J.M., Donnai, D., de Ravel, T.J., Veltman, J.A. et al. (2006) CHARGE syndrome: the phenotypic spectrum of mutations in the CHD7 gene. *J. Med. Genet.*, **43**, 306–314.
- Sanlaville, D. and Verloes, A. (2007) CHARGE syndrome: an update. *Eur. J. Hum. Genet.*, **15**, 389–399.
- Vissers, L.E., van Ravenswaaij, C.M., Admiraal, R., Hurst, J.A., de Vries, B.B., Janssen, I.M., van der Vliet, W.A., Huys, E.H., de Jong, P.J., Hamel, B.C. et al. (2004) Mutations in a new member of the chromodomain gene family cause CHARGE syndrome. *Nat. Genet.*, **36**, 955–957.
- Sanlaville, D., Etchevers, H.C., Gonzales, M., Martinovic, J., Clément-Ziza, M., Delezoide, A.L., Aubry, M.C., Felet, A., Chemouny, S., Cruaud, C. et al. (2006) Phenotypic spectrum of CHARGE syndrome in fetuses with CHD7 truncating mutations correlates with expression during human development. *J. Med. Genet.*, **43**, 211–217.
- Aramaki, M., Udaka, T., Kosaki, R., Makita, Y., Okamoto, N., Yoshihashi, H., Oki, H., Nanao, K., Moriyama, N., Oki, S. et al. (2006) Phenotypic spectrum of CHARGE syndrome with CHD7 mutations. *J. Pediatr.*, **148**, 410–414.
- Wincent, J., Holmberg, E., Strömland, K., Soller, M., Mirzaei, L., Djureinovic, T., Robinson, K., Anderlid, B. and Schoumans, J. (2008) CHD7 mutation spectrum in 28 Swedish patients diagnosed with CHARGE syndrome. *Clin. Genet.*, **74**, 31–38.
- Woodage, T., Basrai, M.A., Baxevanis, A.D., Hieter, P. and Collins, F.S. (1997) Characterization of the CHD family of proteins. *Proc. Natl Acad. Sci. USA*, **14**, 11472–11477.
- Flaus, A., Martin, D.M., Barton, G.J. and Owen-Hughes, T. (2006) Identification of multiple distinct Srd2 subfamilies with conserved structural motifs. *Nucleic Acids Res.*, **31**, 2887–2905.
- Flanagan, J.F., Blus, B.J., Kim, D., Clines, K.L., Rastinejad, F. and Khorasanizadeh, S. (2007) Molecular implications of evolutionary differences in CHD double chromodomains. *J. Mol. Biol.*, **369**, 334–342.
- Hall, J.A. and Georgel, P.T. (2007) CHD proteins: a diverse family with strong ties. *Biochem. Cell Biol.*, **85**, 463–476.
- Marfella, C.G. and Iribalzano, A.N. (2007) The Chd family of chromatin remodelers. *Mutat. Res.*, **618**, 30–40.
- Delmas, V., Stokes, D.G. and Ferry, R.P. (1993) A mammalian DNA-binding protein that contains a chromodomain and an SNF2/SWI2-like helicase domain. *Proc. Natl Acad. Sci. USA*, **90**, 2414–2418.
- Zhang, Y. and Reinberg, D. (2001) Transcription regulation by histone methylation: interplay between different covalent modifications of the core histone tails. *Genes Dev.*, **15**, 2343–2360.
- Becker, P.B. and Hürz, W. (2002) ATP-dependent nucleosome remodeling. *Annu. Rev. Biochem.*, **71**, 247–273.
- Pray-Grant, M.G., Daniel, J.A., Schieltz, D., Yates, J.R. 3rd and Grant, P.A. (2005) Chd1 chromodomain links histone H3 methylation with SAGA- and SLIK-dependent acetylation. *Nature*, **27**, 434–438.
- Thompson, B.A., Tremblay, V., Lin, G. and Bochar, D.A. (2008) CHD8 is an ATP-dependent chromatin remodeling factor that regulates beta-catenin target genes. *Mol. Cell Biol.*, **28**, 3894–3904.
- Song, J.J. and Kingston, R.E. (2008) WDR5 interacts with mixed lineage leukemia (MLL) protein via the histone H3-binding pocket. *J. Biol. Chem.*, **12**, 35258–35264.
- Schnetz, M.P., Bartels, C.F., Shastri, K., Balasubramanian, D., Zentner, G.E., Balaji, R., Zhang, X., Song, L., Wang, Z., Laframboise, T. et al. (2009) Genomic distribution of CHD7 on chromatin tracks H3K4 methylation patterns. *Genome Res.*, **19**, 590–601.
- Mannan, A.U., Krawen, P., Sauter, S.M., Boehm, J., Chronowska, A., Paulus, W., Neesen, J. and Engel, W. (2006) ZFYVE27 (SPG33), a novel spastin-binding protein, is mutated in hereditary spastic paraplegia. *Am. J. Hum. Genet.*, **79**, 351–357.
- Deardorff, M.A., Kaur, M., Yasger, D., Rampuria, A., Korolev, S., Pie, J., Gil-Rodríguez, C., Arnedo, M., Loeys, B., Kline, A.D. et al. (2007) Mutations in cohesin complex members SMC3 and SMC1A cause a mild variant of cornelia de Lange syndrome with predominant mental retardation. *Am. J. Hum. Genet.*, **80**, 485–494.
- Félix, T.M., Hanshaw, B.C., Mueller, R., Bitoun, P. and Murray, J.C. (2006) CHD7 gene and non-syndromic cleft lip and palate. *Am. J. Med. Genet. A*, **1**, 2110–2114.
- Jongmans, M.C., Hoefloot, L.H., van der Donk, K.P., Admiraal, R.J., Magee, A., van de Laar, I., Hendriks, Y., Verheij, J.B., Walpole, I., Brunner, H.G. et al. (2008) Familial CHARGE syndrome and the CHD7 gene: a recurrent missense mutation, intrafamilial recurrence and variability. *Am. J. Med. Genet. A*, **1**, 43–50.
- Remy, I. and Michnick, S.W. (2004) A cDNA library functional screening strategy based on fluorescent protein complementation assays to identify novel components of signaling pathways. *Methods*, **32**, 381–388.
- Saha, A., Wittmeyer, J. and Cairns, B.R. (2006) Chromatin remodelling: the industrial revolution of DNA around histones. *Nat. Rev. Mol. Cell Biol.*, **7**, 437–447.
- Yuan, C.C., Zhao, X., Florens, L., Swanson, S.K., Washburn, M.P. and Hernandez, N. (2007) CHD8 associates with human Staf and contributes to efficient U6 RNA polymerase III transcription. *Mol. Cell Biol.*, **27**, 8729–8738.
- Dou, Y., Milne, T.A., Tackett, A.J., Smith, E.R., Fukuda, A., Wysocka, J., Allis, C.D., Chait, B.T., Hess, J.L. and Roeder, R.G. (2005) Physical association and coordinate function of the H3K4 methyltransferase MLL1 and the H4K16 acetyltransferase MOF. *Cell*, **17**, 873–885.
- Ishihara, K., Oshimura, M. and Nakao, M. (2006) CTCF-dependent chromatin insulator is linked to epigenetic remodeling. *Mol. Cell*, **1**, 733–742.
- Rodríguez-Paredes, M., Ceballos-Chávez, M., Esteller, M., García-Domínguez, M. and Reyes, J.C. (2009) The chromatin remodeling factor CHD8 interacts with elongating RNA polymerase II and controls expression of the cyclin E2 gene. *Nucleic Acids Res.*, **37**, 2449–2460.
- Daubresse, G., Dearing, R., Moore, L., Papoulas, O., Zakrajsek, I., Waldrip, W.R., Scott, M.P., Kennison, J.A. and Tamkun, J.W. (1999) The *Drosophila* kismet gene is related to chromatin-remodeling factors and is required for both segmentation and segment identity. *Development*, **126**, 1175–1187.
- Therrien, M., Morrison, D.K., Wong, A.M. and Rubin, G.M. (2000) A genetic screen for modifiers of a kinase suppressor of Ras-dependent rough eye phenotype in *Drosophila*. *Genetics*, **156**, 1231–1242.
- Srinivasan, S., Armstrong, J.A., Dearing, R., Dahlsveen, I.K., McNeill, H. and Tamkun, J.W. (2005) The *Drosophila* trithorax group protein Kismet facilitates an early step in transcriptional elongation by RNA Polymerase II. *Development*, **132**, 1623–1635.

2866 *Human Molecular Genetics, 2010, Vol. 19, No. 14*

36. Srinivasan, S., Dorigi, K.M. and Tamkun, J.W. (2008) *Drosophila* Kismet regulates histone H3 lysine 27 methylation and early elongation by RNA polymerase II. *PLoS Genet.*, **4**, e1000217.
37. Khattak, S., Lee, B.R., Cho, S.H., Ahn, J. and Spoerl, N.A. (2002) Genetic characterization of *Drosophila* Mi-2 ATPase. *Gene*, **26**, 107–114.
38. Xue, Y., Wong, J., Moreno, G.T., Young, M.K., Côté, J. and Wang, W. (1998) NURD, a novel complex with both ATP-dependent chromatin-remodeling and histone deacetylase activities. *Mol. Cell.*, **2**, 851–861.
39. Zahir, F., Firth, H.V., Baross, A., Delaney, A.D., Eydoux, P., Gibson, W.T., Langlois, S., Martin, H., Willatt, L., Marra, M.A. *et al.* (2007) Novel deletions of 14q11.2 associated with developmental delay, cognitive impairment and similar minor anomalies in three children. *Med. Genet.*, **44**, 556–561.
40. Allen, M.D., Religa, T.L., Freund, S.M. and Bycroft, M. (2007) Solution structure of the BRK domains from CHD7. *J. Mol. Biol.*, **31**, 1135–1140.

3.2 Identification and characterization of FAM124B as a novel component of a CHD7 and CHD8 containing complex

Mutations in the chromodomain helicase DNA binding protein 7 gene (*CHD7*) lead to CHARGE syndrome, an autosomal dominant heterogeneous disorder. Earlier, we could show that a part of CHD7 interacts with a part of CHD8, another chromodomain helicase DNA binding protein which has been recently demonstrated to be involved in the pathogenesis of neurodevelopmental (NDD) and autism spectrum disorders (ASD). We searched for novel CHD7 and CHD8 interacting partners using stable isotope labeling by amino acids in cell culture (SILAC) in combination with mass spectrometry. As result we identified as a potential interaction partner of both CHD7 and CHD8 a new uncharacterized protein, named FAM124B (Family with sequence similarity 124B). Furthermore, the confirmation of the SILAC results by co-immunoprecipitation and yeast two hybrid experiments demonstrated that FAM124B is a potential novel component of a CHD7 and CHD8 containing complex. Interestingly, our studies of Fam124B expression in E12.5 mouse embryos and in adult mouse brain show an overlap of the Fam124B expression with the expression patterns of Chd7 and Chd8. Therefore we conclude that Fam124B is a novel protein possibly involved in the pathogenesis of CHARGE syndrome and neurodevelopmental disorders.

Tserendulam Batsukh, Yvonne Schulz, Stephan Wolf, Tamara I. Rabe, Thomas Oellerich, Henning Urlaub, Inga-Marie Schaefer, Silke Pauli

Status: submitted to PLoS ONE (Impact factor 4.41).

Author contributions to the work:

- 1. Tserendulam Batsukh:** Generated the constructs; performed the experiments; involved in the manuscript writing.
- 2. Yvonne Schulz:** helped in paraffin embedding and sectioning of mouse embryonic tissues.
- 3. Stephan Wolf:** provided all mice for the experiments and was involved in mouse care.
- 4. Tamara I. Rabe:** helped in *in situ* hybridization experiments and assisted in interpretation of the *in situ* hybridization results.
- 5. Thomas Oellerich and Henning Urlaub:** advised and were involved in SILAC experiments; performed the mass-spectrometry of SILAC probes and did the data analysis.

6. Inga-Marie Schaefer: helped us in interpreting the immunohistochemical stainings on different mouse tissues and assisted in picture creations.
7. Silke Pauli: conceived and made experimental design; interpreted the data and prepared the manuscript.

Identification and characterization of FAM124B as a novel component of a CHD7 and CHD8 containing complex

Tserendulam Batsukh¹, Yvonne Schulz¹, Stephan Wolf¹, Tamara I. Rabe², Thomas Oellerich³, Henning Urlaub³, Inga-Marie Schaefer⁴, Silke Pauli¹

¹Institute of Human Genetics, University Medical Center, Göttingen, Germany

²Department of Molecular Cell Biology, Max Planck Institute for Biophysical Chemistry, Göttingen, Germany

³Bioanalytical Mass Spectrometry Group, Max Planck Institute for Biophysical Chemistry, Göttingen, Germany

⁴Department of Pathology, University Medical Center, Göttingen, Germany

ABSTRACT

Background: Mutations in the chromodomain helicase DNA binding protein 7 gene (CHD7) lead to CHARGE syndrome, an autosomal dominant multiple malformation disorder. Proteins involved in chromatin remodeling typically act in multiprotein complexes. We could previously demonstrate that a part of human CHD7 interacts with a part of human CHD8, another chromodomain helicase DNA binding protein presumably being involved in the pathogenesis of neurodevelopmental (NDD) and autism spectrum disorders (ASD). Because identification of novel CHD7 and CHD8 interacting partners will provide further insights into the pathogenesis of CHARGE syndrome and ASD/NDD, we searched for additional associated polypeptides using the method of stable isotope labeling by amino acids in cell culture (SILAC) in combination with mass spectrometry.

Principle findings: The hitherto uncharacterized FAM124B (Family with sequence similarity 124B) was identified as a potential interaction partner of both CHD7 and CHD8. We confirmed the result by co-immunoprecipitation studies and showed by direct yeast two hybrid experiments a direct binding to the CHD8 part. Furthermore, we characterized FAM124B as a mainly nuclear localized protein with a widespread expression in embryonic and adult mouse tissues.

Conclusion: Our results demonstrate that FAM124B is a potential interacting partner of a CHD7 and CHD8 containing complex. From the overlapping expression pattern between Chd7 and Fam124B at murine embryonic day E12.5 and the high expression of Fam124B in the developing mouse brain, we conclude that Fam124B is a novel protein possibly involved in the pathogenesis of CHARGE syndrome and neurodevelopmental disorders.

Key words: *FAM124B*, *CHD8*, *CHD7*, interaction studies, expression pattern

INTRODUCTION

In humans, *CHD7* (NM_017780) is one of nine members of the chromodomain helicase DNA binding domain (CHD) family that plays a role in controlling gene expression by ATP-dependent chromatin remodeling. Mutations in the *CHD7* gene are the major cause of CHARGE syndrome (OMIM 214800), an autosomal dominant congenital malformation disorder characterized by the combination of eye, ear, craniofacial structure, and heart defects [1-6]. However, in 5-10% of patients with a typical presentation of CHARGE syndrome and in 40-60% of patients with an atypical presentation the underlying cause of the symptoms remains unclear [7]. For other autosomal dominant disorders, e.g. Noonan syndrome, a genetic heterogeneity is known, wherein mutations in different genes lead to a near similar phenotype. Therefore, we suggest that also in CHARGE syndrome mutations in one or more unknown genes are involved in the pathogenesis of this disease.

Proteins involved in chromatin remodeling are typically found in multiprotein complexes. In recent and earlier studies different *CHD7* interacting partners have been described [8-13]. In human neural crest-like cells *CHD7* was shown to be associated with components of the BAF- (Brahma associated factor complex) and PBAF - complexes (Polybromo containing complex) [10]. Both belong to the SWI/SNF-family of ATP-dependent chromatin remodeling complexes and can act as transcriptional activators or repressors [14]. In murine embryonic stem (ES) cells a co-localization between *Chd7* and the proteins p300, Oct4, Sox2, Nanog, Smad1 and Stat3 at enhancer elements was shown [9] leading to the hypothesis that these proteins are cofactors in enhancer promoter interactions [9]. *CHD7* was also found to be associated with treacle, the protein that is involved in the pathogenesis of Treacher Collins syndrome [12]. These studies demonstrate that there are numerous *CHD7* interacting partners, leading to the suggestion that there are cell type specific compositions of *CHD7* containing complexes and that the subunits may change during development [7].

Recently, we could demonstrate that a part of the human *CHD7* protein interacts with a part of the *CHD8* protein, another CHD family member. Studies in *Drosophila melanogaster* demonstrated that *kismet* is the only gene related to the human subgroup III members (*CHD6*-*CHD9*). *Kismet* has a functional role in transcriptional regulation by promoting early elongation by RNA Polymerase II as well as by recruiting the histone methyltransferases ASH1 and TRX to chromatin [15]. Rodriguez-Paredes et al. suggested that in mammals the function of *kismet* is overtaken by several subgroup III members (*CHD6*-*CHD9*) [16] and we

hypothesized that CHD7 and CHD8 build a core component of a complex with similar functions such as *kismet* [11]. CHD8 was found to be associated with the WAR complex [17]. This complex includes WDR5, ASH2L and RbBP5 (WAR) and is known as a subcomplex of mixed lineage leukemia (MLL) complexes, the *Drosophila* homolog to TRX complexes. The MLL complexes act as histone H3 Lys-4 methyltransferases [18].

Furthermore, CHD8 binds directly beta-catenin and regulates negatively beta-catenin-targeted gene expression [17]. Microdeletions, chromosomal rearrangements disrupting *CHD8* as well as de novo missense and nonsense mutations in the *CHD8* gene were described in autism spectrum (ASD) and in neurodevelopmental (NDD) disorder patients, indicating that alterations in *CHD8* can contribute to ASD and NDD [19-22].

Identification of novel CHD7 and CHD8 interacting partners will provide further insights into the pathogenesis of CHARGE syndrome and ASD/NDD. Therefore, we tried to detect new binding partners by using the method of stable isotope labeling by amino acids in cell culture (SILAC) in combination with mass spectrometry. We identified FAM124B (Family with sequence similarity 124B) as a potential interaction partner of both CHD7 and CHD8. Additionally, we confirmed the interaction by co-immunoprecipitation and performed direct yeast two hybrid experiments. Furthermore, we examined the intracellular localization and tissue-specific expression of Fam124B during mouse embryogenesis and in adult mouse tissues.

RESULTS

Identification of FAM124B as part of the CHD7 and CHD8 interactomes

In order to identify novel CHD7 and CHD8 interaction partners we applied stable isotope labeling by amino acids in cell culture (SILAC) in combination with mass spectrometry [23,24] (Figure 1). To achieve differential isotope labeling of HeLa cells, one cell batch was cultured in the presence of lysine and arginine containing light (L) isotopes of carbon and nitrogen (^{12}C and ^{14}N , L-lysine and L-arginine) while the other batch was cultured in the presence of lysine and arginine containing heavy (H) isotopes of carbon and nitrogen ($^{13}\text{C}_6$ $^{15}\text{N}_2$ -lysine and $^{13}\text{C}_6$ $^{15}\text{N}_4$ -arginine). Accordingly, the two culture conditions confer distinct molecular masses on the cellular proteins and in this way proteins derived from SILAC-labeled cells can be distinguished and thus attributed to the L- or H-labeled cell batch by mass spectrometry. For elucidation of the CHD7- or CHD8 interactomes, the H-labeled cells were firstly co-transfected with the plasmids CHD7-CR1-3-pCMV-HA (containing amino acids 1593 - 2178, NP_060250.2, in fusion with an HA-tag) and CHD8-pCMV-cmyc (spanning

amino acids 1789 – 2302, NP_065971.2, in fusion with an cmyc-tag). 24 hours post transfection, expression of the tagged proteins was confirmed by western blotting. Subsequently the respective H-labeled cells were lysed and the CHD7 part was purified by anti-HA immunoprecipitation. As a negative control the same immunoprecipitation was performed in lysates of non-transfected L-labeled HeLa cells. The purified proteins from both the H- and L-states were then pooled in equimolar amounts and subsequently digested with the endoproteinase trypsin. Derived peptides were identified by liquid-chromatography (LC)-coupled tandem mass spectrometry (MS/MS), allocated to the corresponding proteins by database search and finally quantified using the MaxQuant software. An at least five-fold enrichment of heavy versus light peptides was considered to mark proteins that were specifically co-purified with the HA-tagged CHD7 part. The same experimental workflow was also performed with inverse labeling. In at least three biological replicates FAM124B was co-purified with CHD7 and CHD8, which identifies this so far uncharacterized protein as a novel effector of the CHD7/8 interactome (Table S1-S3).

Full length cloning and transcript analysis of FAM124B

Information of the genomic and cDNA structure of FAM124B was obtained from NCBI database. In humans, two transcript variants are described. Transcript variant 1 contains two exons with the ATG in exon one and the stop codon in exon 2 resulting in a protein with 455 amino acids (NP_001116251.1). Transcript variant 2 contains an alternate exon with an in-frame stop codon leading to a shorter protein product with 272 amino acids (NP_079061.2). In mice, one transcript homologous to the human transcript variant 1 containing 456 amino acids was described (NP_775601.1). We validated the information by full length cloning and sequencing of human and mouse cDNAs derived from HeLa cells and mouse adult brain tissue, respectively.

FAM124B co-immunoprecipitates with a part of CHD7 and a part of CHD8

Co-Immunoprecipitation studies on HeLa cells were performed to confirm the CHD7-CHD8-FAM124B interaction. HeLa cells were co-transfected with either the CHD7-CR1-3-pCMV-HA (amino acids 1593 - 2178, NP_060250.2) plasmid and FAM124B-1,3-pCMV-cmyc (transcript variant 1, NP_001116251.1) or with CHD8-pCMV-cmyc (amino acids 1789 - 2302, NP_065971.2) and FAM124B-1,3-pCMV-HA (transcript variant 1, NP_001116251.1). Total protein was isolated after 24 hours. Immunoprecipitation with either the anti-CHD7 (abcam, ab31824) or the anti-CHD8 antibody (abcam, ab84527) and detection with either the anti-cmyc (abcam, ab9106) or anti-HA antibody (Roche) lead to an approximately 51 kDa

band corresponding to the estimated size of FAM124B transcript variant 1 (Figure 2A). Reciprocal immunoprecipitation with anti-cmyc antibody and detection with the anti-CHD7 antibody demonstrated a specific band of ~ 70 kDa, the estimated size for the CHD7 part fused to the HA-tag (Figure 2B). Using the anti-HA-antibody for precipitation, we detected a ~ 68 kDa band corresponding to the estimated size of the CHD8 part fused to the cmyc tag (Figure 2C) by using the anti-CHD8 antibody.

The same experimental procedure was then performed with the plasmid FAM124B-1,2-pCMV-HA (transcript variant 2, NP_079061.2). Similar to the results for the FAM124B transcript variant 1, we could demonstrate an interaction with the CHD7 and CHD8 part with FAM124B transcript variant 2 (Figure 2D-F).

FAM124B interacts directly with a part of CHD8

Y2H experiments were performed to determine a direct interaction between CHD7, CHD8 and both variants of FAM124B using the following plasmids: FAM124B-1,3-pGADT7 (full lengths transcript variant 1), FAM124B-1,2-pGADT7 (full lengths transcript variant 2), CHD7-CR1-3-pGBKT7 (amino acids 1591-2181, NP_060250.2) and CHD8-pGBKT7 (amino acids 1789–2302, NP_065971.2). The yeast two hybrid experiments revealed that both transcripts of FAM124B directly interact with the CHD8 part, while no direct interaction with the CHD7 part, spanning the amino acids 1591-2181, could be observed (Figure 3). Because FAM124B transcript variants 1 and 2 have in common exon 1, we hypothesized that the FAM124B-CHD8 interacting area is located within exon 1 of FAM124B.

Subcellular localization of FAM124B in HeLa cells

To determine the subcellular localization of endogenous FAM124B in HeLa cells, we performed immunofluorescence staining by using a rabbit anti-FAM124B antibody (ProteinTech). FAM124B is localized mainly in the nucleus (Figure 4A). To test the specificity of the polyclonal anti-FAM124B antibody, we transiently transfected HeLa cells with either the plasmid FAM124B-1,3-pCMV-HA or the FAM124B-1,3-pCMV-cmyc to overexpress hemagglutinin (HA) or cmyc epitope tagged FAM124B-1,3 (transcript variant 1, NP_001116251.1). By using the rabbit anti-FAM124B antibody, the overexpressed protein was detectable mainly in the nucleus at an exposure time of 200 msec. By raising the exposure time to 2 sec, overexpressed and endogenous FAM124B could be observed. Immunofluorescence staining of recombinant HA tagged FAM124B using the anti-HA antibody (Roche) or staining of the recombinant cmyc tagged FAM124B using the anti-cmyc-

antibody (abcam, ab9106) confirmed the results that FAM124B is preferentially expressed in the nucleus and that the rabbit anti-Fam124B antibody is specific (Figure 4B, C).

Tissue specific expression of murine Fam124B

The expression pattern of murine Fam124B was studied by semiquantitative reverse transcription polymerase chain reaction (RT-PCR) on RNA of wild type CD1 mouse tissues and E9.5 and E12.5 embryos (Figure 5A). The RT-PCR results were validated by quantitative real-time PCR (qRT-PCR) in 3 biological and 3 technical replicates (data not shown). Relative mRNA expression levels were determined by using ΔC_t values and were normalized to the housekeeping genes *Gapdh*, *Hprt* and *Sdha*. Although, quantitative RT-PCR shows a high variability of the Fam124B expression status in different animals, the semiquantitative RT-PCR results could be confirmed, with highest expression rate in lung and lowest in liver. Immunohistochemical staining (IHC) performed on adult mouse tissues confirmed the semiquantitative and quantitative RT-PCR results (Figure 5B). Furthermore, we evaluated the expression level of Fam124B in sections of adult mouse brains. Immunohistochemical examination demonstrated an expression of Fam124B in different brain areas (Figure 6A). Fam124B is highly expressed in the cortex, the hippocampus subfields 1-3 (CA1-3), the dentate gyrus, the caudate putamen, and the cerebellum. In situ hybridization (ISH) of cortex and hippocampus sections with a full-length Fam124B RNA probe supported the results obtained by IHC (Figure 7A, B).

To explore the expression pattern of Fam124B during mouse development, we extended our IHC studies to sections of E12.5 mouse embryos, the timepoint when organogenesis takes place. Similar to adult mouse tissues, Fam124B expression at E12.5 was observed in different inner organs, with lowest expression in liver tissue (Figure 8A-H). In the developing heart, high expression was detected particularly in the endothelial cells of the atrium and along the trabeculated endocardium of the ventricle, while no expression could be observed in blood cells (Figure 8D). At E12.5 when the developing lung is not yet divided into lobes, Fam124B expression could be observed in the stroma cells and in the epithelial cells of the segmental bronchi (Figure 8G). Furthermore, Fam124B was expressed in the developing cochlea and the surrounding tissue (Figure 8E) as well as in neural cells. The dorsal root ganglia and the precartilaginous condensation zones in the neural arch showed Fam124B expression, while Fam124B expression was significantly reduced in the cartilage (Figure 8B). High Fam124B expression could be found in the spinal cord (Figure 8F) and in the developing brain (Figure 9).

DISCUSSION

Loss of function mutations in *CHD7* lead to CHARGE syndrome, a well known malformation syndrome affecting several organs and sensory systems. CHD7 regulates the transcription of tissues-specific target genes through the mechanism of ATP-dependent chromatin remodeling [7-9, 12]. Chromatin remodeling proteins are typically found in large multiprotein complexes. For CHD7 several tissues-specific interacting partners are described [9, 10, 12, 13]. Thus, it can be suggested that there are cell type and developmental stage specific compositions of CHD7 containing complexes. However, the precise complex compositions for each tissue are still unknown. In an earlier study, we could demonstrate that a part of human CHD7 interacts with a part of human CHD8 both directly and indirectly, via potential linker proteins [11]. Loss of function mutations in *CHD8* as well as de novo missense mutations were described in autism spectrum (ASD) and neurodevelopmental (NDD) disorder patients [19-22]. Interestingly, Betancur and colleagues described autism spectrum disorders in about two thirds of children with CHARGE syndrome [25], which supports our hypothesis of a CHD7-CHD8 containing complex regulating the same cell type specific target genes.

The identification and characterization of associated factors of a CHD7-CHD8 containing complex might play an important role in understanding the pathophysiology of CHARGE syndrome and ASD/NDD. Therefore, to further characterize this complex and to identify additional associated polypeptides interacting with the recently described human CHD7 and CHD8 part, we used the method of stable isotope labeling by amino acids in cell culture (SILAC) in combination with mass spectrometry. As a result of three biological replicates we identified the hitherto uncharacterized protein FAM124B as a potential interacting partner. In humans, two FAM124B transcript variants are present, while in mice, only one transcript, homologous to the human transcript variant 1, exists. The interaction of both human FAM124B transcript variants with the CHD7 and CHD8 part was confirmed by co-immunoprecipitation experiments. Direct yeast-two hybrid studies were performed to specify the FAM124B - CHD7 - CHD8 interaction areas. Both transcripts of human FAM124B interact directly with the CHD8 part containing the amino acids 1789–2302 (NP_065971.2), while the FAM124B - CHD7 interaction is an indirect interaction or the interacting area is outside of the used CHD7 part spanning amino acids 1591-2181 (NP_060250.2). The biological role of human FAM124B or its orthologs in *P.troglodytes*, *C.lupus*, *B.taurus*, *R.norvegicus*, *M.musculus*, *G.gallus*, *D.rerio* is still unknown. Bioinformatic analysis of the amino acid sequence failed to identify any known functional domain. To gain further insight into the biological role of FAM124B and its mouse ortholog, we examined the subcellular

localization and the expression pattern. Immunofluorescence microscopy indicates that endogenous FAM124B is localized mainly in the nucleoplasm. CHD8 is described as a nuclear localized protein [26]. Concerning CHD7, a dual localization in the nucleoplasm and in the nucleolus was observed [12]. Therefore, we suggest, that the interaction between FAM124B, CHD8 and CHD7 may take place in the nucleoplasm.

We could detect Fam124B expression in various adult mouse tissues, with highest expression in lung and heart, followed by kidney, brain and testis, whereas it was lowest expressed in liver. No Fam124B expression could be observed in blood cells. In adult mouse brain sections, we demonstrated Fam124B expression in several areas. Within the brain, high expression levels were found in the stratum granulosum of the cortex, stratum granulosum and purkinjense of the cerebellum, thalamic nuclei, caudate putamen, and hippocampus.

CHD8 expression was previously found in various adult mouse tissues including heart, brain, spleen, lung, liver, skeletal muscle, kidney, and testis [26]. CHD7 expression pattern was determined by semiquantitative RT-PCR on several adult tissues including retina, cornea, brain, skeletal muscle, heart, kidney and lung [1]. Accordingly to these previously described data we could observe an overlapping expression pattern between CHD7, Chd8 and Fam124B in adult mouse tissues. Because CHARGE syndrome is a developmental disorder and NDD/ASD are caused by abnormal brain development, we extended our Fam124B expression studies to embryonic tissues. The expression pattern of CHD7 during development has been studied in embryos of different mammalian species, before [4, 5, 27-29]. During mouse development, Chd7 was found to be expressed at E12.5 in a wide range of head tissues (several brain areas with highest expression in proximity to the ventricles, in the choroid plexus, developing olfactory epithelium, ganglia of the cranial nerves, otic and optic pits, and the developing inner ear) and several regions of the body (especially the dorsal root ganglia and lung epithelium, as well as stomach epithelium, kidney, and heart) [27]. Fam124B expression at E12.5 was found in a variety of embryonic tissues (e.g. several brain areas, spinal cord, dorsal root ganglia, developing cochlea and surrounding tissues, lung, heart, and kidney), as well. Similar to the results of adult mouse tissues, Fam124B expression at E12.5 correlated in many embryonic tissues with the Chd7 expression pattern, and therefore Fam124B was found to be expressed in organs affected in CHARGE syndrome.

It has already been shown that CHD7 binds to methylated histone H3 lysine 4 (H3K4) at enhancer elements and modify cell type specific gene expression in a fine-tuning manner [8, 9]. Schnetz and colleagues hypothesized that the binding of a CHD7 containing complex to enhancer elements may modulate the expression rate of target genes through enhancer-

promotor interactions [8, 9]. In mouse ES cells, a subset of Chd7 sites colocalize with p300, Oct4, Sox2 and Nanog. The subset of Chd7 sites, which are not co-occupied by these proteins, can also enhance transcription [9]. However, the associated factors of these Chd7 sites are still unknown. Possibly, the newly identified Fam124B may serve as an associated factor involved in Chd7 enhancer-mediated transcription. Furthermore, the high Fam124B expression in the developing mouse brain and in neuronal tissues at embryonic day E12.5 might indicate a role of FAM124B together with CHD8 in neurodevelopmental and autism spectrum disorders.

In summary, we identified FAM124B, a nuclear protein, as a binding partner of a part of CHD7 and CHD8. We conclude that FAM124B is an associated factor of a CHD7 and CHD8 containing complex. Fam124B is widely expressed at mouse developmental stage E12.5 with an overlapping correlation to Chd7 expression and high expression in the developing mouse brain. Therefore, we assume a role for FAM124B in the pathogenesis of CHARGE syndrome and NDD/ASD. The results of our interaction studies, the subcellular localization, and expression profile of FAM124B provide valuable information and represent a starting point for further functional investigations on FAM124B and its possible role in CHARGE syndrome and NDD/ASD.

MATERIALS AND METHODS

Ethics statement/mouse strains

The animal studies are approved by the Institutional Animal Care and Use Committee of the University of Göttingen. All mouse studies were performed on CD1 wildtype mice.

Stable isotope labeling by amino acids in cell culture (SILAC) and mass spectrometry (MS)

Two HeLa cell populations were grown in SILAC DMEM culture media (10% dialyzed FBS and 1% penstrep) (PAA Laboratories GmbH, Pasching, Austria; Thermo Fisher Scientific, Waltham, MA). The “light” SILAC medium was supplemented with unlabeled L-lysine and L-arginine, while the “heavy” SILAC medium was supplemented with arginine and lysine containing heavy isotopes of carbon and nitrogen ($^{13}\text{C}_6$ -lysine and $^{13}\text{C}_6^{15}\text{N}_4$ -arginine). Upon metabolic labeling of the cells this lead to a mass shift of +6 and +10 Da per incorporated arginine and lysine, respectively. After at least 5 cell passages, co-transfection with the previously described plasmids CHD7-CR1-3-pCMV-HA and CHD8-pCMV-cmyc [11] into either L- or H-labeled HeLa cells was performed. Non transfected L- or H-labeled cells were used as negative control. After transient co-transfection, the cells were incubated at 37°C for

24 hours, then washed with DPBS (PAN BIOTECH GmbH, Aidenbach, Germany) and trypsinized (Invitrogen, Carlsbad, CA, USA). To isolate the same amount of protein from both cell cultures, cell populations were accurately counted under microscope using counting chambers (Neubauer haemocytometer) (approximately $1 - 1,2 \times 10^7$ cells were used) before cell lysis, which was performed as described by Oellerich et al. (2011) [24]. Protein lysates were incubated with 4 μg of monoclonal anti-Ha antibody (Roche Diagnostik GmbH, Mannheim, Germany) at 4°C overnight. Proteins coupled with the antibody were incubated at 4°C with 100 μl of protein G (Immunoprecipitation Kit, Roche Diagnostik GmbH, Mannheim, Germany) for further 2 hours. Centrifugation at 350 rpm for 3 min was carried out to collect the agarose beads. To remove unbound proteins, the beads were washed two times in 500 ml lysis buffer and one time with 1 ml washing buffer 2 (Immunoprecipitation Kit, Roche Diagnostik GmbH, Mannheim, Germany). The beads were resuspended in 50 μl NuPAGE LDS Sample buffer (Invitrogen, Carlsbad, CA, USA) supplemented with 0.1 M DTT. After denaturation for 10 min at 95°C, the denatured H- and L-labeled proteins were pooled in equimolar amounts and subsequently the samples were separated by size using an 1D-PAGE (Invitrogen, Carlsbad, CA, USA) followed by coomassie blue staining. Each gel lane was cut into 23 gel slices. Proteins from each slice were in-gel digested with trypsin (Promega, Madison, WI) according to the protocol described by Shevchenko et al. (2006) [30]. MS measurements were carried out using a nanoflow HPLC (Agilent, Boeblingen, Germany) coupled to a nanoelectrospray LTQ-Orbitrap XL mass spectrometer (Thermo Fisher Scientific, Waltham, MA) as described by Nikolov et al. (2011) [31].

RNA isolation and semiquantitative reverse-transcription PCR

Total RNA was isolated from HeLa cells, MRC-CV1 cells or different mouse tissues using Trizol reagent (Invitrogen, Carlsbad, CA, USA). Homogenizing was carried out with Tissue lyser LT (Qiagen GmbH, Hilden, Germany). 5 μg of total RNA from each sample was reverse-transcribed using Superscript II reverse transcriptase (Invitrogen, Carlsbad, CA, USA). For each PCR reaction 0.5 μl undiluted cDNA and 0.2 μl platinum taq polymerase (Invitrogen, Carlsbad, CA, USA) was used. Human cDNA isolated from HeLa and MRC-CV1 cells were amplified using the following primers: 5'-CCTTCTACACACGCTGTCTTTG-3' as forward primer and 5'-GGGGATGAGCTATGCAACCTAAG-3' as reverse primer. RT-PCR on mouse tissues was carried out using the following primer pair: forward primer 5'-GGTGGCCTTCATCATAATCTTC-3' and reverse primer 5'-CCAGTCACACTCTTGCTTCTGT-3'. The correct sequence was confirmed by sequence analysis.

Quantitative RT-PCR

Realtime PCR reactions were performed using 1µl of 1:10 diluted cDNA from different CD1 mouse tissues, SYBR green (Invitrogen, Carlsbad, CA, USA) and the gene-specific primers forward 5'-CCGTGTGTTCCCATCAGCAG-3' and reverse 5'-CTCCTCCTCCGGCTCCTTG-3'. Relative mRNA expression levels were determined using Δ Ct values and were normalized to the housekeeping genes *Gapdh*, *Hprt* and *Sdha*. The experiment was performed in three biological and 3 technical replicates.

Co-immunoprecipitation

For co-immunoprecipitation studies we generated the plasmids FAM124B-1,3-pCMV-HA (transcript variant 1, NP_001116251.1), FAM124B-1,2-pCMV-HA (transcript variant 2, NP_079061.2), FAM124B-1,3-pCMV-cmyc (transcript variant 1, NP_001116251.1) and FAM124B-1,2-pCMV-cmyc (transcript variant 2, NP_079061.2) by cloning the human full-length sequence of transcript variant 1 and transcript variant 2 in frame to the hemagglutinin (HA) epitope tag into the pCMV-HA vector (Clontech, Mountain View, CA, USA) or in frame to the N-terminal c-Myc epitope tag into the pCMV-Myc vector (Clontech, Mountain View, CA, USA) by using the In fusion advantage kit (Clontech, Mountain View, CA, USA) according to the company's protocol. The correct reading frame and sequence was confirmed by sequence analysis.

HeLa cells were cultured in 50 ml flask (Sarstedt, Newton, NC, USA) and were cotransfected with CHD7-CR1-3-pCMV-HA (amino acids 1593 - 2178, NP_060250.2) and either FAM124B-1,3-pCMV-cmyc or FAM124B-1,2-pCMV-cmyc. Additionally, we co-transfected HeLa cells with CHD8-pCMV-cmyc (amino acids 1789 - 2302, NP_065971.2) and either FAM124B-1,3-pCMV-HA or FAM124B-1,2-pCMV-HA. After 24h of incubation at 37 °C, co-immunoprecipitations were carried out as previously described [11]. For immunoblotting we used the following antibodies: anti-c-Myc (abcam, ab9106) at a dilution of 1:2000, anti-HA (Roche Diagnostik GmbH, Mannheim, Germany) at a dilution of 1:1000, goat anti-CHD7 (abcam, ab 65097) at a dilution of 1:2000, rabbit anti-CHD8 (abcam, ab84527) at a dilution of 1:2000. The following antibodies were used for detection: goat anti-rabbit IgG peroxidase secondary antibody (Sigma-aldrich, St.Louis, MO, USA) for anti-c-Myc and anti-CHD8, goat anti-Rat secondary antibody conjugated with horseradish peroxidase (Thermo Scientific, Rockford, IL, USA) for anti-HA, donkey anti-goat IgG peroxidase secondary antibody (Santa-Cruz Biotechnologies, California, USA) for anti-CHD7.

Yeast two hybrid

For yeast two hybrid studies we generated the constructs FAM124B-1,3-pGBKT7 (transcript variant 1, NP_001116251.1), FAM124B-1,2-pGBKT7 (transcript variant 2, NP_079061.2), FAM124B-1,3-pGADT7 (transcript variant 1, NP_001116251.1) and FAM124B-1,2-pGADT7 (transcript variant 2, NP_079061.2). The human full-length sequence of transcript variant 1 and transcript variant 2 were subcloned in frame to the ATG of the pGBKT7 or pGADT7 vector (Clontech, Mountain View, CA) by using the In fusion advantage kit (Clontech, Mountain View, CA). All constructs were transformed into Y2HGold strain cells (Clontech, Mountain View, CA) and tested for toxicity and autoactivation of the bait or prey reporter genes. No toxicity for the yeast cells could be observed, but the FAM124B-1,3-pGBKT7 and FAM124B-1,2-pGBKT7 showed autoactivation. Therefore, the further experiments were performed with the FAM124B-1,3-pGADT7 and FAM124B-1,2-pGADT7 constructs. These both plasmids were co-transformed into Y2HGold strain cells together with either the CHD7-CR1-3-pGBKT7 (amino acids 1591-2181, NP_060250.2) or the CHD8-pGBKT7 (amino acids 1789–2302, NP_065971.2) plasmids. The direct Yeast two hybrid was performed according to the manufactures' protocol.

Cryosections

Adult brains from CD1 mice were isolated and fixed overnight in 4% paraformaldehyde (PFA) solution prepared in sterile PBS with DEPC water at 4°C with gentle shaking. On the next day, the tissues were washed 3 times with sterile PBS/DEPC at 4°C and incubated in autoclaved/sterile 30% Sucrose at 4°C with gentle shaking till the tissues sank down. Then the brains were incubated for 30 minutes to 1 hour at 4°C in a 1:1 mixture containing 30% sucrose and Jung tissue freezing medium (Leica Microsystems, Nussloch, Germany), following an incubation in tissue freezing medium at 4°C for 30 minutes and embedded on dry ice in tissue freezing medium. The frozen block was kept till usage at -80°C and cut by cryo-microtome (Leica Instrument, Nussloch, Germany) with 20 µm thickness and stucked on Menzel Superfrost microscope slides (Thermo Scientific, Rockford, IL, USA).

In situ hybridization

In situ hybridization was performed on cryosections of adult brain from CD1 mice. The following primer pairs were used to amplify by RT-PCR the whole coding region of *Fam124B*: forward 5'- GCCATGGATGAGATACAGGAA-3' and reverse 5'- CATGAATGGGGCTGACTCTTA-3'. The PCR product was subcloned into pGEMT easy vector (Promega, Madison, WI) and transformed into *E.coli*. Positive plasmids were isolated

and sequenced. For probe amplification from a correct plasmid the following primers were used for the Sp6 transcript: pGEM-T-Sp6-F (ACGTTCGCATGCTCCCG) and pGEM-T-R2 (CCAGGCTTTACTTTATGCTTCC) and for the T7 transcript: PCR-T7 (CTGCGCAACTGTTGGG) and pGEM-T-R1 (AGGCGGCCGCGAATTCAC). The PCR products were gel extracted and DIG-labelled RNA probes were synthesized using the DIG RNA Labeling Kit (SP6/T7) (Roche Diagnostik GmbH, Mannheim, Germany) according to the manufacturer's protocol. Synthesized probes were ethanol precipitated and resuspended in 100 µl of DEPC water/formamide 1:1 mixture and kept till usage at -20°C. Non-radioactive in situ hybridization have been done according to Moorman et al. (2001) The results have been observed using a BX60 microscope (Olympus, Hamburg, Germany) and images were processed by the analysis program (CellSens Dimension, Olympus).

Immunohistochemistry on cells

HeLa and MRC-CV1 cells were transfected with the FAM124B-1,3-pCMV-HA construct. Cell culture, staining procedure and fluorescence imaging was carried out as described previously [11]. As a blocking solution 10% sheep serum diluted in DPBS with 0.1% Tween 20 (TPBS) was used. Rabbit anti-FAM124B antibody (Proteintech Group, Chicago, IL) was diluted at 1:50. As secondary antibody anti-rabbit IgG conjugated with Cy3 (Sigma-Aldrich, St.Louis, MO, USA) antibody was used at a dilution of 1:400.

Immunohistochemistry on paraffin embedded tissues

Adult wild type CD1 mouse tissues and E12.5 embryos were paraffin embedded according to standard procedures. From the paraffin embedded tissues 7µm sections were made and incubated overnight at 45 °C. After a three time Xylene incubation (10, 5, 5 minutes) a series of ethanol incubation (100%, 95%, 90%, 80%, 70%, 50%) and a washing step with DPBS for 2 minutes followed. Slides were cooked with antigen retrieval buffer (citric acid 0.1M; EDTA 0.01%, pH 6.2) in a steam cooker for 10 minutes and allowed retrieval buffer to cool down on ice for at least 10 minutes. Endogenous peroxidase activity was blocked using 6% H₂O₂ solution in water for 15 minutes. The solution was tapped off from the slides and blocked with horse serum (Vectastain Universal Quick kit, Vector Laboratories, Burlingame, CA) for 30 minutes in a humidity chamber at room temperature. Rabbit anti-FAM124B (Protein Tech), rabbit anti-CHD7 (abcam, ab31824) and rabbit anti-CHD8 (abcam, ab84527) antibodies were diluted at 1:50, 1:50 and 1:100, respectively. The primary antibodies were incubated at 4°C overnight. After washing with TPBS for 5 minutes, a Pan specific secondary antibody (Vectastain Universal Quick kit, Vector Laboratories, Burlingame, CA) was applied for

maximum 10 minutes and washed again with TPBS for 5 minutes. Streptavidin peroxidase (Vectastain Universal Quick kit, Vector Laboratories, Burlingame, CA) was applied on the slides for 5 minutes. Slides were then transferred to TPBS washing buffer for minimum 5 minutes. The staining was developed with DAB substrate (Roche Diagnostik GmbH, Mannheim, Germany) for around 2 minutes. The slides were rinsed for minimum 5 minutes under tap water and counterstain could be done in mayor's hematoxylin for 20-40 seconds and washed with tap water 3-4 times. Mounting of slides were done with Aqua polymount (Polysciences Inc., Warrington, PA). Imaging was performed and processed using a BX60 microscope (Olympus, Hamburg, Germany) and the analySIS program Cell-Sens Dimension.

SUPPORTING INFORMATION

Table S1 Proteins found by SILAC in combination with mass spectrometry 1st experiment (XLS)

Table S2 Proteins found by SILAC in combination with mass spectrometry 2nd experiment (XLS)

Table S3 Proteins found by SILAC in combination with mass spectrometry 3rd experiment (XLS)

ACKNOWLEDGMENTS

We thank W. Engel for his support and helpful discussions and Johanna Mänz for her excellent technical assistance.

REFERENCES

1. Vissers LE, van Ravenswaaij CM, Admiraal R, Hurst JA, de Vrie BB, et al. (2004) Mutations in a new member of the chromodomain gene family cause CHARGE syndrome. *Nat Genet* 36: 955–957.
2. Lalani SR, Safiullah AM, Fernbach SD, Harutyunyan KG, Thaller C, et al. (2006) Spectrum of CHD7 mutations in 110 individuals with CHARGE syndrome and genotype–phenotype correlation. *Am J Hum Genet* 78: 303–314.
3. Jongmans MC, Admiraal RJ, van der Donk KP, Vissers LE, Baas AF, et al. (2006) CHARGE syndrome: the phenotypic spectrum of mutations in the CHD7 gene. *J Med Genet* 43: 306–314.

4. Sanlaville D, Etchevers HC, Gonzales M, Martinovic J, Clément-Ziza M, et al. (2006) Phenotypic spectrum of CHARGE syndrome in fetuses with CHD7 truncating mutations correlates with expression during human development. *J Med Genet* 43: 211-217.
5. Aramaki M, Udaka T, Kosaki R, Makita Y, Okamoto N, et al. (2006) Phenotypic spectrum of CHARGE syndrome with CHD7 mutations. *J Pediatr* 148: 410-414.
6. Wincent J, Holmberg E, Strömmland K, Soller M, Mirzaei L, et al. (2008) CHD7 mutation spectrum in 28 Swedish patients diagnosed with CHARGE syndrome. *Clin Genet* 74: 31-38.
7. Janssen N, Bergman EH Jorieke, Swertz MA, Tranebjaerg L, Lodahl M, et al. (2012) Mutation Update on the CHD7 Gene Involved in CHARGE Syndrome. *Hum Mutat* doi: 10.1002/humu.22086
8. Schnetz MP, Bartels CF, Shastri K, Balasubramanian D, Zentner GE, et al. (2009) Genomic distribution of CHD7 on chromatin tracks H3K4 methylation patterns. *Genome Res* 19: 590-601.
9. Schnetz MP, Handoko L, Akhtar-Zaidi B, Bartels CF, Pereira CF, et al. (2010) CHD7 targets active gene enhancer elements to modulate ES cell-specific gene expression. *PLoS Genet* 6: e1001023.
10. Bajpai R, Chen DA, Rada-Iglesias A, Zhang J, Xiong Y, et al. (2010) CHD7 cooperates with PBAF to control multipotent neural crest formation. *Nature* 463: 958–962.
11. Batsukh T, Pieper L, Koszucka AM, vonVelsen N, Hoyer-Fender S, et al. (2010) CHD8 interacts with CHD7, a protein which is mutated in CHARGE syndrome. *Hum Mol Genet* 19: 2858–2866.
12. Zentner GE, Hurd EA, Schnetz MP, Handoko L, Wang C, et al. (2010a) CHD7 functions in the nucleolus as a positive regulator of ribosomal RNA biogenesis. *Hum Mol Genet* 19: 3491–3501.
13. Takada I, Mihara M, Suzawa M, Ohtake F, Kobayashi S, et al. (2007) A histone lysine methyltransferase activated by non-canonical wnt signalling suppresses PPAR-gamma transactivation. *Nat Cell Biol* 9: 1273–1285.
14. Ho L and Crabtree GR. (2010) Chromatin remodelling during development. *Nature* 28: 474-84. Review

15. Srinivasan S, Dorighi KM, Tamkun JW. (2008) *Drosophila* kismet regulates histone H3 lysine 27 methylation and early elongation by RNA polymerase II. *PLoS Genet* 4: e1000217.
16. Rodríguez-Paredes M, Ceballos-Chávez M, Esteller M, García-Domínguez M and Reyes JC. The chromatin remodeling factor CHD8 interacts with elongating RNA polymerase II and controls expression of the cyclin E2 gene. *Nucleic Acids Res* 37: 2449-2460.
17. Thompson BA, Tremblay V, Lin G and Bochar DA. (2008) CHD8 is an ATP-dependent chromatin remodeling factor that regulates beta-catenin target genes. *Mol Cell Biol* 28: 3894-3904.
18. Yokoyama A, Cleary ML. (2008) Menin critically links MLL proteins with LEDGF on cancer-associated target genes. *Cancer Cell* 14: 36-46.
19. Zahir F, Firth HV, Baross A, Delaney AD, Eydoux P, et al. (2007) Novel deletions of 14q11.2 associated with developmental delay, cognitive impairment and similar minor anomalies in three children. *Med Genet* 44: 556-561.
20. Talkowski ME, Rosenfeld JA, Blumenthal I, Pillalamarri V, Chiang C, et al. (2012) Sequencing Chromosomal Abnormalities Reveals Neurodevelopmental Loci that Confer Risk across Diagnostic Boundaries. *Cell* 149: 525-537.
21. O’Roak BJ, Vives L, Girirajan S, Karakoc E, Krumm N, et al. (2012) Sporadic autism exomes reveal a highly interconnected protein network of de novo mutations. *Nature* 485: 246-250.
22. Neale BM, Kou Y, Liu L, Ma'ayan A, Samocha KE, Sabo A, et al. (2012) Patterns and rates of exonic de novo mutations in autism spectrum disorders. *Nature* 485: 242-245.
23. Ong SE, Blagoev B, Kratchmarova I, Kristensen DB, Steen H, et al. (2002) Stable Isotope Labeling by Amino Acids in Cell Culture, SILAC, as a Simple and Accurate Approach to Expression Proteomics. *Mol Cell Proteomics* 1: 376-386.
24. Oellerich T, Bremes V, Neumann K, Bohnenberger H, Dittmann K, Hsiao HH, Engelke M, Schnyder T, Batista FD, Urlaub H, Wienands J. (2011) The B-cell antigen receptor signals through a preformed transducer module of SLP65 and CIN85. *EMBO J* 30: 3620–3634.
25. Betancur, C. (2011) Etiological heterogeneity in autism spectrum disorders: more than 100 genetic and genomic disorders and still counting. *Brain Res* 1380: 42–77.

26. Ishihara K, Oshimura M. and Nakao M. (2006) CTCF-dependent chromatin insulator is linked to epigenetic remodeling. *Mol Cell* 1: 733-742.
27. Bosman EA, Penn AC, Ambrose JC, Kettleborough R, Stemple DL, et al. (2005) Multiple mutations in mouse *Chd7* provide models for CHARGE syndrome. *Hum Mol Genet* 14: 3463–3476.
28. Hurd EA, Capers PL, Blauwkamp MN, Adams ME, Raphael Y, et al. (2007) Loss of *Chd7* function in gene-trapped reporter mice is embryonic lethal and associated with severe defects in multiple developing tissues. *Mamm Genome* 18: 94–104.
29. Bergman JE, Bosman EA, van Ravenswaaij-Arts CM, Steel KP. (2010) Study of smell and reproductive organs in a mouse model for CHARGE syndrome. *Eur J Hum Genet* 18: 171–177.
30. Shevchenko A, Tomas H, Havlis J, Olsen JV, Mann M. (2006) In-gel digestion for mass spectrometric characterization of proteins and proteomes. *Nat Protoc.* 1: 2856-2860.
31. Nikolov M, Stützer A, Mosch K, Krasauskas A, Soeroes S, Stark H, Urlaub H, Fischle W. (2011) Chromatin affinity purification and quantitative mass spectrometry defining the interactome of histone modification patterns. *Mol Cell Proteomics.* 10: M110.005371.

FIGURES

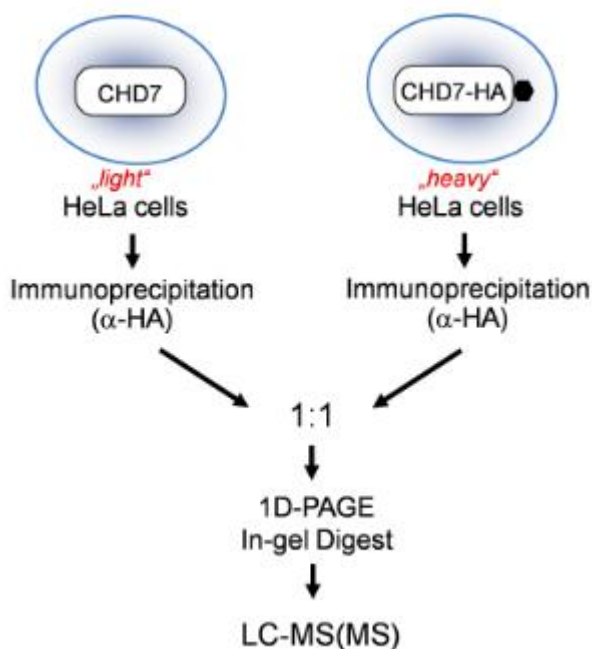


Figure 1: Schematic overview of the SILAC approach.

“Heavy”-labeled cells were co-transfected with the plasmids CHD7-CR1-3-pCMV-HA (containing amino acids 1593 - 2178, NP_060250.2, in fusion with an HA-tag) and CHD8-pCMV-cmyc (spanning amino acids 1789 - 2302, NP_065971.2, in fusion with an cmyc-tag). The CHD7 part was purified by anti-HA immunoprecipitation. As a negative control the same immunoprecipitation was performed in lysates of non-transfected “Light”-labeled HeLa cells. Purified proteins from both cell cultures were pooled in equimolar amounts and in-gel digested, followed by liquid-chromatography (LC)-coupled tandem mass spectrometry.

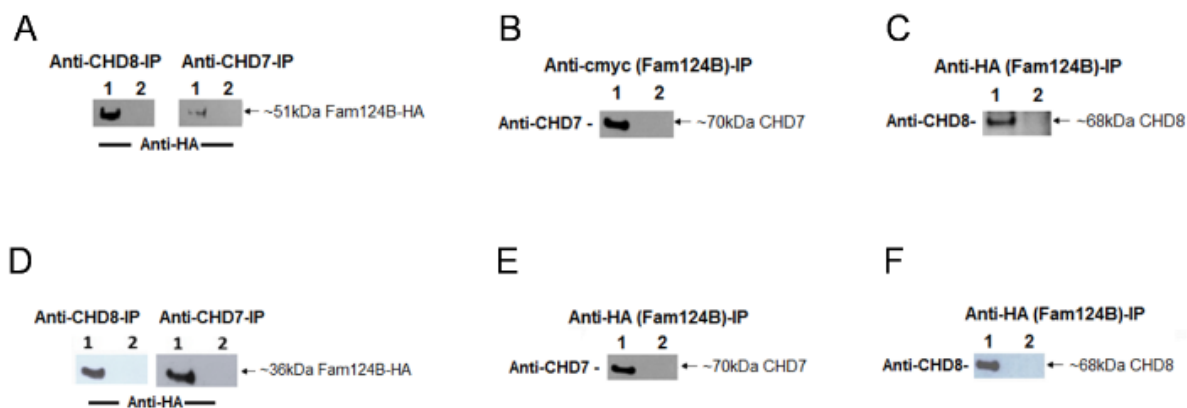


Figure 2: Co-immunoprecipitation of FAM124B with a part of CHD7 and CHD8.

HeLa cells were co-transfected with either the CHD7-CR1-3-pCMV-HA (amino acids 1593 - 2178, NP_060250.2) plasmid and FAM124B-1,3-pCMV-cmyc/FAM124B-1,3-pCMV-HA (transcript variant 1, NP_001116251.1) or with CHD8-pCMV-cmyc (amino acids 1789 - 2302, NP_065971.2) and FAM124B-1,3-pCMV-HA (transcript variant 1, NP_001116251.1).

(A) Using the anti-CHD8 (abcam, ab84527) or the anti-CHD7 (abcam, ab31824) antibody for precipitation, we detected with the anti-HA antibody (Roche) an approximately 51 kDa band corresponding to the estimated size of FAM124B transcript variant 1. Lane 1: co-transfected Co-IP, lane 2: untransfected HeLa cells as negative control. (B) Reciprocal immunoprecipitation with anti-cmyc antibody (precipitating FAM124B transcript variant 1), and detection with the anti-CHD7 antibody lead to a specific band ~ 70 kDa, the estimated size for the CHD7 part fused to the HA-tag. Lane 1: co-transfected Co-IP, lane 2: untransfected HeLa cells as negative control. (C) Reciprocal experiment with anti-HA antibody (precipitating FAM124B transcript variant 1) and detection with the anti-CHD8 antibody detected a specific band ~ 68 kDa, the estimated size for the CHD8 part fused to the cmyc-tag. Lane 1: co-transfected Co-IP, lane 2: untransfected HeLa cells as negative control. (D, E, F) The same experimental procedure was performed for FAM124B transcript variant 2, demonstrating a specific interaction of FAM124B transcript variant 2 with the CHD7 and CHD8 part as well. Lane 1: co-transfected Co-IP, lane 2: untransfected HeLa cells as negative control.

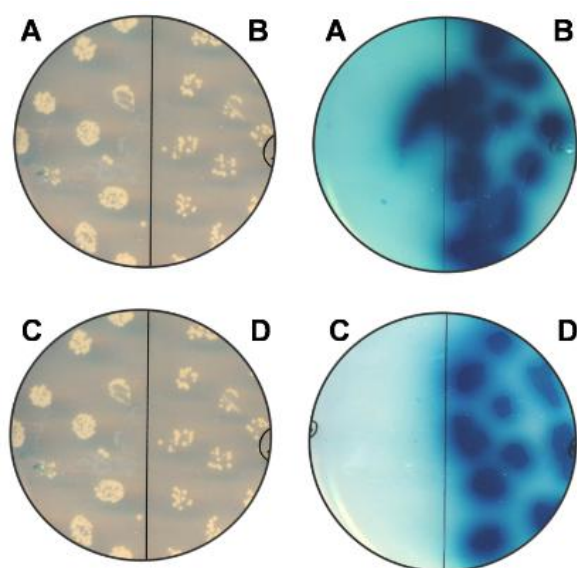


Figure 3: Yeast two hybrid assay.

(A) Direct yeast two hybrid experiment with the constructs FAM124B-1,3-pGADT7 (full lengths transcript variant 1) and CHD7-CR1-3-pGBKT7 (amino acids 1591-2181, NP_060250.2) demonstrating no direct interaction between FAM124B transcript variant 1 and the CHD7 part, while (B) direct yeast two hybrid experiment with the constructs FAM124B-1,3-pGADT7 (full lengths transcript variant 1) and CHD8-pGBKT7 (amino acids 1789–2302, NP_065971.2) shows a direct interaction. The same experiments were performed for FAM124B transcript variant 2. (C) Direct yeast

two hybrid experiment with the constructs FAM124B-1,2-pGADT7 (full lengths transcript variant 2) and CHD7-CR1-3-pGBKT7 (amino acids 1591-2181, NP_060250.2). **(D)** Direct yeast two hybrid experiment with the constructs FAM124B-1,2-pGADT7 (full lengths transcript variant 2) and CHD8-pGBKT7 (amino acids 1789–2302, NP_065971.2). FAM124B transcript variant 2 interacts directly with the CHD8 part, while no direct interaction with the CHD7 part could be observed.

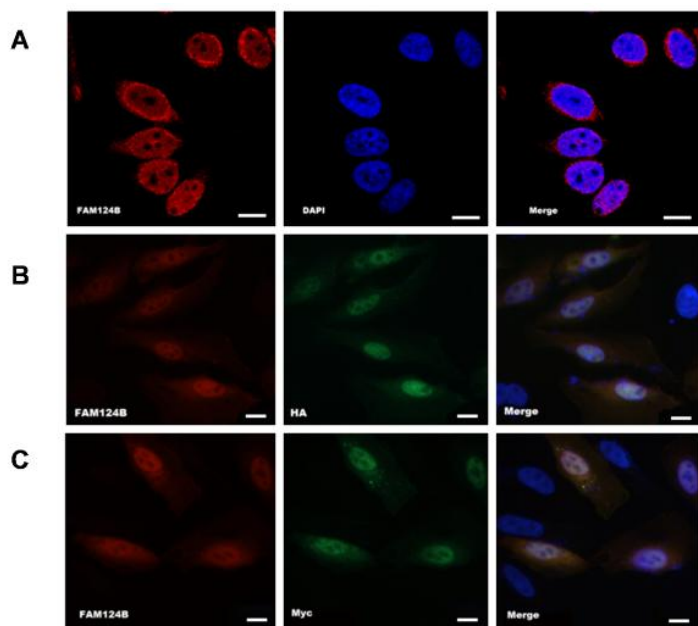


Figure 4: Subcellular localization of FAM124B.

(A) Immunofluorescence staining using a rabbit anti-Fam124B antibody (ProteinTech) on untransfected HeLa cells demonstrating a mainly nuclear localization of endogenous FAM124B.

(B) Immunofluorescence staining using the rabbit anti-Fam124B antibody and the anti-HA antibody on HeLa cells transiently transfected with the plasmid FAM124B-1,3-pCMV-HA (FAM124B transcript variant 1 fused to an hemagglutinin tag) confirmed the mainly nuclear distribution of

FAM124B and demonstrated the specificity of the FAM124B antibody.

(C) Immunofluorescence staining using the rabbit anti-Fam124B antibody and the anti-cmyc antibody on HeLa cells transiently transfected with the plasmid FAM124B-1,3-pCMV-cmyc (FAM124B transcript variant 1 fused to an cmyc tag) confirmed the further results. Scale bar = 10 μ m.

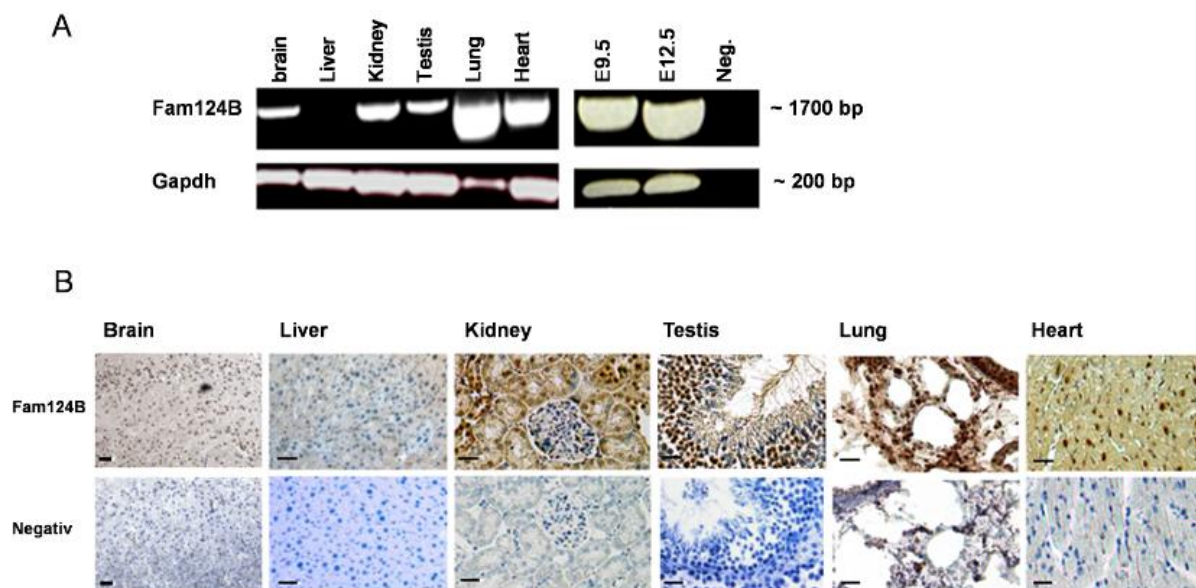


Figure 5: Expression pattern of murine Fam124B

(A) Expression pattern of murine Fam124B by semiquantitative reverse transcription polymerase chain reaction (RT-PCR) on wild type CD1 mouse tissues and E9.5 and E12.5 embryos demonstrating expression in various tissues and during development.

(B) Immunohistochemistry (IHC) performed in adult mouse tissues slightly counterstained with haematoxylin (blue) confirmed the semiquantitative RT-PCR results with high expression (brown) in lung, heart, kidney, moderate expression in brain and testis, and very low expression in liver. Scale bar = 20 μ m.

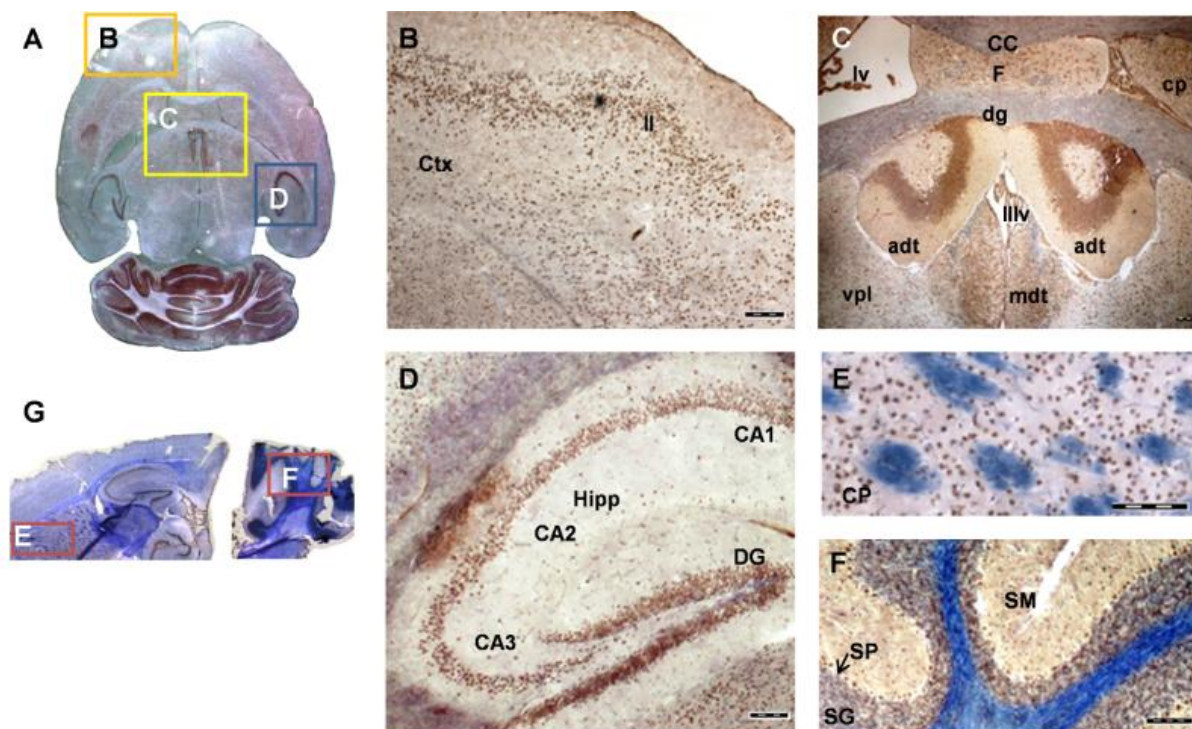


Figure 6: Fam124B expression in the mouse central nervous system.

(A) Overview of horizontal paraffin embedded brain sections (B, C, D). (G) Overview of sagittal brain cryosections (E,F). (B) Cortex, (C) Thalamic nuclei, (D) Hippocampus, (E) Caudate Putamen, (F) Cerebellum.

Ctx = Cortex, CC = Corpus Callosum, Hipp = Hippocampus, CA1-3 = Cornu Ammonis areas, DG = dentate gyrus, CP = Caudate Putamen, adt = anterior dorsal thalamic nucleus, dg = granular layer of dentate gyrus, lv = left ventricle, F = fornix, mdt = mediodorsal thalamic nucleus, IIIv = third ventricle with choroid plexus, vpl = ventral posterior thalamic nucleus, lateral part, SM = stratum moleculare, SP = stratum purkinjense, SG = stratum granulosum, II = stratum granulosum externum. Scale bar = 100 μ m.

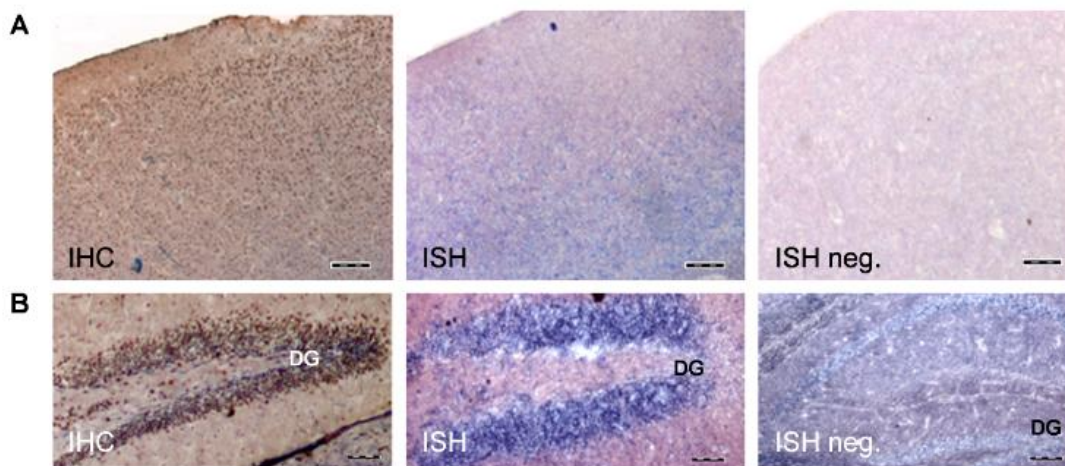


Figure 7: In situ hybridization (ISH) of Fam124B on mouse brain cryosections in comparison with immunostaining (IHC). (A) Cortex, (B) Hippocampus: An overlapping expression pattern could be demonstrated confirming the specificity of the FAM124B antibody. DG = dentate gyrus. Scale bar =100 μ m.

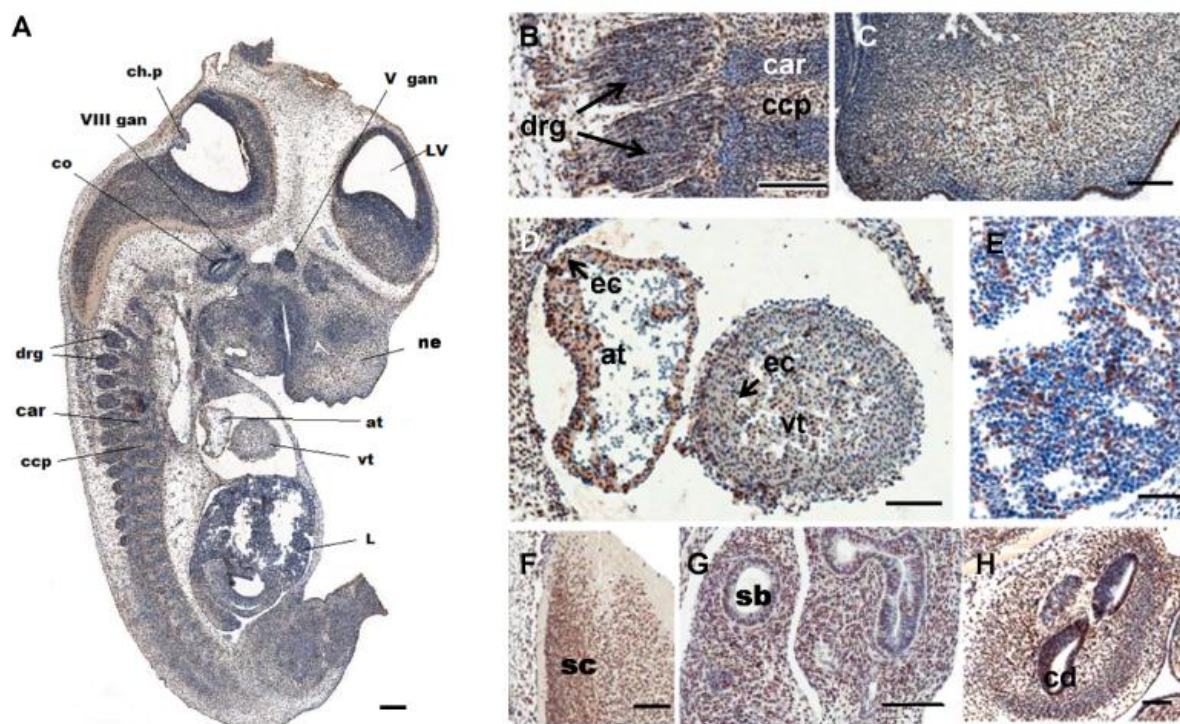


Figure 8: Fam124B expression at murine embryonic stage E12.5

Fam124B expression (brown) was found in a variety of embryonic tissues. Expression could be observed in several brain areas, spinal cord, dorsal root ganglia, developing cochlea and surrounding tissues, lung, heart, and kidney. Low expression was found in the developing liver and no expression (blue) in blood cells.

(A) Overview of Fam124B immunostaining on sagittal section of an E12.5 wildtype embryo slightly counterstained with haematoxylin, scale bar = 200 μ m. Higher magnification of (B) dorsal root ganglia, scale bar = 100 μ m (C) nasal region, scale bar = 100 μ m (D) the developing heart, scale bar = 100 μ m (E) developing liver, scale bar = 50 μ m (F) spinal cord (sc), scale bar = 50 μ m (G) developing lung with segmental bronchus (sb), scale bar = 100 μ m (H) cochlea, and surrounding tissue, scale bar = 100 μ m.

LV = lateral ventricle, ch.p = choroid plexus differentiating from fourth ventricle, co = cochlea, cd = cochlear duct, ne = nasal epithelium, V gan = left trigeminal (V) ganglion, drg = dorsal root ganglion, VIII gan = Vestibulocochlear (VIII) ganglion, at = left atrium of heart, vt = left heart ventricle, ec = endothelial cells, car = cartilage primordium of body of vertebra, ccp = cartilage condensation being primordium of vertebral body.

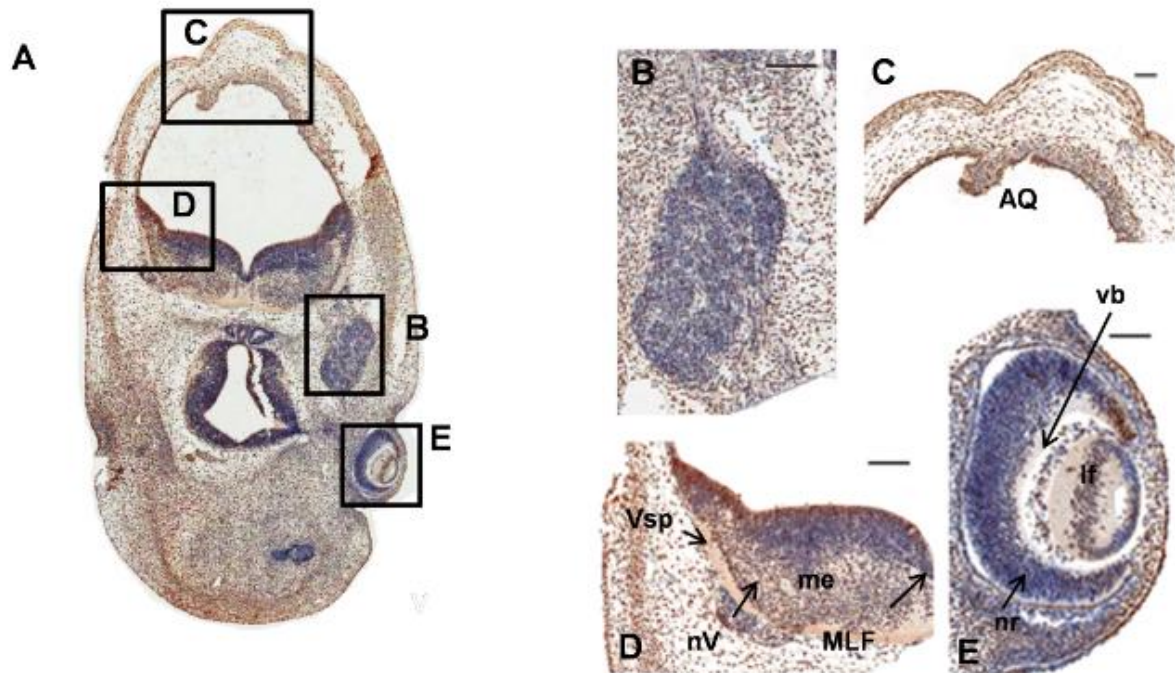


Figure 9: Fam124B expression in the developing brain at murine embryonic stage E12.5

(A) Overview of Fam124B immunostaining of the brain slightly counterstained with haematoxylin. (B) Higher magnification of the trigeminal ganglion, (C) aqueduct of Sylvius with choroid plexus = AQ (D) Higher magnification of the medulla (me) with spinal tract of trigeminal nerve (Vsp), nV = trigeminal nucleus, MLF = medial longitudinal fasciculus (E) Higher magnification of the eye, nr = neural retina, lf = lens fibers, vb = vitreous body. Scale bar = 50 μ m.

PLoS ONE

Identification and characterization of FAM124B as a novel component of a CHD7 and CHD8 containing complex

--Manuscript Draft--

Manuscript Number:	
Article Type:	Research Article
Full Title:	Identification and characterization of FAM124B as a novel component of a CHD7 and CHD8 containing complex
Short Title:	Characterization of FAM124B
Corresponding Author:	Silke Pauli University Medical Center Göttingen, GERMANY
Keywords:	FAM124B; CHD8; CHD7; interaction studies; expression pattern
Abstract	<p>Background: Mutations in the chromodomain helicase DNA binding protein 7 gene (CHD7) lead to CHARGE syndrome, an autosomal dominant multiple malformation disorder. Proteins involved in chromatin remodeling typically act in multiprotein complexes. We could previously demonstrate that a part of human CHD7 interacts with a part of human CHD8, another chromodomain helicase DNA binding protein presumably being involved in the pathogenesis of neurodevelopmental (NDD) and autism spectrum disorders (ASD). Because identification of novel CHD7 and CHD8 interacting partners will provide further insights into the pathogenesis of CHARGE syndrome and ASD/NDD, we searched for additional associated polypeptides using the method of stable isotope labeling by amino acids in cell culture (SILAC) in combination with mass spectrometry.</p> <p>Principle findings: The hitherto uncharacterized FAM124B (Family with sequence similarity 124B) was identified as a potential interaction partner of both CHD7 and CHD8. We confirmed the result by co-immunoprecipitation studies and showed by direct yeast two hybrid experiments a direct binding to the CHD8 part. Furthermore, we characterized FAM124B as a mainly nuclear localized protein with a widespread expression in embryonic and adult mouse tissues.</p> <p>Conclusion: Our results demonstrate that FAM124B is a potential interacting partner of a CHD7 and CHD8 containing complex. From the overlapping expression pattern between Chd7 and Fam124B at murine embryonic day E12.5 and the high expression of Fam124B in the developing mouse brain, we conclude that Fam124B is a novel protein possibly involved in the pathogenesis of CHARGE syndrome and neurodevelopmental disorders.</p>
Order of Authors:	<p>Tserendulam Batsukh</p> <p>Yvonne Schulz</p> <p>Stephan Wolf</p> <p>Tamara I. Rabe</p> <p>Thomas Oellerich</p> <p>Henning Urlaub</p> <p>Inga-Marie Schaefer</p> <p>Silke Pauli</p>
Suggested Reviewers:	<p>Seema R. Lalani, MD Baylor College of Medicine seemal@bcm.edu She worked since years in the field of CHARGE syndrome</p> <p>Bernd Wollnik University of Cologne, Institute of Human Genetics</p>

Powered by Editorial Manager® and Preprint Manager® from Aries Systems Corporation

4. Discussion

Mutations in the chromodomain helicase DNA binding protein 7 gene (*CHD7*) are the underlying cause for CHARGE syndrome, an autosomal dominant inherited heterogeneous multiple malformation syndrome (Vissers et al. 2004). In 10-20% of patients with typical signs of CHARGE syndrome and in 40-50% of patients with an atypical presentation no mutation could be found and therefore the molecular cause is unknown. The characterization of *CHD7* interacting partners can help to understand the pathogenesis of the disease. In our working group a part of *CHD8*, another member of the CHD family of proteins, was identified by yeast two hybrid library screen as a putative interaction partner of *CHD7*. The interaction was confirmed by bimolecular fluorescence assay (BiFC), direct Yeast two Hybrid and Co-IP experiments. Furthermore, we investigated the *CHD7-CHD8* interaction in the presence of 4 *CHD7* missense mutations. Indeed, three out of 4 mutations lead to a loss of interaction by direct interaction studies, while the interaction still remained in Co-IP studies. Because of these results we suggest that *CHD7* and *CHD8* interact directly (shown by the Y2H experiments) and indirectly via additional linker proteins (in Co-IP results). Therefore we searched for additional *CHD7* and *CHD8* associated proteins by using the method of SILAC in combination with mass spectrometry. As a novel interacting partner of a part of *CHD7* and a part of *CHD8* we identified the unknown protein *FAM124B*. We further characterized the expression profile and the subcellular localization of *FAM124B*. Moreover, our results let us suggest that *FAM124B* might be very important for embryonic development and could play a role in the pathogenesis of CHARGE syndrome and autism and neurodevelopmental disorders.

4.1 Known *CHD7* complexes and function

Since the discovery that *CHD7* mutations lead to CHARGE syndrome, its functions have been studied to a greater extent. To date, *CHD7* is known to be involved in several cell and tissue specific complexes (Takada et al. 2007, Bajpai et al. 2010, Schnetz et al. 2009, 2010). In human multipotent neural crest like cells, *CHD7* regulates neural crest and placode formation by binding to components of the BAF/PBAF complex (Bajpai et al. 2010, Fig. 4.1A). BAF/PBAF complexes are chromatin remodeling complexes, which are involved in developmental transitions. The composition of the complex is tissue and developmental stage dependent (Ho & Crabtree 2010).

With an approach of chromatin immunoprecipitation and microarray-based sequence analysis (ChIP-chip) in human colorectal carcinoma cells, human neuroblastoma cells, and mouse ES cells before and after differentiation into neural precursor cells, *CHD7* has been

demonstrated to have tissue and cell type specific temporal functions via localizing to methylated histone H3 lysine 4 (H3K4) in enhancer regions of various genes (Schnetz et al. 2009). A further study in mouse embryonic stem (ES) cells indicates that CHD7 colocalizes with Oct4, Sox2, Nanog, and p300 and functions by binding to enhancers as a transcriptional modulator and fine-tuning the expression levels of ES cell-specific genes in either a positive or negative way (Schnetz et al. 2010, Fig. 4.1B). In addition, CHD7 forms a complex with NLK, SETDB1 and PPAR- γ and binds to methylated lysine 4 and lysine 9 residues on histone H3 at PPAR- γ target promoters in mesenchymal stem cells. Therefore it is suggested that CHD7 is involved in the regulation of cell fate specification (Takada et al. 2007, Fig. 4.1C).

Furthermore, in *Drosophila*, Kismet, a homolog of the human CHD7 protein, has been proven to be crucial for proper axon pruning and development of fly's central nervous system (Melicharek et al. 2010). Another functional study could demonstrate that Kismet promotes early transcriptional elongation through RNA polymerase II by recruiting the histone methyltransferases ASH1 and TRX to chromatin (Srinivasan et al. 2008).

CHD7 is localized in the nucleolus and the nucleoplasm (Zentner et al. 2010, Kita et al. 2012). Interestingly, recently it has been shown that CHD7 codes for two transcripts. The shorter transcript is generated by alternative splicing of exon 6 and contains only one chromodomain. This transcript variant was shown to localize in the nucleolus (Kita et al. 2012). CHD7 regulates positively rRNA biosynthesis and is associated with rDNA (Zentner et al. 2010). Indeed, it has been shown that both CHD7 transcripts regulate 45S precursor rRNA production (Zentner et al. 2010, Kita et al. 2012). Moreover overexpression studies showed that the long CHD7 transcript (CHD7L) supports Sox2-mediated transcriptional regulation whereas the short CHD7 transcript (CHD7S) suppresses it (Kita et al. 2012). Treacher Collins syndrome (TCS) is a multiple congenital anomaly caused by mutations in the *TCOF1* gene, encoding the protein treacle (Valdez et al. 2004, Dixon et al. 2007). TCS and CHARGE syndrome are distinct diseases, but share some common features such as eye and ear defects. Like CHD7, treacle is associated on rDNA and act as a positive regulator of rRNA synthesis. Indeed, Zentner et al. (2010) could show that CHD7 is needed for treacle (*TCOF1*) to associate with rDNA (Fig. 4.1D). These findings imply a functional link between CHARGE syndrome and Treacher Collins syndrome.

These reports show crucial roles for CHD7 in the transcriptional regulation of target genes, its effects on developmental stages and various tissue specific processes and the pathogenetic connection between CHARGE syndrome and other malformation syndromes like Treacher Collins syndrome.

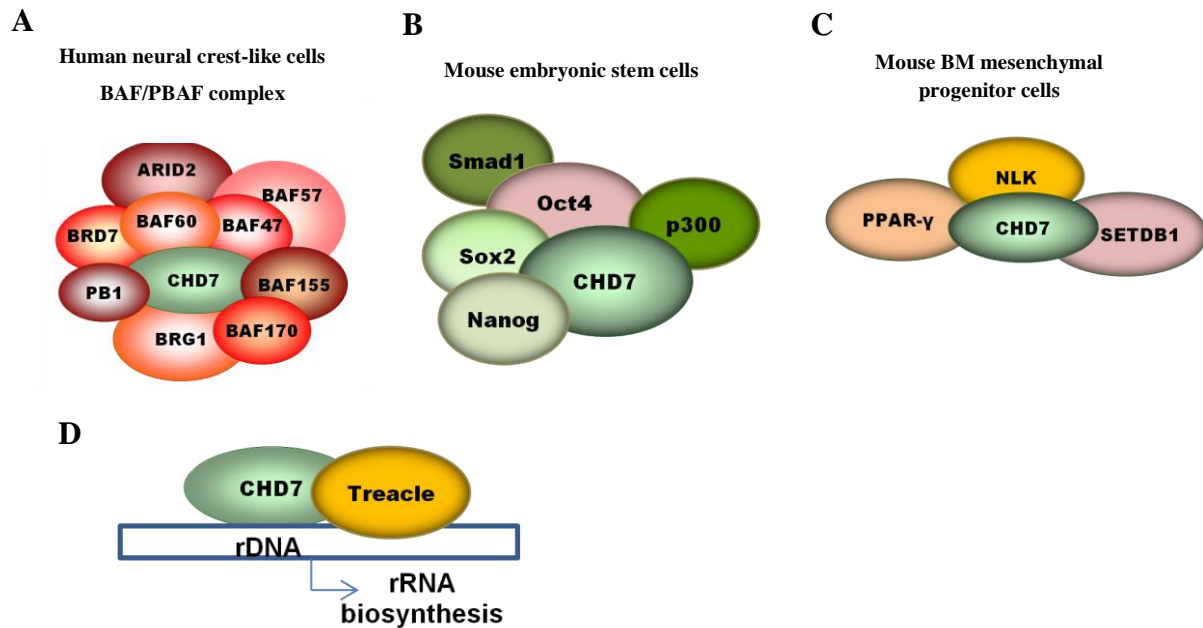


Figure 4.1. Models for CHD7 complexes. **A:** Human neural crest-like cells, BAF/PBAF complex (Bajpai et al. 2010), **B:** A complex in mouse embryonic stem cells (Schnetz et al. 2010), **C:** A complex in mouse bonemarrow mesenchymal progenitor cells (Takada et al. 2007), **D:** CHD7 and Treacle association on rDNA (Zentner et al. 2010).

4.2 Known CHD8 complexes and function

Chromodomain helicase DNA binding protein 8 (CHD8) is a chromatin remodeling enzyme that belongs to the CHD subgroup III. Typical additional domains of this subgroup are three conserved regions (CR1-3), a SANT and two BRK domains. CHD proteins utilize ATP hydrolysis to modify chromatin structure and to regulate transcriptional processes (Marfella & Imbalzano 2007). CHD8 was first described in *Xenopus* by Sakamoto et al. (2000). They named the protein Duplin (for axis duplication inhibitor). It was shown that Duplin is a nuclear protein that directly binds to β -catenin and inhibits Wnt/ β -catenin signaling (Sakamoto et al. 2000). The second chromodomain is responsible for the β -catenin interaction. In addition, they could show that Duplin regulates β -catenin- T-cell factor (Tcf)-dependent downstream genes (Chung et al. 1997, Kobayashi et al. 2002). However, Duplin is an N-terminal fragment of Chd8 which lacks the catalytic Snf2 helicase domain and all further domains. Later, full length of CHD8 has been shown to bind also directly to β -catenin (Thompson et al. 2008).

Nishiyama et al. (2004) created Duplin knock-out mice. Duplin mutant homozygous embryos show growth retardation accompanied by massive apoptosis leading to death at E7.5. Later they demonstrated CHD8 binds to both p53 and histone H1 proteins. The p53–CHD8–histone H1 complex is required for suppression of p53 target genes transcription, and therefore

prevents apoptosis induced by genotoxicity (Nishiyama et al. 2009, Fig. 4.2A). Interestingly, the Wnt signaling pathway is regulated by CHD8 in a similar way. CHD8 promotes the β -catenin–CHD8–histone H1 trimeric complex on chromatin (Nishiyama et al. 2012, Fig. 4.2B).

CHD8 is shown to be involved in various protein complexes depending on the cell type and developmental stage. Mouse *Chd8* has been shown to play a role in Ctf-dependent insulator function by binding directly Ctf (11-zinc finger protein or CCCTC-binding factor) (Ishihara et al. 2006). Furthermore, various experiments on smooth muscle cells (SMCs) could demonstrate that complexes including CHD8, Serum Response Factor (SRF) and CCTF play an essential role in differentiation and maintenance/survival of SMCs (Rodenberg et al. 2010, Fig. 4.2C).

Additionally, CHD8 was copurified with a large protein complex including Wdr5, Ash2L, and RbBP5 (WAR), which are known members of the Mixed Lineage Leukemia (MLL) histone modifying complex (Dou et al. 2005, Thompson et al. 2008, Yates et al. 2010, Fig. 4.2D). MLL1 or 2, the trithorax orthologs in *Drosophila*, built together with RbBP5-WDR5 and ASH2L a complex which acts as a methyltransferase. This complex composition regulates the *HOXA2* gene transcription in a positive manner (Hess 2004, Wysocka et al. 2005). In contrary, it has been demonstrated through CHD8 shRNA downregulation in pluripotent human testicular embryonal carcinoma cell lines that CHD8 with the WAR complex members WDR5, ASH2L and RbBP5 negatively regulates *HOXA2* expression (Yates et al. 2010).

CHD8 interacts with the human Staf protein for efficient U6 gene transcription in vivo and it has been demonstrated by Chip analysis that CHD8 binds to both Pol II and Pol III snRNA promoters (Yuan et al. 2007). Moreover, CHD8 binds specifically to histone H3 di-methylated at lysine 4 with its chromodomains (Rodríguez-Paredes et al. 2009). CHD8 also binds the elongating form of RNA polymerase II to control the expression of cyclin E2 and thymidylate synthetase (TYMS) (Rodríguez-Paredes et al. 2009).

In addition, CHD8 is associated directly with the androgen receptor (AR) which could demonstrate a role for CHD8 in AR-mediated regulation of target genes (Menon et al. 2010). Collectively, CHD8 has various interaction partners depending on the cell type. Depending on the complex partners CHD8 functions in different processes like repressing apoptosis, differentiation and survival of SMCs, transcriptional repression and regulation of specific target genes.

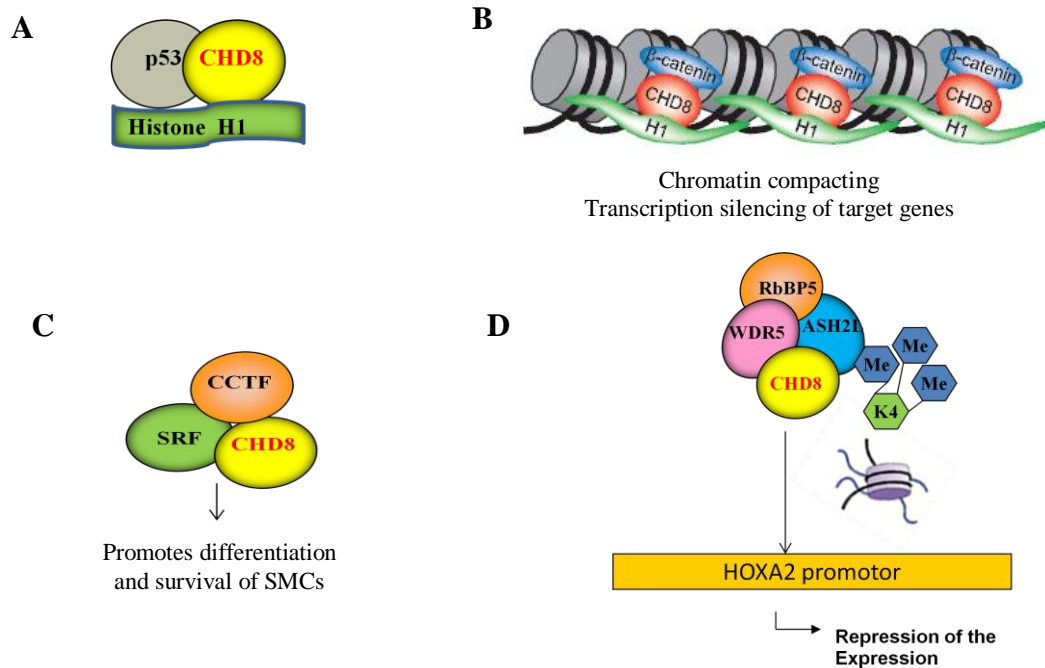


Figure 4.2. Models for CHD8 complexes. **A:** p53–CHD8–histone H1 complex regulates apoptosis during embryogenesis (Nishiyama et al. 2009), **B:** CHD8 interacts with β -catenin and subsequently recruits histone H1, resulting in chromatin compaction and transcriptional silencing of Wnt target genes (adapted and modified from Nishiyama et al. 2012), **C:** CHD8, SRF and CCTF complex is important for differentiation and survival of smooth muscle cells (Rodenberg et al. 2010), **D:** The human WAR (WDR5, RbBp5, ASH2L) complex repress *HOXA2* gene expression when CHD8 is included (Thompson et al. 2008).

4.3 CHD8 builds together with CHD7 a complex

In our working group we searched for CHD7 interaction partners by performing yeast two hybrid library screen of a human fetal brain library. CHD8 was identified as a potential CHD7 interaction partner. The interaction was confirmed by direct yeast two hybrid and in HeLa cells by Co-IP and BiFC-assay (bimolecular fluorescence complementation assay). Interestingly, when we narrow down the interacting area of CHD8, a region of unknown functions without predicted domains was identified. The predicted sizes of the CHD7 and CHD8 proteins are 334 kDa and 290 kDa, respectively. Because of such a huge size of the endogenous CHD7 and CHD8 proteins, western blot detection needs to be done by a harsh nuclear isolation protocol as well as wet blotting technique. CHD8 is expressed relatively strong in HeLa cells (Nishiyama et al. 2009, 2012), whereas endogenous CHD7 expression is very low. Therefore, we were not able to perform Co-IP experiments with endogenous CHD7 in HeLa cells (data not shown). To demonstrate, the endogenous CHD7-CHD8 interaction we used the new method of Proximity Ligation Assay (PLA, Olink) (Fig. 4.3). In this method, two target

proteins can be detected with specific antibodies produced in two different species. Specific oligonucleotide labeled secondary antibodies (PLA probes) generates fluorescence spots only when the two PLA probes have bound in close proximity. In our case, the PLA probes produce red fluorescence spots.

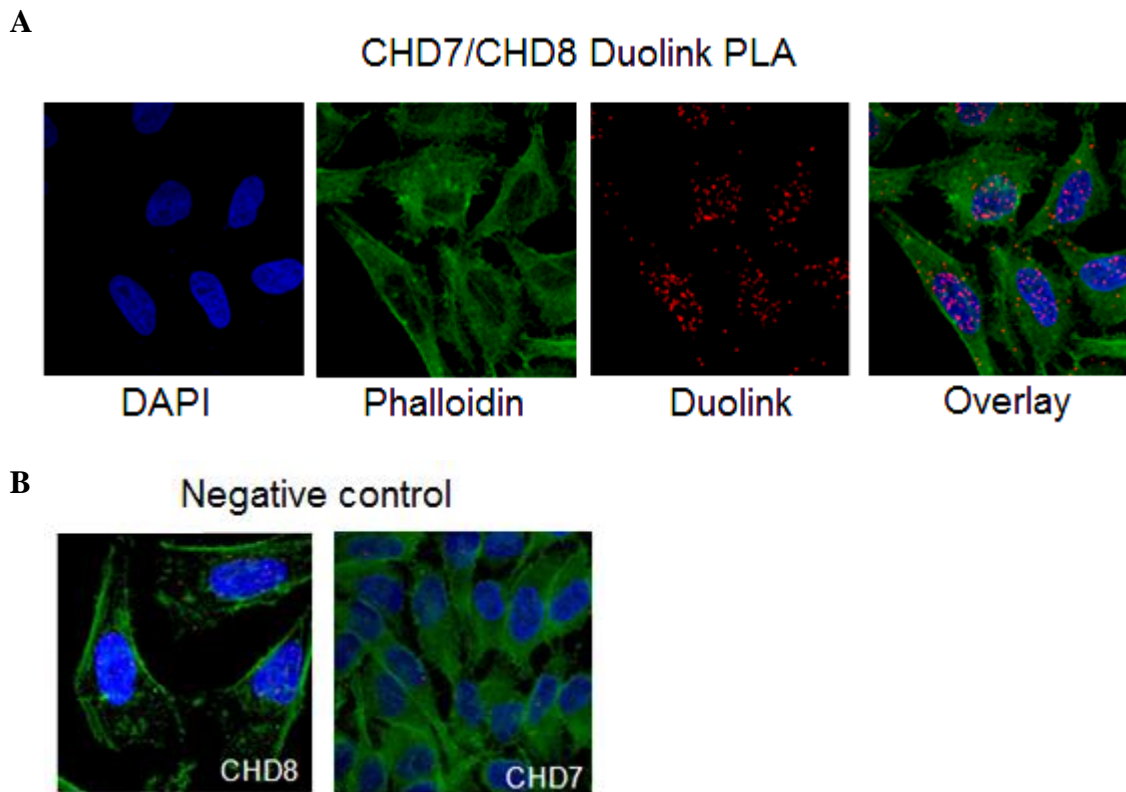


Figure 4.3. CHD7 and CHD8 endogenous interaction in HeLa cells shown by the Duolink PLA method.

Cell nuclei were counterstained with DAPI and cytoskeleton was stained by Phalloidin/FITC. Interacting areas are visualized as red fluorescence spots. **A:** CHD7 and CHD8 interaction can be seen in the nucleus. **B:** Technical negative control for the CHD7 and CHD8 antibodies. The primary CHD7 and CHD8 antibodies are used separately with 2 PLA probes. There are very few red dots in negative control which indicates antibodies do bind specifically (done by Yvonne Schulz 2011).

Moreover, in mammals CHD3 and CHD4, two other members of the CHD family, build together a core component of the NuRD complex (Xue et al. 1998, Hall & Georgel 2007). In lower organisms like *Drosophila*, not all orthologs of the known human CHD genes are existing. For instance, *Kismet* is the only ortholog of all human CHD subgroup III members in *Drosophila*. *Kismet* mutant *Drosophila* larvae showed more severe influence on some transcription factors than CHD7, CHD8 or CHD9 solely did in mammals (Srinivasan et al. 2005, Rodríguez-Paredes et al. 2009). Because of these observations, it is suggested that other CHD subgroup members might have overtaken functions of *Kismet*. Furthermore, it is hypothesized that depletion of one CHD subgroup member leads to a gene-specific, but not a

general influence (Rodríguez-Paredes et al. 2009). Deletions of the region 14q11.2 including the CHD8 and SUPT16H gene have been found in three patients with facial dysmorphism, developmental delay and cognitive impairments (Zahir et al. 2007). The authors concluded that haploinsufficiency of either the CHD8 and/or the SUPT16H are the reason for the phenotype in the patients (Zahir et al. 2007). Even though these patients' phenotype is different from CHARGE syndrome, we considered that missense mutations in the *CHD8* gene disturbing the function of its interacting partner CHD7 might lead to CHARGE syndrome. Therefore, we analyzed in our working group 25 CHD7 negative CHARGE syndrome patients for missense mutations in the CHD8 gene. We did not find a pathogenic CHD8 mutation in our collective (Batsukh et al. 2010). Interestingly, it has been reported recently that some patients with autism (ASD) and neurodevelopmental disorders (NDD) have de novo missense or nonsense mutations in the *CHD8* gene as well as microdeletions (Zahir et al. 2007, Neale et al. 2012, O'Roak et al. 2012, Talkowski et al. 2012). Because of these results, it is now clear that *CHD8* mutations are not an underlying cause of CHARGE syndrome, but interestingly about two thirds of children with CHARGE syndrome suffer from autism spectrum disorders (Betancur 2011). Our findings that CHD7 and CHD8 interact with each other might shed some light in the understanding of the connection between ASDs/NDDs and CHARGE syndrome.

4.4 Evaluating the effect of 4 CHD7 missense mutations on the interaction between CHD8 and CHD7

We wanted to check if the CHARGE syndrome causing CHD7 missense mutations have an effect on the CHD7-CHD8 interaction (Batsukh et al. 2010). We studied the three known CHD7 mutations (p.His2096Arg, p.Val2102Ile and p.Gly2108Arg) (Felix et al. 2006, Lalani et al. 2006, Jongmans et al. 2008) as well as a mutation newly identified in our lab (p.Trp2091Arg). All four missense mutations are within the CHD7 part involved in the CHD7-CHD8 interaction (Batsukh et al. 2010). Interestingly, all four missense mutations lead to a phenotype in the patients classified as atypical CHARGE syndrome (Felix et al. 2006, Lalani et al. 2006, Jongmans et al. 2008, Batsukh et al. 2010). In direct Y2H experiments three (p.Trp2091Arg, p.His2096Arg and p.Gly2108Arg) of the four missense mutations disrupt the CHD7-CHD8 interaction. Our patient with the missense mutation p.Trp2091Arg has bilateral coloboma and microphthalmia of the left eye, microcephaly, unilateral deafness and mental retardation (Batsukh et al. 2010). Only one out of five affected members of two families with the missense mutation p.Gly2108Arg fulfilled the diagnostic criteria for CHARGE syndrome while the others showed a very mild phenotype (Jongmans et al. 2008)

In contrast, Co-IP interaction study showed no disruption in CHD7-CHD8 interaction by the four missense mutations in the CHD7 part. While the Y2H is a good technique to test direct interactions between proteins, the Co-IP is a method which allows purifying the whole complex. Because of the Co-IP results, we hypothesize that there must be a linker protein which still keeps the mutated CHD7 together with CHD8 in the same complex (Batsukh et al. 2010). Therefore, we further searched for possible linker proteins that could help us to understand the pathomechanism behind CHD7 mutations (see next 4.5).

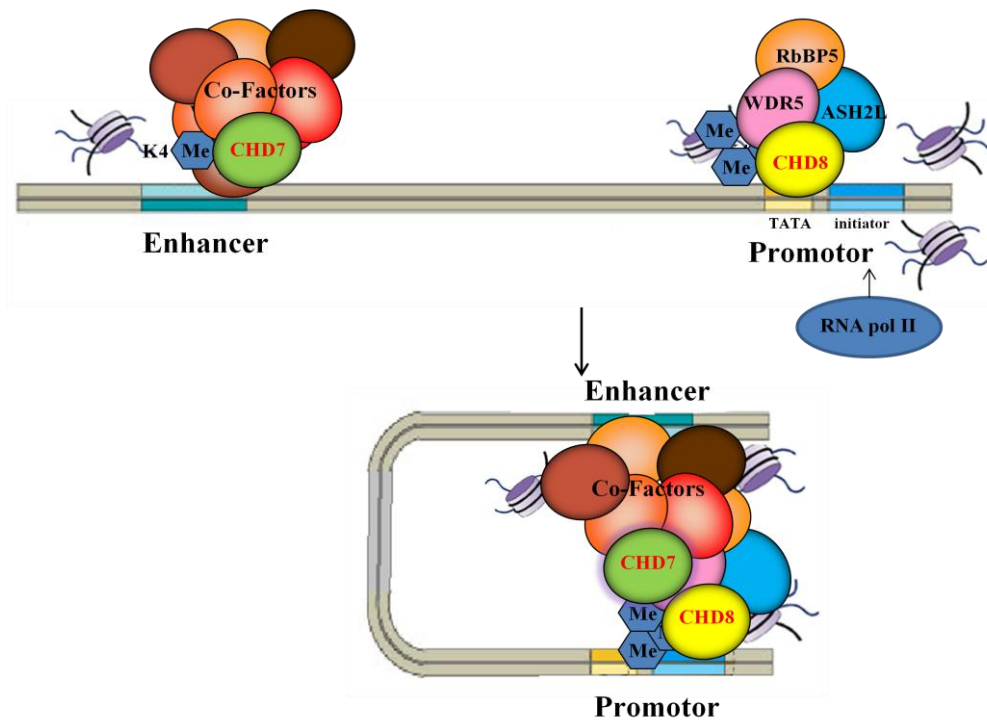


Figure 4.4. Hypothetical Enhancer and Promoter interaction via CHD7 and CHD8 containing protein/transcription factors (TF) complex mediated DNA-loop model. Protein and protein interactions between various TFs (including CHD7 and CHD8) and RNA pol II activate transcription (Modified from Garrath & Grisham Biochemistry, 1999) (Thompson et al. 2008, Schnetz et al. 2010).

Collectively, from these studies we suggest a hypothetical DNA-loop model which is mediated by CHD7 and CHD8 containing protein complexes and leading to an enhancer and promoter interaction (Fig. 4.4). Furthermore, it can be postulated that CHD7 and CHD8 can build a core component of one big complex, probably present in a cell type and developmental stage specific manner. Further characterization of these complexes can help to understand the pathogenesis of CHARGE syndrome.

4.5 FAM124B is associated with CHD7 and CHD8

Our interaction study of CHD7 and CHD8 led us to conclude that both proteins are components of a huge complex, with additional proteins acting as linker proteins between

CHD7 and CHD8. Therefore, we used the method of SILAC in combination with mass-spectrometry to further characterize such complex. In particular, we could find FAM124B as a potential interaction partner of CHD7 and CHD8 in all three repetitions of the experiment (manuscript in submission stage: Batsukh et al. 2012). We could confirm the interaction of FAM124B with both CHD7 and CHD8 by Co-IP. However, a direct interaction investigated by Yeast two hybrid experiments could only be demonstrated for both FAM124B transcripts with a CHD8 part, containing a region of unknown function and one BRK domain (amino acids 1789–2302). No interaction could be seen between FAM124B and the CHD7 part containing the CR1-3/SANT domain region (amino acids 1591-2181). Probably FAM124B interacts with CHD7 by binding to another than the tested region or via CHD8 or additional proteins (see 4.7).

4.6. Subcellular localization and expression profile of Fam124B in comparison of Chd7 and Chd8

We further investigated the subcellular localization of FAM124B. We could demonstrate that endogenous FAM124B is localized mainly in the nucleoplasm. CHD8 is a nuclear protein (Ishihara et al. 2006) whereas CHD7 is shown to be expressed in nucleolus and nucleoplasm (Zentner et al. 2010, Kita et al. 2012). Thus, we suggest the interaction between FAM124B, CHD8 and CHD7 might be in the nucleoplasm.

CHD7 expression patterns in all analyzed species (Human, mouse, chicken, zebrafish) are congruent with the organs affected in CHARGE syndrome (Bosman et al. 2005, Lalani et al. 2006, Sanlaville et al. 2006, Aramaki et al. 2007, Patten et al. 2012). Therefore, we analyzed the expression of Fam124B in comparison with Chd7 and Chd8 by immunostaining on different adult and embryonic mouse tissues (Fig 4.5-7). All the positive stained cells show brown color. The expression pattern of Fam124B correlates in the cornu ammonis of the hippocampus and in the cortex nicely with the Chd8 expression pattern. Chd7, Chd8 and Fam124B are all three highly expressed in the stratum purkinjense of the cerebellum (Fig. 4.5). Because it is known that Chd8 and Chd7 are highly expressed during early embryogenesis and the expression is decreased in some adult tissues (Nishiyama et al. 2004, 2009, Bosman et al. 2005) we expanded our studies on E12.5 mouse embryos.

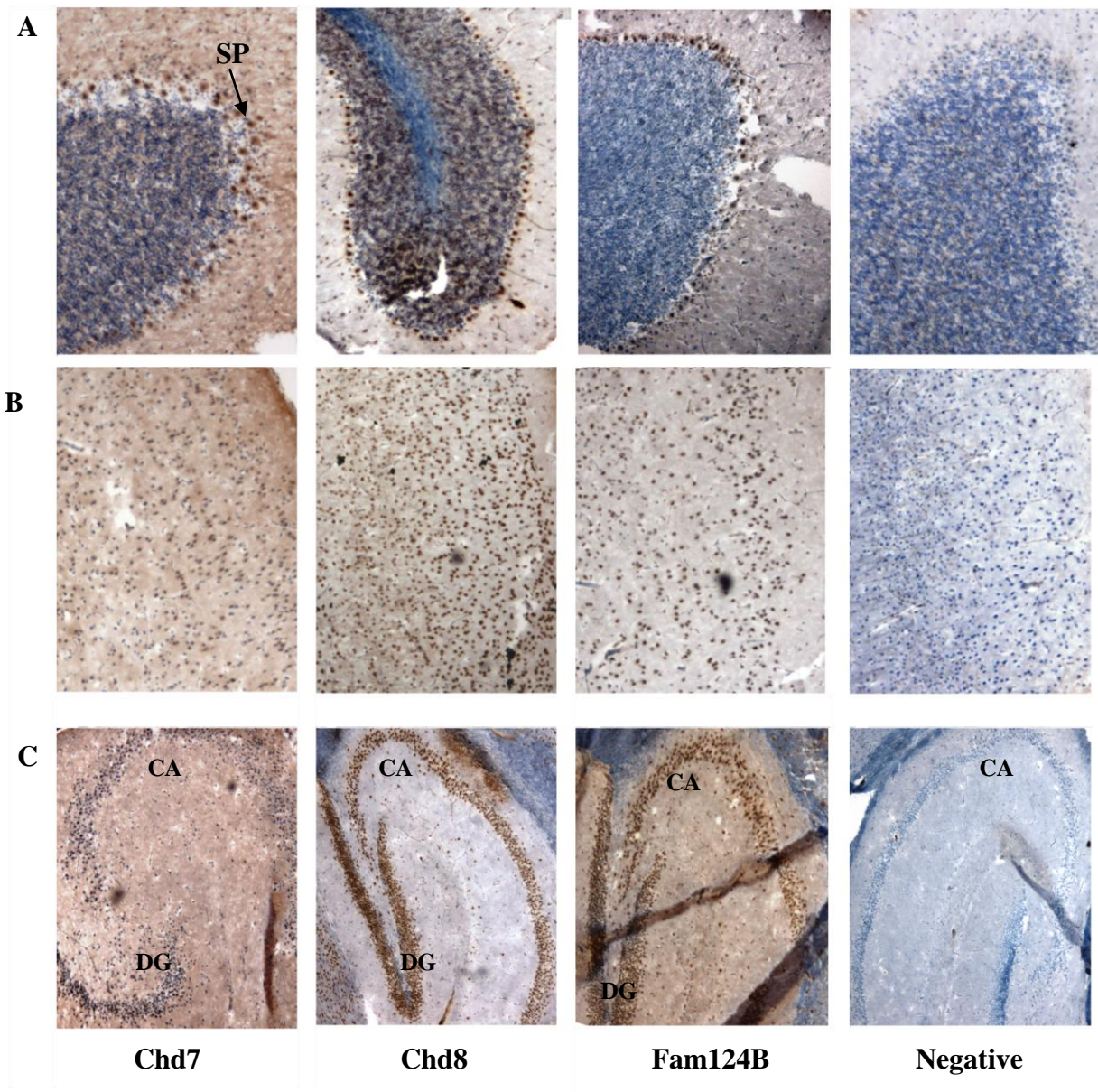


Figure 4.5. Immunostaining Fam124B of adult brain shown in comparison with Chd7 and Chd8.

Counterstained with hematoxylin eosin. **A:** Cerebellum, SP- stratum purkinjense; **B:** cortex area, **C:** Cornu ammonis of hippocampus (CA) and dentate gyrus (DG) area.

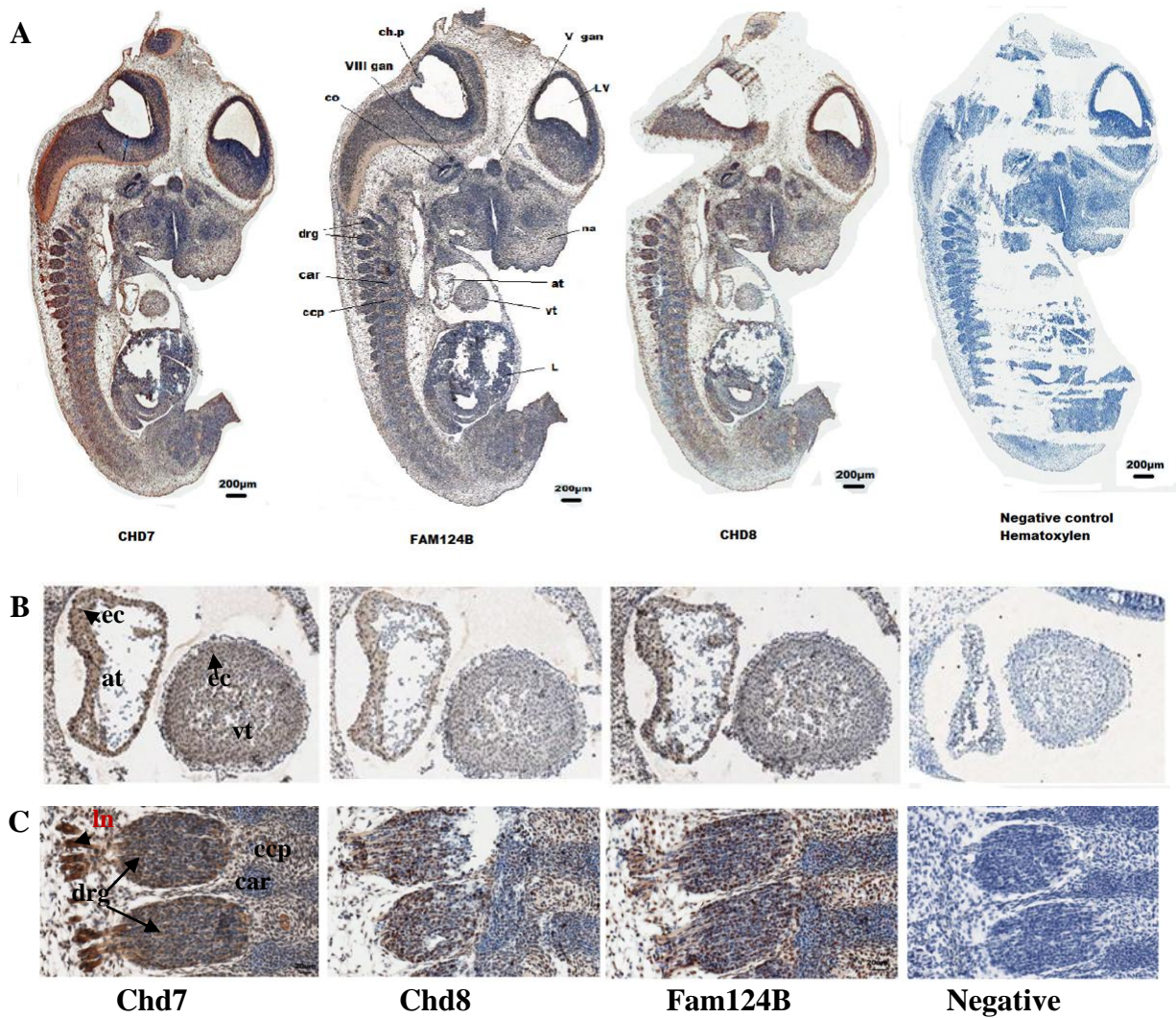


Figure 4.6. Chd7, Chd8 and Fam124B immunostainings on sagittal sections of an E12.5 wildtype embryo. Counterstained with hematoxylin eosin. **A:** Overview of immunostainings on sagittal section of an E12.5 wildtype embryo, LV = lateral ventricle, ch.p = choroid plexus differentiating from fourth ventricle, co = cochlea, cd = cochlear duct, ne = nasal epithelium, V gan = left trigeminal (V) ganglion, drg = dorsal root ganglion, VIII gan = Vestibulocochlear (VIII) ganglion, L = liver, na= nasal region, ccp = **B:** the developing heart, at = left atrium of heart, vt = left heart ventricle, ec = endothelial cells, **C:** dorsal root ganglion, car = cartilage primordium of body of vertebra, ccp = cartilage condensation being primordium of vertebral body, ln=lumbar nerve, drg=dorsal root ganglion.

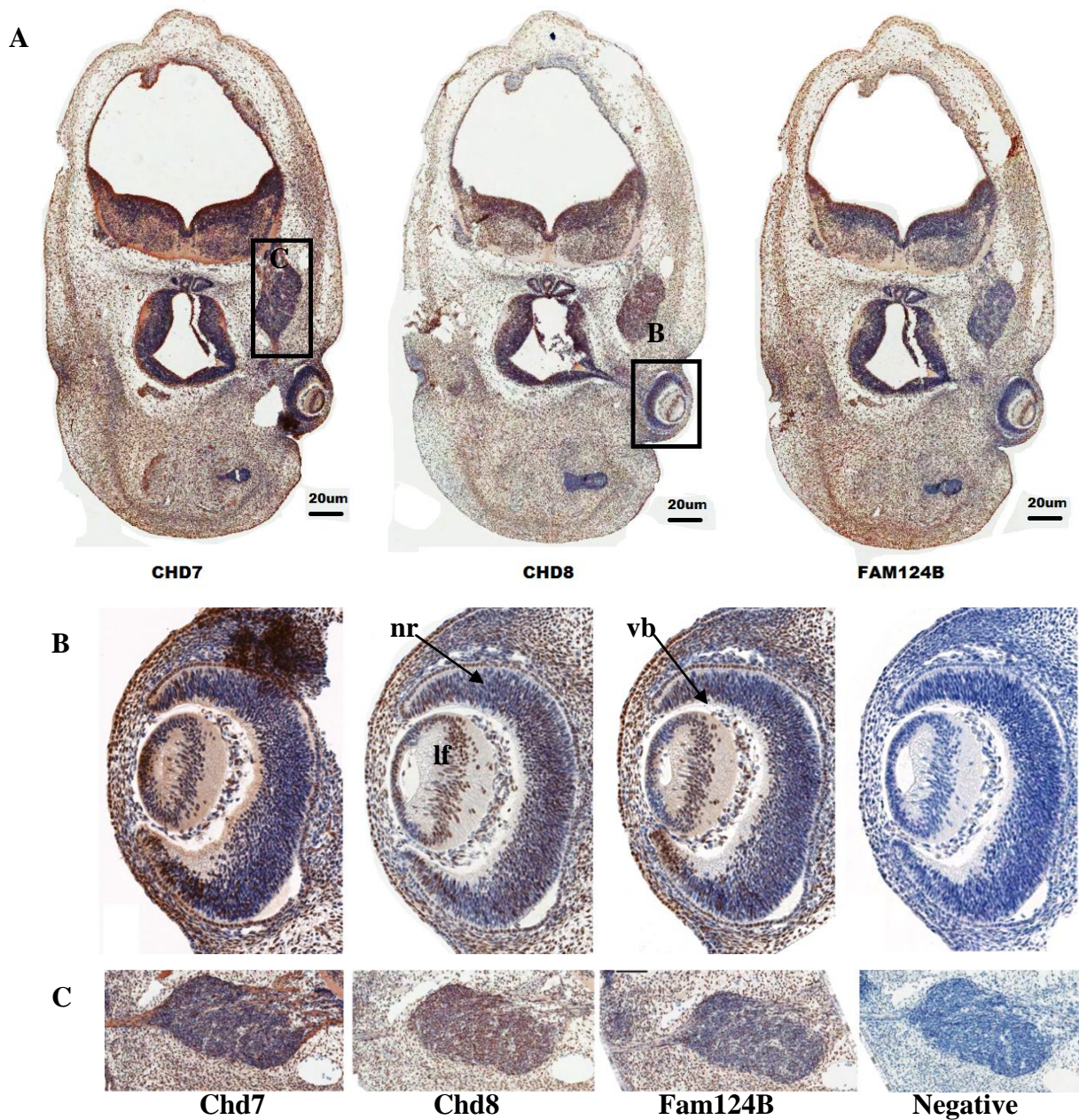


Figure 4.7. Chd7, Chd8 and Fam124B immunostaining on coronal sections of the E12.5 mouse embryo.

Counterstained with hematoxylin eosin. **A:** Overview of the immunostaining of E12.5 embryo, **B:** Higher magnification of the embryonic eye, nr = neural retina, lf = lens fibers, vb = vitreous body, **C:** Higher magnification of the trigeminal ganglion.

In sagittal and coronal sections of E12.5 embryos, the developing heart, the dorsal root ganglia, and the developing eyes were strongly stained by the Chd7, Chd8 and Fam124B antibodies (Fig. 4.6, 4.7). Our Chd7 results fit with the results of Chd7 expression study performed on E12.5 mouse tissues, which demonstrated high expression in the developing brain (ventricles, hypothalamus, olfactory epithelium, olfactory tissues, pituitary, olfactory

sensory neurons, vestibulocochlear ganglion, dorsal root ganglia, developing lung and heart) (Bosman et al. 2005). Lowest expression could be observed in the developing liver (Fig. 4.6). Fam124B expression at E12.5 was found in several brain areas, spinal cord, dorsal root ganglia, cochlea and surrounding tissues, lung, heart, and kidney. Therefore, Fam124B expression pattern correlates in many embryonic tissues with the Chd7 expression pattern.

We demonstrated that FAM124B is a nuclear protein which possibly builds together with CHD7 and CHD8 a complex. Fam124B is highly expressed at mouse developmental stage E12.5 with an overlapping correlation to Chd7 expression and a correlation to Chd8 expression especially in the developing mouse brain. Therefore, we assume a role for FAM124B in the pathogenesis of CHARGE syndrome and ASD/NDD.

4.7 Structure and Function of FAM124B

FAM124B is localized on chromosome 2q36.2. It has two transcripts in human and chimpanzee and only one in mouse and other species which is homologous to the longer human transcript. FAM124B is an evolutionary highly conserved protein which could have an important role in the cell (see 4.6). By bioinformatic prediction programs, we could not find any functional domain in FAM124B. Interestingly, alignment of the amino acid sequence of FAM124B from human to zebrafish revealed an area containing human amino acids 109-255 which show 100% homology between the species (Fig. 4.8). These data imply us that this region could contain an important hitherto unknown domain motif or this region is of functional relevance. Further investigations to clarify this aspect are needed.

In our study we could show that *in vivo* and *in vitro* FAM124B is localized in the nucleoplasm (manuscript in submission Batsukh et al. 2012). No previous characterization and functional studies on FAM124B gene have been performed. In order to identify additional proteins which interact with FAM124B, we overexpressed the FAM124B transcript variant 1 (longer transcript variant, NP_001116251.1 3) in HeLa cells and performed a pull down with the anti-Ha (Roche) antibody followed by SDS-PAGE electrophoresis separation and mass-spectrometry analysis (data not shown). Interestingly, two times out of three repetitions of the experiment we detected treacle, the protein mutated in Treacher Collins syndrome. It was shown that treacle and CHD7 bind to rDNA. Furthermore, it was demonstrated that the absence of CHD7 impaired the ability of treacle to bind rDNA (Zentner et al. 2010). Therefore, the authors suggest a connection between CHD7 and treacle and moreover they hypothesized a functional link between CHARGE and Treacher Collins syndrome (see 4.1). From our data we suggested that possibly treacle builds a complex together with CHD7, CHD8 and FAM124B.

145	SFDNYEDAIRLYEMILQREATLQKSNFCFFVLYASKSFALQLSLKQLPPGMSVDPKESSVLQFKVQEIGQLVPLLNPFCM	224	[Homo sapiens] Human
145	SFDNYEDAVRLYEMILQREATLQKSNFCFFVLYASKSFALQLSLKQLPPGMSVDPKESSVLQFKVQEIGQLVPLLNPFCI	224	[Pan troglodytes] Chimpanzee
145	SFDNYEDAIRLYEMILQREATLQKSNFCFFVLYASKSFALQLSLKQLPPGMSVDPKESSVLQFKVQEIGQLVPLLNPFCI	224	[Pongo abelii] Orangutan
145	SFDNYEDAIRLYAMILQREATLQKSNFCFFVLYSTETFALQLSLKQLPLGTSVDPKEASVLQFKVQEIGQLVPLLPHPCV	224	[Bos taurus] Cow
145	SFDNYEDAIRLYEMILQREATLQKSNFCFFVLYATNSFALQLSLKQLPPGMSVDPKSSVLQFKVREIGQLVPLLNPFCI	224	[Callithrix jacchus] Marmoset
145	SFDNYEDAIRLYELILQKEATLQKSNFCFFVLYATESFALQLSLKQLPLGVSVDPKESSVLQFKVQEIGQLVPLLPHPCV	224	[Canis lupus familiaris] Dog
145	SFDNYEDAIRLYEMILQREATLQKSDFCFFVLYATESFTLQSLKQLPLGMAVDPKEASVLQFKVQEIGQLVPLLPHPCV	224	[Sus scrofa] Pig
145	SFDNYDDAVGLYEMILRKEATVRKSNFCFFVLYATRTIAVQLCLKQLPIGMAEPKESLLQFKVQEMGQLVPLLNPFCI	224	[Gallus gallus] Chicken
145	SFDNYEDAIRLYEMILQRDATVQKSNFCFFVLYATEGFSLQLSLKQLPLGMPVDPKESSVLQFKVQEIGQLVPLLNPFCV	224	[Cricetulus griseus] Hamster
145	SFDNYEDAIRLYEMILLQRDATVQKSDFCFFVLYATEGFSLQLSLKQLPLGMSVDPKESSVLQFKVQEIGQLVPLLNPFCV	224	[Mus musculus] Mouse
145	SFDNYEDAIRLYEMILLQRDATVQKSDFCFFVLYATEGFSLQLSLKQLPLGMSVDPKESSVLQFKVQEIGQLVPLLNPFCV	224	[Rattus norvegicus] Rat
147	SFDNYEDIVRLYETVLQKRAEEQKPGFCWFTLLAEQGFSLQLAIKQLSPGVRVEPCQSAVLQFRVREIGQLVPLLNPNTCS	226	[Xenopus tropicalis] Frog
144	SCDNYEDAVRLYETILQKEATTQKAGFCFFVLYSTTHSVQLSIKQLHPGISVQVKDACALQFAIHAVGQLVPLLPHYPCV	223	[Danio rerio] Zebrafish

Figure 4.8. A homologous part of FAM124B protein alignment from Human to Zebrafish by Constraint-based Multiple alignment tool (COBALT, <http://www.ncbi.nlm.nih.gov/tools/cobalt/>). 145 to 224 amino acid sequence of Human FAM124B shows 100% homology with all the other species.

Additionally, we could identify 3 times KU70, an ATP-dependent helicase II as a FAM124B interaction partner. KU70 was shown to interact with p53, a protein which interacts with CHD8 (Feki et al. 2005, Nishiyama et al. 2009). Therefore, FAM124B might have like CHD7 or CHD8 different functions, is involved in different mechanisms and is part of different complexes, maybe in a cell type and developmental stage dependent manner.

4.8 Future endeavors and perspectives

In the current study we have identified two new components of CHD7 containing complexes, CHD8 and FAM124B.

CHD8 mutations or disruptions are reported to be responsible for ASD/NDDs. Autism spectrum disorders are commonly associated with CHARGE syndrome. With the current study we provide the first functional link between these two conditions. A further characterization of CHD7 and CHD8 containing complexes is necessary to get deeper insights into the pathomechanism behind ASD/NDD and CHARGE or other related malformation syndromes. Such functional link at the molecular level was described in the literature for CHARGE syndrome and Treacher Collins syndrome, a clinically distinct disorder but affecting the same organ systems. *TCOF1*, the gene mutated in Treacher Collins syndrome and *CHD7* co-associate at rDNA (Zentner et al. 2010). Possibly, the characterization of CHD7 and CHD8 complexes can also explain the overlap in the clinical features between CHARGE and other related disorders.

CHARGE syndrome belongs to the group of “neurocristopathies”. Many of the symptoms seen in those syndromes are hypothesized to be the result from abnormalities in the

development, migration, or interaction of the cephalic neural crest cells (Siebert et al. 1985). Indeed, Bajpai et al. (2010) could demonstrate by CHD7 knockdown studies in *Xenopus laevis* embryos that CHD7 is crucial for neural crest cell (NCC) formation and migration into the pharyngeal arches. We could observe the same effect in our group (Fig. 4.9).

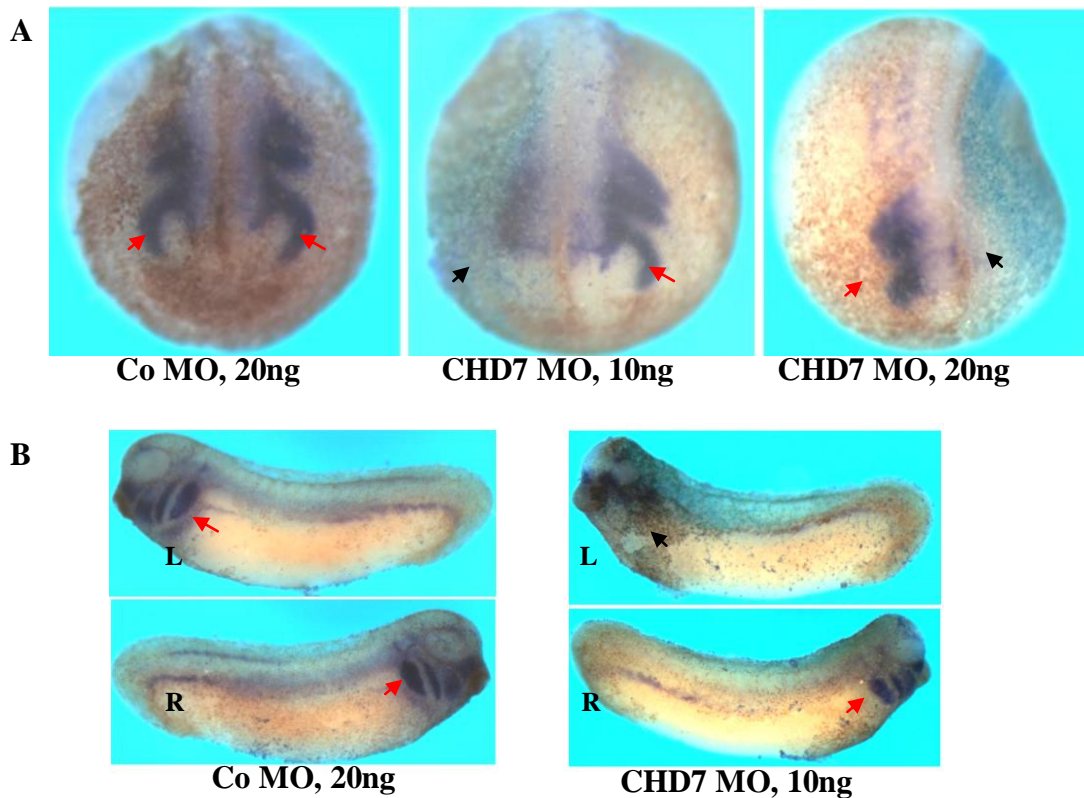


Figure 4.9. Effect of CHD7 knockdown on expression of transcription factor Twist involved in neural crest formation. Two cell-stage *Xenopus laevis* embryos were injected with Control morpholino (CoMO, 20ng) and CHD7 morpholino (CHD7 MO, 10ng and 20ng) asymmetrically into a single blastomere and analyzed by whole mount *in situ* hybridization at neurula stage (st.21 and 26) to visualize expression pattern of Twist, a transcription factor that controls early neural crest formation. **A:** *Xenopus laevis* stage 21. **B:** stage 26, left (L) and right (R) side of the embryos. Red arrows indicate migrating neural crest cells while black arrow shows disrupted neural crest migration which CHD7 MO was injected. In CHD7 knockdown part, neural crest formation is severely affected which shows no expression of Twist (done by Yvonne Schulz 2012).

In the current study we identified the hitherto uncharacterized protein FAM124B as a novel component of a CHD7 and CHD8 containing complex. We examined the expression profile and subcellular localization but functional studies are still needed. It will be interesting to prove if a knockdown of FAM124B in *Xenopus laevis* embryos will lead to an abnormal formation and migration of neural crest cells, as well. Furthermore, it will be of great interest if an overexpression of FAM124B in *Xenopus laevis* embryos with a CHD7 knockdown can

rescue the CHD7/CHARGE phenotype and if a knockdown of FAM124B and CHD7 together show a more severe synergistic effect.

Additionally, the creation and characterization of a “loss of function” FAM124B mouse model will provide information if a mutated FAM124B lead to CHARGE or a CHARGE related syndrome. In our working group, a FAM124B mutation screening of CHD7 negative CHARGE patients is already in progress. We believe that such studies can elucidate another gene involved in CHARGE syndrome and can explain the multiple defects seen in the patients.

5. References

- Adams ME, Hurd EA, Beyer LA, Swiderski DL, Raphael Y, Martin DM. (2007)** Defects in vestibular sensory epithelia and innervation in mice with loss of Chd7 function: implications for human CHARGE syndrome. *J Comp Neurol.* 504:519–532.
- Airio A, Pukkala E, Isomaki H. (1995)** Elevated cancer incidence in patients with dermatomyositis: a population based study. *J Rheumatol.* 22:1300–1303.
- Akhtar A, Zink D, Becker PB. (2000)** Chromodomains are protein-RNA interaction modules. *Nature.* 407:405–409.
- Allis CD, Jenuwein T, Reinberg D, Caparros ML (editors). (2007)** Epigenetics, Cold Spring Harbor Laboratory Press, Cold Spring Harbor, New York. p.240.
- Aramaki M, Udaka T, Kosaki R, Makita Y, Okamoto N, Yoshihashi H, Oki H, Nanao K, Moriyama N, Oku S, Hasegawa T, Takahashi T, Fukushima Y, Kawame H, Kosaki K. (2006)** Phenotypic spectrum of CHARGE syndrome with CHD7 mutations. *J Pediatr.* 148:410-414.
- Asakura Y, Toyota Y, Muroya K, Kurosawa K, Fujita K, Aida N, Kawame H, Kosaki K, Adachi M. (2008)** Endocrine and radiological studies in patients with molecularly confirmed CHARGE syndrome. *J Clin Endocrinol Metab.* 93:920–924.
- Bagchi A, Papazoglu C, Wu Y, Capurso D, Brodt M, Francis D, Bredel M, Vogel H, Mills AA. (2007)** CHD5 is a tumor suppressor at human 1p36. *Cell.* 128(3):459-475.
- Bajpai R, Chen DA, Rada-Iglesias A, Zhang J, Xiong Y, Helms J, Chang CP, Zhao Y, Swigut T, Wysocka J. (2010)** CHD7 cooperates with PBAF to control multipotent neural crest formation. *Nature.* 463(7283):958-962.
- Batsukh T, Pieper L, Koszucka AM, von Velsen N, Hoyer-Fender S, Elbracht M, Bergman JE, Hoefsloot LH, Pauli S. (2010)** CHD8 interacts with CHD7, a protein which is mutated in CHARGE syndrome. *Hum Mol Genet.* 19(14):2858-2866.
- Bergman JE, Bosman EA, van Ravenswaaij-Arts CM, Steel KP. (2010)** Study of smell and reproductive organs in a mouse model for CHARGE syndrome. *Eur J Hum Genet.* 18(2):171-177.
- Bergman JE, Bocca G, Hoefsloot LH, Meiners LC, van Ravenswaaij-Arts CM. (2011a.)** Anosmia predicts hypogonadotropic hypogonadism in CHARGE syndrome. *J Pediatr.* 158:474–479.

- Bergman JE**, Janssen N, Hoefsloot LH, Jongmans MC, Hofstra RM, van Ravenswaaij- Arts CM. (2011b) CHD7 mutations and CHARGE syndrome: the clinical implications of an expanding phenotype. *J Med Genet.* 48:334–342.
- Betancur C.** (2011) Etiological heterogeneity in autism spectrum disorders: more than 100 genetic and genomic disorders and still counting. *Brain Res.*1380:42-77.
- Blake KD**, Davenport SL, Hall BD, Hefner MA, Pagon RA, Williams MS, Lin AE, Graham Jr JM. (1998) CHARGE association: an update and review for the primary pediatrician. *Clin Pediatr (Phila).* 37:159–173.
- Bosman EA**, Penn AC, Ambrose JC, Kettleborough R, Stemple DL, Steel KP. (2005) Multiple mutations in mouse *Chd7* provide models for CHARGE syndrome. *Hum Mol Genet.* 14(22):3463-3476.
- Bouazoune K**, Mitterweger A, Langst G, Imhof A, Akhtar A, Becker PB, Brehm A. (2002) The dMi-2 chromodomains are DNA binding modules important for ATP-dependent nucleosome mobilization. *Embo J.* 21:2430–2440.
- Boyer LA**, Latek RR, Peterson CL. (2004) The SANT domain: a unique histone-tail-binding module? *Nat Rev Mol Cell Biol.* 5(2):158-163.
- Brehm A**, Tufteland KR, Aasland R, Becker PB. (2004) The many colours of chromodomains. *Bioessays.* 26(2):133-140.
- Carta C**, Pantaleoni F, Bocchinfuso G, Stella L, Vasta I, Sarkozy A, Digilio C, Palleschi A, Pizzuti A, Grammatico P, Zampino G, Dallapiccola B, Gelb BD, Tartaglia M. (2006) Germline missense mutations affecting KRAS Isoform B are associated with a severe Noonan syndrome phenotype. *Am J Hum Genet.* 79(1):129-135.
- Cirstea IC**, Kutsche K, Dvorsky R, Gremer L, Carta C, Horn D, Roberts AE, Lepri F, Merbitz-Zahradnik T, König R, Kratz CP, Pantaleoni F, et al. (2010) A restricted spectrum of NRAS mutations causes Noonan syndrome. *Nat Genet.* 42(1):27-29.
- Chung CD**, Liao J, Liu B, Rao X, Jay P, Berta P, Shuai K. (1997) Specific inhibition of Stat3 signal transduction by PIAS3. *Science.* 278(5344):1803-1805.
- Cleary JO**, Price AN, Thomas DL, Scambler PJ, Kyriakopoulou V, McCue K, Schneider JE, Ordidge RJ, Lythgoe MF. (2009) Cardiac phenotyping in ex vivo murine embryos using microMRI. *NMR Biomed.* 22:857–866.

- Deardorff** MA, Kaur M, Yaeger D, Rampuria A, Korolev S, Pie J, Gil-Rodríguez C, Arnedo M, Loeys B, Kline AD, Wilson M, Lillquist K, et al. (2007) Mutations in cohesin complex members SMC3 and SMC1A cause a mild variant of cornelia de Lange syndrome with predominant mental retardation. *Am J Hum Genet.* 80(3):485-494.
- Dixon** J, Trainor P, Dixon MJ. (2007) Treacher Collins syndrome. *Orthod Craniofac Res.* 10(2):88-95. Review.
- Dodé C, Hardelin JP.** (2009) Kallmann syndrome. *Eur J Hum Genet.* 17(2):139-46.
- Dou** Y, Milne TA, Tackett AJ, Smith ER, Fukuda A, Wysocka J, Allis CD, Chait BT, Hess JL, Roeder RG. (2005) Physical association and coordinate function of the H3 K4 methyltransferase MLL1 and the H4 K16 acetyltransferase MOF. *Cell.* 121(6):873-885.
- Eberharter** A, Vetter I, Ferreira R, Becker PB. (2004) ACF1 improves the effectiveness of nucleosome mobilization by ISWI through PHD-histone contacts. *Embo J.* 23:4029–4039.
- Feki** A, Jefford CE, Berardi P, Wu JY, Cartier L, Krause KH, Irminger-Finger I. (2005) BARD1 induces apoptosis by catalysing phosphorylation of p53 by DNA-damage response kinase. *Oncogene.* 24(23):3726-3736.
- Felix** TM, Hanshaw BC, Mueller R, Bitoun P, Murray JC. (2006) CHD7 gene and nonsyndromic cleft lip and palate. *Am J Med Genet A.* 140:2110–2114.
- Fischle** W, Wang Y, Jacobs SA, Kim Y, Allis CD, Khorasanizadeh S. (2003) Molecular basis for the discrimination of repressive methyl-lysine marks in histone H3 by Polycomb and HP1 chromodomains. *Genes Dev.* 17:1870–1881.
- Flanagan** JF, Mi LZ, Chruszcz M, Cymborowski M, Clines KL, Kim Y, Minor W, Rastinejad F, Khorasanizadeh S. (2005) Double chromodomains cooperate to recognize the methylated histone H3 tail. *Nature.* 438:1181–1185.
- Garrath** RH, **Grisham** CM. (1999) *Biochemistry*, second edition, Figure 31.32.
- Gaspar-Maia** A, Alajem A, Polesso F, Sridharan R, Mason MJ, Heidersbach A, Ramalho-Santos J, McManus MT, Plath K, Meshorer E, Ramalho-Santos M. (2009) Chd1 regulates open chromatin and pluripotency of embryonic stem cells. *Nature.* 460(7257):863-868.
- Ge** Q, Nilasena DS, O'Brien CA, Frank MB, Targoff IN. (1995) Molecular analysis of a major antigenic region of the 240-kD protein of Mi-2 autoantigen. *J Clin Invest.* 96:1730–1737.

- Gui Y, Guo G, Huang Y, Hu X, Tang A, Gao S, Wu R, Chen C, Li X, Zhou L, He M, Li Z, Sun X, Jia W, Chen J, et al. (2011)** Frequent mutations of chromatin remodeling genes in transitional cell carcinoma of the bladder. *Nat Genet.* 43(9):875-878.
- Hall JA, Georgel PT. (2007)** CHD proteins: a diverse family with strong ties. *Biochem Cell Biol.* 85(4):463-476.
- Heintzman ND, Hon GC, Hawkins RD, Kheradpour P, Stark A, Harp LF, Ye Z, Lee LK, Stuart RK, Ching CW, Ching KA, Antosiewicz-Bourget JE, et al. (2009)** Histone modifications at human enhancers reflect global cell-type-specific gene expression. *Nature.* 459(7243):108-112.
- Hess JL. (2004)** MLL: a histone methyltransferase disrupted in leukemia. *Trends Mol. Med.* 10:500–507.
- Ho L, Crabtree GR. (2010)** Chromatin remodelling during development. *Nature.* 463:474–484.
- Horsch U, Scheele A (editors). (2011)** Compendium on CHARGE syndrome. Median-Verlag von Killisch-Horn GmbH. Heidelberg. p.11
- Hurd EA, Capers PL, Blauwkamp MN, Adams ME, Raphael Y, Poucher HK, Martin DM. (2007)** Loss of Chd7 function in gene-trapped reporter mice is embryonic lethal and associated with severe defects in multiple developing tissues. *Mamm Genome.* 18:94–104.
- Hurd EA, Poucher HK, Cheng K, Raphael Y, Martin DM. (2010)** The ATP-dependent chromatin remodeling enzyme CHD7 regulates pro-neural gene expression and neurogenesis in the inner ear. *Development.* 137:3139–3150.
- Ishihara K, Oshimura M, Nakao M. (2006)** CTCF-dependent chromatin insulator is linked to epigenetic remodeling. *Mol Cell.* 23(5):733-742.
- Jacobs-McDaniels NL, Albertson RC. (2011)** Chd7 plays a critical role in controlling left-right symmetry during zebrafish somitogenesis. *Dev Dyn.* 240(10):2272-2280.
- Janssen N, Bergman JE, Swertz MA, Tranebjaerg L, Lodahl M, Schoots J, Hofstra RM, van Ravenswaaij-Arts CM, Hoefsloot LH. (2012)** Mutation update on the CHD7 gene involved in CHARGE syndrome. *Hum Mutat.* 33(8):1149-1160.
- Jongmans MC, Admiraal RJ, van der Donk KP, Vissers LE, Baas AF, Kapusta L, van Hagen JM, Donnai D, de Ravel TJ, Veltman JA, Geurts van Kessel A, De Vries BB, et al. (2006)**

CHARGE syndrome: the phenotypic spectrum of mutations in the CHD7 gene. *J Med Genet.* 43:306–314.

Jongmans MC, Hoefsloot LH, van der Donk KP, Admiraal RJ, Magee A, van de Laar I, Hendriks Y, Verheij JB, Walpole I, Brunner HG, van Ravenswaaij CM. (2008) Familial CHARGE syndrome and the CHD7 gene: a recurrent missense mutation, intrafamilial recurrence and variability. *Am J Med Genet A.* 146A(1):43-50.

Kalscheuer VM, Feenstra I, Van Ravenswaaij-Arts CM, Smeets DF, Menzel C, Ullmann R, Musante L, Ropers HH. (2008) Disruption of the TCF4 gene in a girl with mental retardation but without the classical Pitt-Hopkins syndrome. *Am J Med Genet A.* 146A(16):2053-2059.

Kehle J, Beuchle D, Treuheit S, Christen B, Kennison JA, Bienz M, Muller J. (1998) dMi-2, a hunchbackinteracting protein that functions in polycomb repression. *Science.* 282:1897–1900.

Kelley DE, Stokes DG, Perry RP. (1999) CHD1 interacts with SSRP1 and depends on both its chromodomain and its ATPase/helicase-like domain for proper association with chromatin. *Chromosoma.* 108:10–25.

Kim J, Daniel J, Espejo A, Lake A, Krishna M, Xia L, Zhang Y, Bedford MT. (2006) Tudor, MBT and chromo domains gauge the degree of lysine methylation. *EMBO Rep.* 7:397–403.

Kita Y, Nishiyama M, Nakayama KI. (2012) Identification of CHD7(S) as a novel splicing variant of CHD7 with functions similar and antagonistic to those of the full-length CHD7(L). *Genes Cells.* 17(7):536-547.

Kobayashi M, Kishida S, Fukui A, Michiue T, Miyamoto Y, Okamoto T, Yoneda Y, Asashima M, Kikuchi A. (2002) Nuclear localization of Duplin, a beta-catenin-binding protein, is essential for its inhibitory activity on the Wnt signaling pathway. *J Biol Chem.* 277(8):5816-5822.

Krantz ID, McCallum J, DeScipio C, Kaur M, Gillis LA, Yaeger D, Jukofsky L, Wasserman N, Bottani A, Morris CA, Nowaczyk MJ, Toriello H, et al. (2004) Cornelia de Lange syndrome is caused by mutations in NIPBL, the human homolog of *Drosophila melanogaster* Nipped-B. *Nat Genet.* 36(6):631-635.

Lalani SR, Safiullah AM, Molinari LM, Fernbach SD, Martin DM, Belmont JW. (2004) SEMA3E mutation in a patient with CHARGE syndrome. *J Med Genet.* 41:e94.

Lalani SR, Safiullah AM, Fernbach SD, Harutyunyan KG, Thaller C, Peterson LE, McPherson JD, Gibbs RA, White LD, Hefner M, Davenport SL, Graham JM, Bacino CA, Glass NL,

- Towbin JA, et al. (2006) Spectrum of CHD7 mutations in 110 individuals with CHARGE syndrome and genotype–phenotype correlation. *Am J Hum Genet.* 78:303–314.
- Law ME, Templeton KL, Kitange G, Smith J, Misra A, Feuerstein BG, Jenkins RB. (2005) Molecular cytogenetic analysis of chromosomes 1 and 19 in glioma cell lines. *Cancer Genet Cytogenet.* 160:1–14.
- Layman WS, McEwen DP, Beyer LA, Lalani SR, Fernbach SD, Oh E, Swaroop A, Hegg CC, Raphael Y, Martens JR, Martin DM. (2009) Defects in neural stem cell proliferation and olfaction in *Chd7* deficient mice indicate a mechanism for hyposmia in human CHARGE syndrome. *Hum Mol Genet.* 18:1909–1923.
- Layman WS, Hurd EA, Martin DM. (2010) Chromodomain proteins in development: lessons from CHARGE syndrome. *Clin Genet.* 78:11–20.
- Layman WS, Hurd EA, Martin DM. (2011) Reproductive dysfunction and decreased GnRH neurogenesis in a mouse model of CHARGE syndrome. *Hum Mol Genet.* 20:3138–3150.
- Lee YW, Kim SC, Shin YL, Kim JW, Hong HS, Lee YK, Ki CS. (2009) Clinical and genetic analysis of the CHD7 gene in Korean patients with CHARGE syndrome. *Clin Genet.* 75:290–293.
- Lemos TA, Passos DO, Nery FC, Kobarg J. (2003) Characterization of a new family of proteins that interact with the C-terminal region of the chromatin-remodeling factor CHD-3. *FEBS Lett.* 533:14–20.
- Lutz T, Stöger R, Nieto A. (2006) CHD6 is a DNA-dependent ATPase and localizes at nuclear sites of mRNA synthesis. *FEBS Lett.* 580(25):5851-5857.
- Marfella CG, Imbalzano AN. (2007) The Chd family of chromatin remodelers. *Mutat Res.* 618(1-2):30-40.
- Marfella CG, Ohkawa Y, Coles AH, Garlick DS, Jones SN, Imbalzano AN. (2006) Mutation of the SNF2 family member *Chd2* affects mouse development and survival. *J Cell Physiol.* 209(1):162-171.
- Melicharek DJ, Ramirez LC, Singh S, Thompson R, Marendra DR. (2010) *Kismet/CHD7* regulates axon morphology, memory and locomotion in a *Drosophila* model of CHARGE syndrome. *Hum Mol Genet.* 19(21):4253-4264.
- Menon T, Yates JA, Bochar DA. (2010) Regulation of androgen-responsive transcription by the chromatin remodeling factor CHD8. *Mol Endocrinol.* 24(6):1165-1174.

- Messmer S, Franke A, Paro R. (1992)** Analysis of the functional role of the Polycomb chromo domain in *Drosophila melanogaster*. *Genes Dev.* 6(7):1241-1254.
- Min J, Zhang Y, Xu RM. (2003)** Structural basis for specific binding of Polycomb chromodomain to histone H3 methylated at Lys 27. *Genes Dev* 17:1823–1828.
- Musio A, Selicorni A, Focarelli ML, Gervasini C, Milani D, Russo S, Vezzoni P, Larizza L. (2006)** X-linked Cornelia de Lange syndrome owing to SMC1L1 mutations. *Nat Genet.* 38(5):528-530.
- Nava C, Hanna N, Michot C, Pereira S, Pouvreau N, Niihori T, Aoki Y, Matsubara Y, Arveiler B, Lacombe D, Pasmant E, Parfait B, Baumann C, Héron D, Sigaudy S, et al. (2007)** Cardio-facio-cutaneous and Noonan syndromes due to mutations in the RAS/MAPK signalling pathway: genotype-phenotype relationships and overlap with Costello syndrome. *J Med Genet.* 44(12):763-771.
- Neale BM, Kou Y, Liu L, Ma'ayan A, Samocha KE, Sabo A, Lin CF, Stevens C, Wang LS, Makarov V, Polak P, Yoon S, et al. (2012)** Patterns and rates of exonic de novo mutations in autism spectrum disorders. *Nature.* 485(7397):242-245.
- Nishiyama M, Nakayama K, Tsunematsu R, Tsukiyama T, Kikuchi A, Nakayama KI. (2004)** Early embryonic death in mice lacking the beta-catenin-binding protein Duplin. *Mol Cell Biol.* 24(19):8386-8394.
- Nishiyama M, Oshikawa K, Tsukada Y, Nakagawa T, Iemura S, Natsume T, Fan Y, Kikuchi A, Skoultchi AI, Nakayama KI. (2009)** CHD8 suppresses p53-mediated apoptosis through histone H1 recruitment during early embryogenesis. *Nat Cell Biol.* 11(2):172-182.
- Nishiyama M, Skoultchi AI, Nakayama KI. (2012)** Histone H1 recruitment by CHD8 is essential for suppression of the Wnt- β -catenin signaling pathway. *Mol Cell Biol.* 32(2):501-512.
- O'Roak BJ, Vives L, Girirajan S, Karakoc E, Krumm N, Coe BP, Levy R, Ko A, Lee C, Smith JD, Turner EH, Stanaway IB, Vernot B, Malig M, Baker C, et al. (2012)** Sporadic autism exomes reveal a highly interconnected protein network of de novo mutations. *Nature.* 485(7397):246-250.
- Pagon RA, Graham Jr JM, Zonana J, Yong SL. (1981)** Coloboma, congenital heart disease, and choanal atresia with multiple anomalies: CHARGE association. *J Pediatr.* 99:223–227.

- Patten SA**, Jacobs-McDaniels NL, Zaouter C, Drapeau P, Albertson RC, Moldovan F. (2012) Role of Chd7 in zebrafish: a model for CHARGE syndrome. *PLoS One*. 7(2):e31650.
- Pena PV**, Davrazou F, Shi X, Walter KL, Verkhusha VV, Gozani O, Zhao R, Kutateladze TG. (2006) Molecular mechanism of histone H3K4me3 recognition by plant homeodomain of ING2. *Nature*. 442:100–103.
- Pray-Grant MG**, Daniel JA, Schieltz D, Yates JR 3rd, Grant PA. (2005) Chd1 chromodomain links histone H3 methylation with SAGA- and SLIK-dependent acetylation. *Nature*. 433:434–438.
- Ragvin A**, Valvatne H, Erdal S, Arskog V, Tufteland KR, Breen K, AM OY, Eberharther A, Gibson TJ, Becker PB, Aasland R. (2004) Nucleosome binding by the bromodomain and PHD finger of the transcriptional cofactor p300. *J Mol Biol*. 337:773–788.
- Randall V**, McCue K, Roberts C, Kyriakopoulou V, Beddow S, Barrett AN, Vitelli F, Prescott K, Shaw-Smith C, Devriendt K, Bosman E, Steffes G, et al. (2009) Great vessel development requires biallelic expression of Chd7 and Tbx1 in pharyngeal ectoderm in mice. *J Clin Invest*. 119:3301–3310.
- Razzaque MA**, Nishizawa T, Komoike Y, Yagi H, Furutani M, Amo R, Kamisago M, Momma K, Katayama H, Nakagawa M, Fujiwara Y, Matsushima M, et al. (2007) Germline gain-of-function mutations in RAF1 cause Noonan syndrome. *Nat Genet*. 39(8):1013-1017.
- Roberts AE**, Araki T, Swanson KD, Montgomery KT, Schiripo TA, Joshi VA, Li L, Yassin Y, Tamburino AM, Neel BG, Kucherlapati RS. (2007) Germline gain-of-function mutations in SOS1 cause Noonan syndrome. *Nat Genet*. 39(1):70-74.
- Rodenberg JM**, Hoggatt AM, Chen M, Touw K, Jones R, Herring BP. (2010) Regulation of serum response factor activity and smooth muscle cell apoptosis by chromodomain helicase DNA-binding protein 8. *Am J Physiol Cell Physiol*. 299(5):C1058-1067.
- Rodríguez-Paredes M**, Ceballos-Chávez M, Esteller M, García-Domínguez M, Reyes JC. (2009) The chromatin remodeling factor CHD8 interacts with elongating RNA polymerase II and controls expression of the cyclin E2 gene. *Nucleic Acids Res*. 37(8):2449-2460.
- Sakamoto I**, Kishida S, Fukui A, Kishida M, Yamamoto H, Hino S, Michiue T, Takada S, Asashima M, Kikuchi A. (2000) A novel beta-catenin-binding protein inhibits beta-catenin-dependent Tcf activation and axis formation. *J Biol Chem*. 275(42):32871-32878.

- Sanlaville D**, Etchevers HC, Gonzales M, Martinovic J, Clément-Ziza M, Delezoide AL, Aubry MC, Pelet A, Chemouny S, Cruaud C, Audollent S, Esculpavit C, et al. (2006) Phenotypic spectrum of CHARGE syndrome in fetuses with CHD7 truncating mutations correlates with expression during human development. *J Med Genet.* 43(3):211-217.
- Sarkozy A**, Carta C, Moretti S, Zampino G, Digilio MC, Pantaleoni F, Scioletti AP, Esposito G, Cordeddu V, Lepri F, Petrangeli V, Dentici ML, et al. (2009) Germline BRAF mutations in Noonan, LEOPARD, and cardiofaciocutaneous syndromes: molecular diversity and associated phenotypic spectrum. *Hum Mutat.* 30(4):695-702.
- Schnetz MP**, Bartels CF, Shastri K, Balasubramanian D, Zentner GE, Balaji R, Zhang X, Song L, Wang Z, Laframboise T, Crawford GE, Scacheri PC. (2009) Genomic distribution of CHD7 on chromatin tracks H3K4 methylation patterns. *Genome Res.* 19(4): 590–601.
- Schnetz MP**, Handoko L, Akhtar-Zaidi B, Bartels CF, Pereira CF, Fisher AG, Adams DJ, Flicek P, Crawford GE, Laframboise T, Tesar P, Wei CL, Scacheri PC. (2010) CHD7 targets active gene enhancer elements to modulate ES cell-specific gene expression. *PLoS Genet.* 6(7):e1001023.
- Schubbert S**, Zenker M, Rowe SL, Böll S, Klein C, Bollag G, van der Burgt I, Musante L, Kalscheuer V, Wehner LE, Nguyen H, West B, Zhang KY, Sistermans E, Rauch A, et al.(2006) Germline KRAS mutations cause Noonan syndrome. *Nat Genet.* 38(3):331-336.
- Schwab U**, Stein H, Gerdes J, Lemke H, Kirchner H, Schaadt M, Diehl V. (1982) Production of a monoclonal antibody specific for Hodgkin and Sternberg-Reed cells of Hodgkin's disease and a subset of normal lymphoid cells. *Nature.* 299:65–67.
- Seelig HP**, Moosbrugger I, Ehrfeld H, Fink T, Renz M, Genth E. (1995) The major dermatomyositis-specific Mi-2 autoantigen is a presumed helicase involved in transcriptional activation. *Arthritis Rheum.* 38:1389–1399.
- Seelig HP**, Renz M, Targoff IN, Ge Q, Frank MB. (1996) Two forms of the major antigenic protein of the dermatomyositis-specific Mi-2 autoantigen. *Arthritis Rheum.* 39:1769–1771.
- de la Serna IL**, Ohkawa Y, Imbalzano AN. (2006) Chromatin remodelling in mammalian differentiation: lessons from ATP-dependent remodellers. *Nat Rev Genet.* 7(6):461-473.
- Shi X**, Hong T, Walter KL, Ewalt M, Michishita E, Hung T, Carney D, Pena P, Lan F, Kaadige MR, Lacoste N, Cayrou C, Davrazou F, Saha A, Cairns BR, et al. (2006) ING2 PHD domain links histone H3 lysine 4 methylation to active gene repression. *Nature.* 442:96–99.

- Shur I, Benayahu D. (2005)** Characterization and functional analysis of CReMM, a novel chromodomain helicase DNA-binding protein. *J Mol Biol.* 352:646–655.
- Shur I, Socher R, Benayahu D. (2006)** In vivo association of CReMM/CHD9 with promoters in osteogenic cells. *J Cell Physiol.* 207:374–378.
- Siebert JR, Graham Jr JM, MacDonald C. (1985)** Pathologic features of the CHARGE association: support for involvement of the neural crest. *Teratology.* 31:331–336.
- Sillibourne JE, Delaval B, Redick S, Sinha M, Doxsey SJ. (2007)** Chromatin remodeling proteins interact with pericentrin to regulate centrosome integrity. *Mol Biol Cell.* 18(9):3667-3680.
- Sims RJ 3rd, Nishioka K, Reinberg D. (2003)** Histone lysine methylation: a signature for chromatin function. *Trends Genet.* 19:629–639.
- Sims RJ 3rd, Chen CF, Santos-Rosa H, Kouzarides T, Patel SS, Reinberg D. (2005)** Human but not yeast CHD1 binds directly and selectively to histone H3 methylated at lysine 4 via its tandem chromodomains. *J Biol Chem.* 280:41789–41792.
- Sims JK, Wade PA. (2011)** SnapShot: Chromatin remodeling: CHD. *Cell.* 144(4):626-626.e1.
- Smith CL and Peterson CL. (2005)** ATP-dependent chromatin remodeling. *Curr Top Dev Biol.* 65:115–148.
- Solari F, Ahringer J. (2000)** NURD-complex genes antagonise Ras-induced vulval development in *Caenorhabditis elegans*. *Curr Biol.* 10:223–226.
- Srinivasan S, Armstrong JA, Deuring R, Dahlsveen IK, McNeill H, Tamkun JW. (2005)** The *Drosophila trithorax* group protein Kismet facilitates an early step in transcriptional elongation by RNA Polymerase II. *Development.* 132(7):1623-1635.
- Srinivasan S, Dorigi KM, Tamkun JW. (2008)** *Drosophila* kismet regulates histone H3 lysine 27 methylation and early elongation by RNA polymerase II. *PLoS Genet.* 4(10):e1000217
- Talkowski ME, Rosenfeld JA, Blumenthal I, Pillalamarri V, Chiang C, Heilbut A, Ernst C, Hanscom C, Rossin E, Lindgren AM, Pereira S, Ruderfer D, et al. (2012)** Sequencing chromosomal abnormalities reveal neurodevelopmental loci that confer risk across diagnostic boundaries. *Cell.* 149(3):525-537.

- Tartaglia M, Mehler EL, Goldberg R, Zampino G, Brunner HG, Kremer H, van der Burgt I, Crosby AH, Ion A, Jeffery S, Kalidas K, Patton MA, et al. (2001)** Mutations in PTPN11, encoding the protein tyrosine phosphatase SHP-2, cause Noonan syndrome. *Nat Genet.* 29(4):465-468.
- Thompson PM, Gotoh T, Kok M, White PS, Brodeur GM. (2003)** CHD5, a new member of the chromodomain gene family, is preferentially expressed in the nervous system. *Oncogene.* 22:1002–1011.
- Thompson BA, Tremblay V, Lin G, Bochar DA. (2008)** CHD8 is an ATP-dependent chromatin remodeling factor that regulates beta-catenin target genes. *Mol Cell Biol.* 28(12):3894-3904.
- Tong JK, Hassig CA, Schnitzler GR, Kingston RE, Schreiber SL. (1998)** Chromatin deacetylation by an ATP-dependent nucleosome remodelling complex. *Nature.* 395:917–921.
- Tonkin ET, Wang TJ, Lisgo S, Bamshad MJ, Strachan T. (2006)** NIPBL, encoding a homolog of fungal Scc2-type sister chromatid cohesion proteins and fly Nipped-B, is mutated in Cornelia de Lange syndrome. *Nat Genet.* 36(6):636-641.
- Tsukiyama T. (2002)** The in vivo functions of ATP-dependent chromatin-remodelling factors. *Nat Rev Mol Cell Biol.* 3(6):422-429. Review.
- Valdez BC, Henning D, So RB, Dixon J, Dixon MJ. (2004)** The Treacher Collins syndrome (TCOF1) gene product is involved in ribosomal DNA gene transcription by interacting with upstream binding factor. *Proc Natl Acad Sci USA.* 101(29):10709-10714.
- Verloes A. (2005)** Updated diagnostic criteria for CHARGE syndrome: a proposal. *Am J Med Genet A.* 133:306–308.
- Vissers LE, van Ravenswaaij CM, Admiraal R, Hurst JA, de Vries BB, Janssen IM, van der Vliet WA, Huys EH, de Jong PJ, Hamel BC, Schoenmakers EF, Brunner HG, et al. (2004)** Mutations in a new member of the chromodomain gene family cause CHARGE syndrome. *Nat Genet.* 36(9):955-957.
- Vuorela P, La-Mello S, Saloranta C, Penttinen M, Poyhonen M, Huoponen K, Borozdin W, Bausch B, Botzenhart EM, Wilhelm C, Kaariainen H, Kohlhase J. (2007)** Molecular analysis of the CHD7 gene in CHARGE syndrome: identification of 22 novel mutations and evidence for a low contribution of large CHD7 deletions. *Genet Med.* 9:690–694.

- Wade PA, Jones PL, Vermaak D, Wolffe AP. (1998)** A multiple subunit Mi-2 histone deacetylase from *Xenopus laevis* cofractionates with an associated Snf2 superfamily ATPase. *Curr Biol.* 8:843–846.
- Wang HB, Zhang Y. (2001)** Mi2, an auto-antigen for dermatomyositis, is an ATP-dependent nucleosome remodeling factor. *Nucleic Acids Res.* 29:2517–2521.
- Wessels K, Bohnhorst B, Luhmer I, Morlot S, Bohring A, Jonasson J, Epplen JT, Gadzicki D, Glaser S, Gohring G, Malzer M, Hein A, and others. (2010)** Novel CHD7 mutations contributing to the mutation spectrum in patients with CHARGE syndrome. *Eur J Med Genet.* 53:280–285.
- White PS, Thompson PM, Gotoh T, Okawa ER, Igarashi J, Kok M, Winter C, Gregory SG, Hogarty MD, Maris JM, Brodeur GM. (2005)** Definition and characterization of a region of 1p36.3 consistently deleted in neuroblastoma. *Oncogene.* 24(16):2684-2694.
- Williams CJ, Naito T, Arco PG, Seavitt JR, Cashman SM, De Souza B, Qi X, Keables P, Von Andrian UH, Georgopoulos K. (2004)** The chromatin remodeler Mi-2beta is required for CD4 expression and T cell development. *Immunity.* 20(6):719-733.
- Williams MS. (2005)** Speculations on the pathogenesis of CHARGE syndrome. *Am J Med Genet A.* 133:318–325.
- Wincent J, Holmberg E, Stromland K, Soller M, Mirzaei L, Djureinovic T, Robinson KL, Anderlid BM, Schoumans J. (2008)** CHD7 mutation spectrum in 28 Swedish patients diagnosed with CHARGE syndrome. *Clin Genet.* 74:31–38.
- Wolffe AP. (1992)** New insights into chromatin function in transcriptional control. *FASEB J.* 6(15):3354-3361. Review.
- Woodage T, Basrai MA, Baxevanis AD, Hieter P, Collins FS. (1997)** Characterization of the CHD family of proteins. *Proc Natl Acad Sci U S A.* 94(21):11472-11477.
- Wysocka J, Myers MP, Laherty CD, Eisenman RN, Herr W. (2003)** Human Sin3 deacetylase and trithorax-related Set1/Ash2 histone H3-K4 methyltransferase are tethered together selectively by the cell-proliferation factor HCF-1. *Genes Dev.* 17: 896–911.
- Xue Y, Wong J, Moreno GT, Young MK, Cote J, Wang W. (1998)** NURD, a novel complex with both ATP dependent chromatin-remodeling and histone deacetylase activities. *Mol Cell.* 2:851–861.

- Yates** JA, Menon T, Thompson BA, Bochar DA. (2010) Regulation of HOXA2 gene expression by the ATP-dependent chromatin remodeling enzyme CHD8. *FEBS Lett.* 584(4):689-693.
- Yoshida** T, Hazan I, Zhang J, Ng SY, Naito T, Snippert HJ, Heller EJ, Qi X, Lawton LN, Williams CJ, Georgopoulos K. (2008) The role of the chromatin remodeler Mi-2 β in hematopoietic stem cell self renewal and multilineage differentiation. *Genes Dev.* 22:1174–1189.
- Yuan** CC, Zhao X, Florens L, Swanson SK, Washburn MP, Hernandez N. (2007) CHD8 associates with human Staf and contributes to efficient U6 RNA polymerase III transcription. *Mol Cell Biol.* 27(24):8729-8738.
- Zahir** F, Firth HV, Baross A, Delaney AD, Eydoux P, Gibson WT, Langlois S, Martin H, Willatt L, Marra MA, Friedman JM. (2007) Novel deletions of 14q11.2 associated with developmental delay, cognitive impairment and similar minor anomalies in three children. *J Med Genet.* 44(9):556-561.
- Zenker** M, Voss E, Reis A. (2007) Mild variable Noonan syndrome in a family with a novel PTPN11 mutation. *Eur J Med Genet.* 50(1):43-47.
- Zentner** GE, Hurd EA, Schnetz MP, Handoko L, Wang C, Wang Z, Wei C, Tesar PJ, Hatzoglou M, Martin DM, Scacheri PC. (2010) CHD7 functions in the nucleolus as a positive regulator of ribosomal RNA biogenesis. *Hum Mol Genet.* 19(18):3491-3501.
- Zhang** Y, LeRoy G, Seelig HP, Lane WS, Reinberg D. (1998) The dermatomyositis-specific autoantigen Mi2 is a component of a complex containing histone deacetylase and nucleosome remodeling activities. *Cell.* 95:279–289.

6. Abbreviations

aa	amino acid
ASD	Autism Spectrum Disorder
ASH1	Absent, Small or Homeotic 1
ATP	adenosintriphosphate
BAF	Brahma associated factor complex
BiFC	bimolecular fluorescence complementation
bp	base pair
BSA	bovine serum albumin
BRK	Brahma and Kismet domain
°C	degree Celsius
cDNA	complementary DNA
Co-IP	co-immunoprecipitation
CHD	chromodomain helicase DNA-binding
ChIP-chip	chromatin immunoprecipitation ("ChIP") with microarray technology ("chip")
Chromo	chromatin organization modifier
COBALT	Constraint-based Multiple alignment tool
CR	conserved region
Ctcf	11-zinc finger protein or CCCTC-binding factor
Cy3	indocarbocyanine
DAB	3,3'-diaminobenzidine tetrahydrochloride
DAPI	diamidino-2-phenylindole dihydrochloride
dATP	desoxyriboadenosintriphosphate
DMEM	Dulbecco's modified Eagle's medium
DNA	deoxyribonucleic acid
DNase	deoxyribonuclease
DPBS	Dulbecco's phosphate buffered saline
dpc	days post coitum
Duplin	for axis duplication inhibitor
EDTA	ethylene diamine tetra-acetic acid
EGFP	enhanced green fluorescent protein
ESC	embryonic stem cell
et al.	et alii (and others)

FAM124B	Family with sequence similarity 124B
FBS	fetal bovine serum
Fig.	Figure
FITC	fluorescein isothiocyanate
<i>Gapdh</i>	glyceraldehyde-3-phosphate dehydrogenase gene
HEPES	N-(2-hydroxyethyl) piperazin, N'-3-propanesulfoneacid
HPLC	High-performance liquid chromatography
<i>Hprt</i>	hypoxanthine guanine phosphoribosyl transferase gene
HRP	horseradish peroxidase
IgG	immunoglobulin G
ICC	immunocytochemistry
IHC	immunohistochemistry
IHH	idiopathic hypogonadotropic hypogonadism
IPTG	Isopropyl- β -thiogalactopyranoside
ISH	In situ hybridization
kb	kilobase pairs
kDa	kilodalton
LC	liquid-chromatography
min	minute
ml	milliliter
MLL	mixed lineage leukemia
MLPA	Multiplex Ligation-dependent Probe Amplification
MRCV-CV1	human fibroblast cell line
MO	morpholino
mRNA	messenger RNA
MS	mass spectrometry
NCBI	national center for biotechnology information
NDD	neurodevelopmental disorders
ng	nanogram
NIH3T3	mouse embryonic fibroblast cell line
NuRD	nucleosome remodeling and deacetylase
PAGE	polyacrylamide gel electrophoresis
PBAF	Polybromo containing complex
PBS	Phosphate Buffered Saline

PCR	polymerase chain reaction
PFA	paraformaldehyde
pH	preponderance of hydrogen ions
PHD	plant homeo domain
PLA	proximity ligation assay
rDNA	ribosomal DNA
RNA	ribonucleic acid
rpm	rotation per minute
RT	room temperature
RT-PCR	reverse transcriptase-PCR
SANT	Switching-defective protein 3, Adaptor 2, Nuclear receptor corepressor, Transcription factor IIIB
<i>Sdha</i>	succinate dehydrogenase complex, subunit A
SDS	sodium dodecylsulfate
SILAC	stable isotope labeling by amino acids in cell culture
SMC	smooth muscle cell
SNF2	sucrose non-fermenting 2
Taq DNA polymerase	<i>Thermus aquaticus</i> DNA polymerase
TPBS	Phosphate Buffered Saline with Tween-20
Tcf	T-cell factor
TCS	Treacher Collins syndrome
TE	Tris-EDTA buffer
Tris	trihydroxymethylaminomethane
TRX	trithorax
UTR	untranslated region
WAR	WDR5, ASH2L and RbBP5
WT	wild-type
X- α -gal	5-bromo-4-chloro-3-indolyl- α -D-galactopyranoside
Y2H	yeast two hybrid
μ g	microgram
μ l	microliter

The names of nucleic/amino acids are abbreviated in accordance with internationally accepted codes.

7. Acknowledgement

I am so grateful for being able to work and study at the Institute of Human Genetics, under supervision of **Prof. Dr. med. Dr. h. c. Wolfgang Engel**. I would like to express my sincere gratitude to **him** for his helpful comments, excellent guidance, valuable discussions and financial support throughout my PhD study.

I take this opportunity with great pleasure to thank my supervisor, **Dr. Silke Pauli**, who gave me such an interesting project to do. I am sincerely grateful to her generous helps, understandings, friendly and insightful discussions, and expert guidance during the entire course of my PhD work and help in the preparation of the thesis.

My sincere thanks to my co-referee **Prof. Dr. Sigrid Hoyer-Fender** and the other members of the thesis committee **Prof. Dr. Peter Burfeind, Prof. Dr. Hubertus Jarry, Prof. Dr. Jochen Reiss** and **Prof. Dr. Andreas Wodarz** for taking time out from their busy schedule to work as my examiners and for their critical reading of my thesis.

I would like to acknowledge and extend my heartfelt gratitude to all people who helped me, shared the ideas and cooperation, specifically to **Dr. Tamara I. Rabe** for her friendly help for ISH experiments; to **Dr. Henning Urlaub** and **Thomas Oellerich** for SILAC/MS experiment; **Dr. Inga-Marie Schaefer** for interpreting IHC results.

My warm thanks to all of my friends and colleagues who made my life and work in Goettingen with a lot of wonderful memories. I would like to express my special thanks to my Mongolian friends, especially to **Gunjee, Nomintuya, Dembee, Khishgee, Sanaa, Altaa, Baigal, Duuya, Byambaa, Lkhagvaa, Ankhaa, Khaliunaa, Dagii, Chimgee, Oggie, Ali, Sunjee's family** and all others. Moreover, I want to express my gratitude to my lab mates **Yvonne, Johanna, Krzysztof, Neele, Nina, Astrid, Karina, Ralf, Ania, Steffi** and other institute friends **Krishna, Xingbo, Tan, 2xSandra, Nadja, Chiru, Belal, Lukasz, Henning** and **Daria** for their friendly atmosphere, continuous supports and numerous happy moments. To all those whose names are inadvertently left out, please accept my sincere and warmest gratitude.

Special acknowledgements and thanks to my mother, **Mukhjargal Dugarsuren** and all my family members for their love, encouragement and numerous heartfelt supports. Who I am today is because of your love. Also, I would like to mention my dear late dad, **Batsukh Shatar**, and my dear grandma, **Dolgorjav Ravdan**. Thank you for your love, care and wisdoms you taught me. I wish you could have lived to see it happen.

Last but not least, I am so grateful to **Heavenly Father, God**, whose love, blessing, protection and guidance are always with me all the way of my life.

8. Curriculum Vitae

Personal details:

Name: Tserendulam Batsukh
 Place of Birth: Ulaanbaatar, Mongolia
 Date of Birth: 24th March 1984
 Nationality: Mongolian
 Address: Goßler Straße 13/Nord24
 Göttingen 37073, Germany
 Telephone: +49-17625950386
 Email: cq_84@yahoo.com, b.tserendulam@gmail.com

Education:

2009-current PhD study at Institute of Human Genetics, Georg-August University, Goettingen, Germany.
 Topic of PhD thesis: “Novel interaction partners of the chromatin remodeler CHD7, a protein mutated in CHARGE syndrome”.

2005 – 2007 Master of Science at Faculty of Biology, National University of Mongolia, Ulaanbaatar, Mongolia.

2001 - 2005 Bachelor of Science at Faculty of Biology, department of Molecular Biology & Genetics, National University of Mongolia, Ulaanbaatar, Mongolia.

1994 – 2001 Secondary School №11 which is specialized in mathematics and physics, Ulaanbaatar, Mongolia.

1991-1994 Primary School №23 which is specialized in foreign languages, Ulaanbaatar, Mongolia.

Career:

2007-2009 Researcher at Institute of Biology, Mongolian Academy of Sciences, Ulaanbaatar, Mongolia.

9. List of Publications

Batsukh T, Pieper L, Koszucka AM, von Velsen N, Hoyer-Fender S, Elbracht M, Bergman JE, Hoefsloot LH, Pauli S. (2010) CHD8 interacts with CHD7, a protein which is mutated in CHARGE syndrome. *Hum Mol Genet.* 19(14):2858-2866. (doi:10.1093/hmg/ddq189)

Batsukh T, Schulz Y, Wolf S, Rabe TI, Oellerich T, Urlaub H, Schaefer IM, Pauli S. (2012) Identification and characterization of FAM124B as a novel component of a CHD7 and CHD8 containing complex (manuscript in submission stage).